Quantifying variation in the temporal resolution of the visual system

By

Clinton Scott Haarlem

B.Sc. Biology, Leiden University, 2015

M.Sc. Biology - Evolution, Biodiversity and Conservation, Leiden University, 2017

A thesis submitted in partial fulfilment of

the requirements for the degree of

Doctor of Philosophy

2025

School of Natural Sciences

Discipline of Zoology

Trinity College Dublin

Trinity College Dublin

Coláiste na Tríonóide, Baile Átha Cliath

The University of Dublin

Declaration

I declare that this thesis has not been submitted as an exercise for a degree at this or any other university and it is entirely my own work. I agree to deposit this thesis in the University's open access institutional repository or allow the Library to do so on my behalf, subject to Irish Copyright Legislation and Trinity College Library conditions of use and acknowledgement. I consent to the examiner retaining a copy of the thesis beyond the examining period, should they so wish (EU GDPR May 2018).

Clinton Scott Haarlem

Summary

Visual systems have evolved the capacity to process environmental information across multiple domains. Spatial relations, colour and contrast are well known attributes of visual processing, but the temporal aspect of vision is often overlooked. Nevertheless, adequate updating of visual information over time is crucial for creating accurate representations of fleeting real-world phenomena. For example, temporal processing contributes to motion perception and, in certain situations, different temporal integration periods can determine whether one can see anything at all. A higher temporal resolution means that the visual system processes information on a smaller timescale, and thus provides access to potentially more visual information per timeframe.

High visual processing rates may have considerable advantages in many situations, but fast sensory processing is metabolically costly. Additionally, due to physical and physiological constraints, a necessary trade-off exists between high temporal- and high spatial processing. Within the bounds set by these limitations, visual temporal resolution is found to vary greatly in the animal kingdom. This variation is likely driven by specific visual requirements for different species depending on their ecological niche. For temporal resolution to be influenced by different selection pressures, a certain amount of variation must exist not only among species, but also among individuals within a species. How large this variation may be, and which processes may dictate different rates of temporal resolution within an individual are currently unclear. Moreover, the possible selective pressures acting on this trait are relatively unexplored, and it is not clear how different ecological settings may influence temporal resolution.

In this thesis, I use ecological principles, psychophysical experiments, neuroscience and sports science to investigate variability in visual temporal resolution on multiple levels, both among and within species. I create a novel, custom psychophysical paradigm to quantify temporal resolution, using the critical flicker fusion threshold: the point at which a flickering light-source flickers at such high a frequency, that the flicker can no longer be consciously perceived by the individual. With this paradigm, I measure critical flicker fusion thresholds in a sample group of healthy human participants to establish how widely temporal resolution varies within a species. I show that the trait varies substantially among individuals, but is stable over time within individuals.

The existence of paradigms such as the critical flicker fusion threshold suggests that, even though visual perception is experienced as a continuous stream of information, certain

aspects of visual processing may happen in a discrete manner. One hypothesis posits that visual information may be processed in discrete temporal windows, and that stimuli falling within one window are integrated into a single percept (i.e. the fusing together of multiple flashes occurring in close temporal proximity), and stimuli falling in different windows are segregated into separate percepts (i.e. the perception of separate flashes). Previous research has suggested that brainwave activity may be linked with the size of these temporal integration windows, and that certain oscillations in the brain may directly dictate individual temporal resolution. To test this, I assess whether a specific peak brainwave frequency is associated with variation in temporal processing among individuals, and whether small fluctuations in brain oscillations may cause variability in temporal processing within an individual. For this, I carry out an experiment which incorporates electroencephalogram recording, alongside two behavioural measures for visual temporal processing, the critical flicker fusion threshold and the gap-detection task. I show that this peak brainwave frequency is linked with one measure for temporal resolution, but not the other, indicating that the observed relationship may be highly context-specific.

Following on, I examine visual temporal resolution in an ecological context, both within a single species, and in the animal kingdom. First, I explore whether a certain visual processing rate is favoured in individuals occupying specific ecological settings. Using high-level sports as proxies for different ecological settings, I compare critical flicker fusion thresholds in two groups of highly trained athletes and a non-athlete control group. I demonstrate that there is no significant difference in temporal resolution between athletes in visually dynamic settings and athletes in non-visually-dynamic settings. However, temporal processing rates are higher in both athlete groups compared to the non-athlete group, suggesting that visual temporal resolution may, at least in part, be determined by cardiovascular fitness.

Lastly, I take a broad look at the animal kingdom to show that temporal resolution varies widely among species, and is linked with several aspects of ecology, such as foraging strategy and locomotion modality. These results suggest that the overall pace of a species' ecological profile may influence visual processing rates, and that highly dynamic environmental interactions may select for higher temporal resolution.

Acknowledgements

I took the first steps of my PhD journey in the middle of a global pandemic, which was quite a unique, and at times stressful, experience. Navigating a multidisciplinary project and familiarising myself with Trinity from abroad during lockdowns was a difficult process, and having all my social interactions take place on a small computer screen was certainly an interesting way to get to know supervisors and colleagues. Luckily, after nine long months of working remotely, I made my way over to Ireland and I was warmly welcomed by many friendly faces, both familiar and new. So first off, thank you to Ireland for having such wonderful people, and for being such a pleasant and positive place to be. I have had an amazing four years here so far and I plan on having many more.

Many thanks to my supervisors Andrew Jackson, Redmond O'Connell and Kevin Mitchell for all your support and guidance throughout my PhD. I was incredibly lucky to get the opportunity to work on such a multidisciplinary project, and to be guided by three supervisors who were always able to give valuable insights no matter the topic. Thank you for making me feel at home in the different departments I was fortunate enough to work in, and for providing me the opportunity to explore all my interests. I thoroughly enjoyed all our talks on ecology, neuroscience, sports science, animal behaviour, computer programming, engineering and sometimes even philosophy! Thank you also for the moral support during the times when participant recruitment seemed like a hopeless cause and all progress seemed to stall. It worked out in the end.

Much thanks to everyone in Zoology, TCIN, Botany and all the other places in Trinity where I got to meet some amazing people. You all have made my PhD not only a great learning experience, but also great fun. I'll fondly remember all the chats, drinks, cakes, holiday celebrations and symposia. I especially appreciate the fact that you all humoured me by participating in my research as I hunted each and every one of you down with my flashy-light-box. Special shout-out to MacDara and Lauren in Zoology, who absolutely went out of their way to help me recruit participants for my experiments. It is greatly appreciated. In TCIN, big thanks to Pat, who taught me all about how to carry out EEG recording, and to John and Kevin who provided a huge amount of support with MATLAB programming and EEG analysis.

And last, but most definitely not least: Seán. Thank you for your endless support and patience, and for keeping my spirits high. And most importantly, thank you for making this Irish adventure some of the best years of my life so far!

Table of Contents

List of Figures

List of Tables

Chapter 1

General Introduction

Ecological environments can be highly dynamic and incredibly complex, and the fitness of every organism is fundamentally shaped by how it interacts with the world. For an organism to be successful, it must be able to accurately collect, process and interpret information about its surroundings. This practice, known as sensory perception, enables an individual to identify and respond to external stimuli and consequently allows it to forage, detect threats, select mates, find shelter and investigate environmental cues. As such, sensory perception is under strong selective pressure, and a variety of senses have evolved throughout the animal kingdom (Barth & Schmid, 2001; Niven & Laughlin, 2008; Smith, 2008).

Though numerous different types of sensory processing have emerged over evolutionary time, the systems underlying this processing tend to be remarkably similar among species and share many common features. These shared features generally include a specialized organ or grouping of cells which collects external environmental cues and transform them into internal units of information, a nervous system to transport information to the individual's main processing centre and a brain, or something akin to it, to interpret the signal and determine an appropriate response (Smith, 2008). These features are all also vastly complex systems in their own right, and together they carry out highly coordinated processes that allow an individual to bridge its external and internal environments.

Sensory perception is essential for survival, but its dependence on these complex systems has also made it metabolically costly. This evolutionary constraint is one of the main drivers for variation in perceptual processing (Barth & Schmid, 2001; Niven & Laughlin, 2008). All species are forever under pressure to process sensory information in the most cost-effective manner, using the limited hardware available to them through their genetic makeup. Species, and individuals within a species, may experience specific ecological demands that lead them to favour some aspects of perception, while requiring them to reduce, or even forego, others, resulting in adaptations that offer functional benefits in distinct ecological niches and driving individual variation. For example, in certain species, the proportion of different visual pigments in the retina may shift depending on environmental changes (Yokoyama & Yokoyama, 1996). In species such as euryhaline fishes, this shift may aid visual perception in either redder freshwater environments or bluer marine environments during different stages of migration (Beatty, 1966, 1975). As a more extreme example, the Mexican cave tetra (*Astyanax mexicanus*) is a species of fish that exists in two distinct forms: a surface form that

lives in river and stream habitats, and a cave dwelling form. Though they are a single species and can interbreed, the surface form has fully developed and functional eyes, whereas the cave form is blind, with some varieties even lacking eyes entirely. Interestingly, the blind cave form has enhanced olfactory and mechanosensory systems relative to the surface forms (Jeffery, 2005; Kowalko, 2020).

In the context of variation in sensory perception, the visual system is particularly interesting. Image-forming eyes have evolved in only six of the 33 extant metazoan phyla, yet these six make up 96% of the known species alive today (Fernald, 2006). Most visual systems are thus extremely similar due to shared evolutionary origins, yet at the same time visual perception varies extensively among species, and even among individuals of the same species. Visual perception grants access to vast amounts of information and a visual image, or percept, can be made up of numerous elements. These elements may include colour, brightness, contrast, contours, curvatures, straight lines, angles, motion and directionality. The extent to which each of these elements plays a role in vision varies greatly, both among and within species (Emery & Webster, 2019; Halpern et al., 1999; Land & Nilsson, 2012).

One element of visual processing that is not often considered, yet which no visual system can function without, is the element of time. Environments, and therefore visual scenes, are ever in flux, and the only way an individual may perceive changes in its surroundings is if its visual system regularly updates over time. This characteristic of vision is known as temporal resolution, and it directly determines the amount of visual information an individual has access to per timeframe, which makes it a uniquely intriguing concept in the framework of individual variability.

Among species, visual temporal resolution has been shown to be linked with metabolic rate and body mass (Healy et al., 2013). Small-scale case studies have also indicated that fast-moving, highly manoeuvrable species possess faster visual processing abilities than closely related slower species (Boström et al., 2016; O'Carroll et al., 1996; Potier et al., 2020). These findings suggest that high visual temporal resolution may be beneficial in highly dynamic environments, and that this ecological demand may drive selection. For selection processes to act on a trait, a certain degree of natural variation must exist among individuals within a species. Though visual temporal resolution is known to vary widely in the animal kingdom, it is currently not clear what the magnitude of this variation is within a species, or how stable temporal resolution is over time within the same individual, or even where any variation might originate. Due to this gap in the current knowledge in this area, it is unclear to what extent individual variation in temporal resolution might influence behaviour or environmental interactions and, ultimately, how it might shape the occupation of distinct ecological niches.

In this thesis, I will address these questions by using a common psychophysical method, the critical flicker fusion (CFF) threshold, to quantify visual temporal resolution. First, I will employ this method in a cohort of healthy human participants to examine how much visual temporal resolution naturally varies among individuals, and how stable it is over time within individuals. Second, I will focus on a possible neurobiological origin for variation in temporal processing by assessing how a specific neural oscillation in the occipital region of the brain may correlate with visual temporal resolution, both among- and within individuals.

After having established the magnitude, stability and a possible driver for individual variation in visual temporal resolution, I will then explore a potential ecological selection pressure which may drive variation within a species. I will do this by examining whether physical fitness and activity in a visually dynamic setting are correlated with faster temporal resolution in healthy human participants. Lastly, I will investigate how the overall ecological profile of a species may be linked with its temporal resolution, by correlating CFF with multiple mode-of-life characteristics in a large-scale animal dataset.

1.1 Research outline

Chapter 2: Individual variation in visual temporal resolution

One of the main drivers of natural selection is individual variation. Variation can be found in almost all aspects of biology, including in sensory perception. Here, I conduct a psychophysical study to assess the amount of variation among individuals in visual temporal resolution, using critical flicker fusion thresholds. I show that in a healthy cohort of similar ages, the variation in CFF is greater among- than within individuals, and that CFF is relatively stable over time. Additionally, I present a novel testing paradigm for measuring CFF thresholds that is low-cost, portable and produces fast and accurate measurements.

Chapter 3: A potential neurophysiological origin for visual temporal resolution

Within neuroscience, visual gap detection tasks are regularly deployed to measure temporal perception ability and its relation to attention. Previous research has suggested variation in visual temporal resolution may originate in differences in the peak frequency of distinct neural oscillations, but the evidence is controversial. Here, I use both CFF and gap detection as behavioural measures for temporal resolution, alongside electroencephalogram (EEG) recordings of alpha band oscillations to investigate this potential link. I show that higher frequency alpha band oscillations correlate with the ability to perceive shorter gaps in the gap

detection task, but not with having a higher CFF threshold. I discuss how the two behavioural tasks fundamentally differ, and that any links between the examined neural oscillations and temporal resolution may be fragile and highly context-specific.

Chapter 4: Ecological setting and its relation to visual temporal perception

The presence of individual variation in a trait within a species allows for the potential of different ecological settings to place certain selection pressures on the trait. In this chapter I investigate whether a physically or visually dynamic ecological setting may select for higher temporal resolution in human participants, by comparing CFF thresholds among two different groups of athletes and a non-athlete control group. I show that higher temporal resolution is significantly correlated with physical fitness, but not with visually dynamic settings, suggesting that high levels of cardiovascular fitness may be a facilitator of fast temporal processing.

Chapter 5: Evolutionary and ecological correlates of visual temporal perception

All animals that rely on visual perception must be able to process visual information at a certain rate to keep track of an ever-changing environment and to effectively perform the types of behaviours for which the species is evolutionarily adapted. In this chapter, I turn to the animal kingdom to explore whether certain species-specific ecological characteristics are linked with visual processing rate. I show that several of these characteristics, such as habitat light levels, foraging strategy and the manner in which a species locomotes through the environment, are significantly correlated with their CFF thresholds, suggesting that visual temporal resolution is closely linked with a species' overall ecological profile.

Chapter 2

The speed of sight: individual variation in critical flicker fusion thresholds

---

Author contributions

I co-conceived the idea, created the testing paradigm, collected and analysed the data and wrote the manuscript. Andrew Jackson, Redmond O'Connell and Kevin Mitchell all contributed to the conception of the idea, secured funding and contributed to the analysis of the data and writing of the manuscript.

Status

This chapter has been published as:

Haarlem, C. S., O'Connell, R. G., Mitchell, K. J., & Jackson, A. L. (2024). The speed of sight: Individual variation in critical flicker fusion thresholds. *PLoS ONE*, *19*(4 April), 1–13.

2.1 Abstract

The critical flicker fusion threshold is a psychophysical measure commonly used to quantify visual temporal resolution; the fastest rate at which a visual system can discriminate visual signals. Critical flicker fusion thresholds vary substantially among species, reflecting different ecological niches and demands. However, it is unclear how much variation exists in flicker fusion thresholds between healthy individuals of the same species, or how stable this attribute is over time within individuals. In this study, we assessed both inter- and intra-individual variation in critical flicker fusion thresholds in a cohort of healthy human participants within a specific age range, using two common psychophysical methods and three different measurements during each session. The resulting thresholds for each method were highly correlated. We found a between-participant maximum difference of roughly 30 Hz in flicker fusion thresholds and we estimated a 95% prediction interval of 21 Hz. We used random-effects models to compare between- and within-participant variance and found that approximately 80% of variance was due to between-individual differences, and about 10% of the variance originated from within-individual differences over three sessions. Within-individual thresholds did not differ significantly between the three sessions in males, but did in females ($P<0.001$ for two methods and $P<0.05$ for one method), indicating that critical flicker fusion thresholds may be more variable in females than in males.

2.2 Introduction

Visual perception is one of the most salient types of sensory processing found in the animal kingdom, with around 96% of known animal species alive today possessing image forming eyes (Fernald, 2006). Visual systems in nature are incredibly diverse and their specific functions and sensitivities vary greatly depending on a species' ecological demands. However, all sensory processing is constrained by the maximum rate at which the system can parse information. This processing rate is different among species and is known as their temporal resolution (Grothe & Klump, 2000; Healy et al., 2013; Reeves, 1996). A finely tuned visual temporal resolution is necessary to respond appropriately to a dynamic environment and it determines a species' ability to gauge how visual scenes change over time and how accurately it can detect rapid changes in light intensity. The processing of both spatial and temporal information is also crucial for motion perception, and the resolution with which this occurs may offer distinct benefits and drawbacks. A high temporal resolution may offer an increased ability to track fast-moving objects in high luminance conditions, whereas a lower temporal resolution might be more advantageous for the extrapolation of the direction of motion of

slower objects and for increased temporal integration under low luminance conditions (Donner, 2021; Lappin et al., 2009).

One commonly used method to quantify visual temporal resolution is with the critical flicker fusion (CFF) threshold: the point at which an intermittently flashing light flashes at such high a frequency, that individual flashes can no longer be discriminated and the light appears constant. An individual's CFF threshold is dependent on the physical properties of the stimulus, such as its intensity, wavelength, size and its distance from the observer (Hecht & Shlaer, 1936; Inger et al., 2014; Mankowska et al., 2021). As all visual systems rely on the integration and summation of luminous energy, CFF is applicable and generalizable across species, making it a useful proxy for visual temporal resolution research. Using simple experimental paradigms, CFF thresholds can also be determined in several ways: either behaviourally with trained animals, or electro-physiologically with electroretinograms.

As variation between individuals of the same species is present in many aspects of visual perception, we aimed to evaluate whether this is also the case for critical flicker fusion thresholds, using healthy human participants. CFF has been well studied in humans, and previous research has found that critical flicker fusion thresholds are affected by many physiological factors (Muth et al., 2023). For instance, different parts of our retina have different levels of sensitivity to flicker (Hecht & Verrijp, 1933; Lloyd, 1952). Since flickering visual stimuli are processed by the nervous system, CFF thresholds may also be affected by impaired cerebral functioning (Mackie & Beck, 1965; Mark et al., 1958) and by neurological conditions such as Alzheimer's disease (Curran & Wattis, 2000).

Certain physiological stresses such as exercise or physical exhaustion may directly, but temporarily, affect an individual's CFF threshold (Godefroy et al., 2002; Lambourne et al., 2010; Maciejewska et al., 2020). It has also been suggested that CFF might be used as a measure for cortical arousal and central nervous system activity (Clemente-Suarez, 2017; Davranche & Audiffren, 2004; Fuentes et al., 2018; Parkin et al., 1997). Flicker fusion thresholds may even be affected by an individual's blood oxygen content (Hemelryck et al., 2013). CFF thresholds also tend to be lower in older people than in younger people (Brozek & Keys, 1945; Misiak, 1947; Wilson, 1963).

Due to numerous external and internal factors that may affect CFF measurements, many different methods and techniques have been designed to quantify this trait, making it extremely difficult, if not impossible, to compare study results directly. Some methods, such as the classical psychophysical "method of constant stimuli," require a large number of repetitions of each stimulus to produce an accurate measure of performance, resulting in

extremely long testing times and subsequently introducing fatigue as a possible confounding factor (Eisen-Enosh et al., 2017; Gescheider, 1984).

Additionally, CFF studies often rely on small sample sizes and thresholds are generally only reported as group averages, for example when assessing the effects of sex or age on CFF thresholds (Ginsburg et al., 1982; Misiak, 1947; Regal, 1981). Previous research has also placed considerable focus on how CFF thresholds may be affected by physiological or psychological phenomena, or by pharmacological intervention (Carmel et al., 2007; Hindmarch, 1982; Leigh, 1982; Smith & Misiak, 1976). This research is valuable, but leaves the question of how much natural variation exists in CFF thresholds, and whether varying thresholds represent stable individual traits or more fluctuating variation due to other factors.

In the current study, we hypothesized that a considerable amount of natural individual variation exists in CFF thresholds. Additionally, we hypothesized that CFF thresholds are a stable trait within individuals. Quantitatively these predictions will manifest as larger variation among individuals compared to the variation within individuals. To quantify this, we employed a modified combination of several commonly used testing methods to address several questions:

1. We measured the amount of natural variation in CFF thresholds in a healthy cohort of similar age, in the absence of other stressors.
2. We measured the test-retest stability of CFF thresholds over time in order to quantify within-individual variation.
3. We assessed the level of correlation between the different testing methods, and the robustness of using a testing protocol that drastically decreases testing time by combining several methods.

2.3 Methods

2.3.1 Participants

88 participants (53 female, age range 18-35 years) were recruited from Trinity College Dublin. 47 participants completed the task as part of a larger perception study. 11 of these participants were researchers in the School of Psychology and participated voluntarily. The remaining 36 were compensated with either a 10 Euro gift voucher per hour or by teaching credits forming part of their postgraduate research degree at the rate of 1 credit per half-hour of participation, according to the European Credit Transfer System (ECTS). 41 participants completed only the CFF threshold task associated with this study and participated on a

voluntary basis. All participants provided written, informed consent and all participants had normal or corrected-to-normal visual acuity. The study was approved by the Ethics Committee of Trinity College Dublin's School of Psychology (approval ID SPREC052022-01). Participant recruitment and data collection commenced on 1 August 2022 and ended on 6 July 2023.

2.3.2 Apparatus

We measured critical flicker fusion thresholds using a novel measuring device, consisting of an Arduino Uno R3 microprocessor and a standard 5mm diameter, round-lens 4500K white LED light, housed in a black container. An opaque, black viewing tube and goggles with blacked out frames were mounted on top of the container, to standardize viewing distance at ~16 cm and to eliminate almost all ambient light. Flicker frequency of the LED could be adjusted with a rotary encoder dial that either increased or decreased flicker rate in 1 Hz increments (Fig 2.1)[1]. We measured luminance and colour temperature with a ColorCal Mk II. Mean luminance of the LED was ~255 lux. The device was powered by a personal laptop, using a USBC cable. We measured the power input with a Tektronix TDS 210 oscilloscope to ensure stability. The precision and stability of the LED flash timings were measured using a photometer, both before the start of, and after completion of the study. Participants completed the task while seated, with the box placed in front of them on a desk. Participants were allowed to hold or tilt the box as needed to suit their comfort and to prevent neck- or back strain while operating the device.

[1] Flicker was produced with a square waveform, with equal on-off duty cycle.

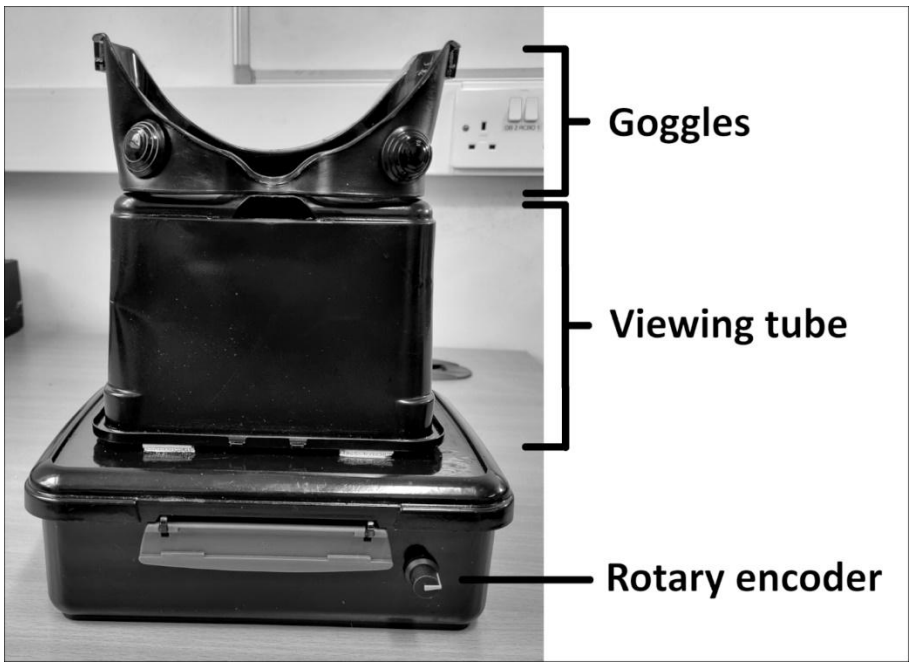

Fig 2.1. CFF measuring apparatus. The LED light and electronic components were housed in an opaque, black box. On top were mounted a viewing tube and goggles with blacked-out frame.

2.3.3 Testing protocol

The experiment was conducted throughout the day, between 9am and 5:30pm. The protocol consisted of a combination of two commonly used psychophysical experimental techniques: the method of limits (MOL) and the method of constant stimuli (MOC). As the method of limits generally produces a fast result, but the method of constant stimuli has a higher level of precision and stability (Eisen-Enosh et al., 2017), we combined the two methods to produce a protocol that took less than 10 minutes to complete. The MOL can be employed in two distinct manners (ascending and descending) and we used both, to give us three different CFF threshold values per participant, per session.

The protocol started with two different measurements of the method of limits: participants observed a constantly lit LED light through the viewing tube and were then instructed to turn the rotary encoder clockwise, to make the light source start flashing. Participants were then asked to keep rotating the dial to increase the flash frequency in 1 Hz increments until flashes could no longer be perceived and the light appeared steady. The frequency at which this occurred was recorded (ascending measurement). The LED light source was then set to a flash frequency of 65 Hz, which a previously conducted pilot study found to be well above the threshold at which participants were generally able to perceive light flashes at the described intensity. This threshold was also consistent with previous findings (Brozek & Keys, 1945;

Eisen-Enosh et al., 2017; Hecht & Shlaer, 1936; Hecht & Verrijp; 1933; Muth et al., 2023). For the second measurement, participants were instructed to observe the light source again, but this time they were asked to turn the dial counter-clockwise to decrease flash frequency, until they first observed flashing. The frequency at which this happened was again recorded (descending measurement). One participant indicated during one session that they were able to perceive flashing at the starting point of 65 Hz. For this session, the starting point was set to 80 Hz instead.

The third step consisted of the method of constant stimuli: for each participant, we took the highest of the two aforementioned recorded thresholds, and created a series of 10 flash frequencies in 1 Hertz steps: 5 frequencies below the recorded threshold, and 4 frequencies above it. Each of the frequencies in the series was then multiplied by 5 to produce a set of 50 stimuli. We then randomized the entire set and presented it to the participant. Participants were then instructed to cycle through all of the 50 frequencies in the series, one by one, using the rotary encoder dial to instantiate the next stimulus in the set. Participants were asked to inform the experimenter for each stimulus whether they observed a steady light or not. The final critical flicker fusion threshold for the individual was determined by calculating the highest frequency in the series at which the user was able to perceive flashing 80% of the time.

2.3.4 Within-individual variation

To investigate the stability of CFF thresholds within individuals, 49 participants completed the task three times, with a minimum of 24 hours between each measurement. Each participant was retested during the same part of the day: either in the morning or in the afternoon.

2.3.5 Statistical analysis

We performed statistical analyses using R version 4.2.1 (R Core Team, 2022) and RStudio version 2023.3.0.386 (Posit Team, 2023). We calculated method of constant stimuli thresholds by creating a binomial generalized linear model for each participant, using the proportion of responses per frequency at which flicker was perceived as response variable and the frequency in Hertz as the explanatory variable. In these models, the range for y was set to 0 – 1, with 0.8 corresponding to an 80% correct score. We therefore calculated the x-value at which y = 0.8 (Fig 2.2). We analysed the between- and within- individual variation with random mixed effects models, using the lme4 package (Bates et al., 2015) and we used Pearson's correlation coefficient to analyse the level of correlation between the three different measurements. Normality of the data was assessed numerically with Shapiro tests and visually with quantile-quantile-plots of model residuals. Quantile-quantile plots were created

using the car package, which contains functions and tools for statistical regression analysis (Fox & Weisberg, 2019).

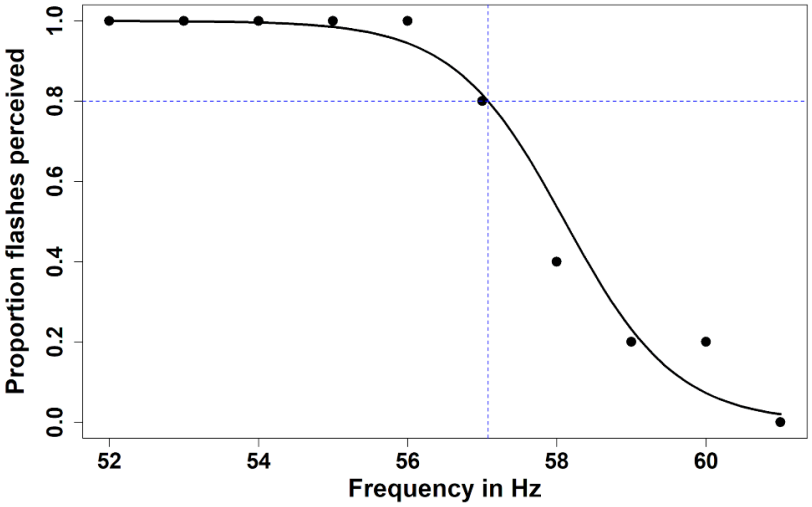

Fig 2.2. Example of CFF-threshold calculation for the method of constant stimuli. We created and plotted binomial models for each participant. The CFF threshold was then calculated for each participant as the x-coordinate at which the proportion of correct responses was equal to 0.8. Shown here as the intersection point of the two dashed blue lines, where y = 0.8 and x = 57.08.

CFF thresholds followed a normal distribution for the method of constant stimuli (P = 0.12) and descending method of limits (P = 0.57), but not for the ascending method of limits (P < 0.05). Visual inspection indicated this was likely due to two extremely low values of 20 and 21 Hz. (Fig 2.3) Quantile-quantile plot indicated a normal distribution otherwise, and Shapiro-Wilks test with the two outliers excluded confirmed normality of the data (P = 0.07). As the two outliers represent natural population variation, they were not excluded from the dataset and parametric analyses were carried out for all three methods.

2.4 Results

2.4.1 Correlation between methods

We obtained three CFF-threshold values for each participant (n = 88): one using the ascending method of limits, one using the descending method of limits and one using a shortened version of the method of constant stimuli. We found a high level of correlation (P<0.001) between all three methods, with Pearson's *r* = 0.93 between MOC and MOL

descending, r = 0.76 between MOC and MOL ascending and r = 0.68 between MOL descending and MOL ascending (Fig 2.3).

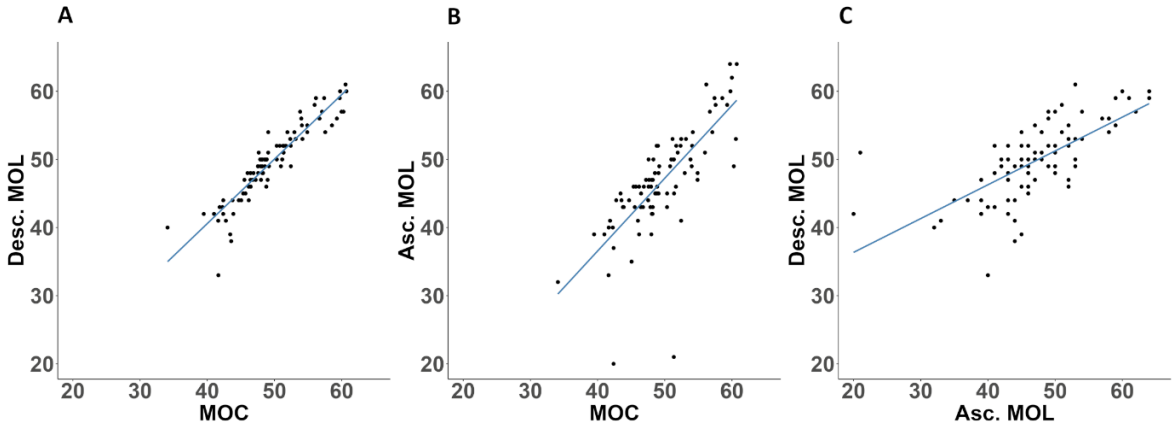

Fig 2.3. Correlation between the different methods. A: correlation between MOC and MOL descending, b: correlation between MOC and MOL ascending, and c: correlation between MOL ascending and MOL descending.

2.4.2 Variation in CFF thresholds

We tested a total of 88 participants and recorded three CFF threshold measurements for each participant. The distribution of CFF values was similar for each method (Fig 2.4). Table 2.1 lists the results for each method used.

Table 2.1. Comparison of the three CFF measuring methods.

Method	Min.	Max.	Mean	SD	Variance	95% PI
MOC	34.09	60.71	49.59	5.41	29.29	± 10.6
Asc. MOL	20	64	46.81	7.63	58.27	± 15
Desc. MOL	33	61	49.66	5.54	30.69	± 10.9

Results of CFF measurement for the method of constant stimuli (MOC), ascending method of limits (Asc. MOL) and descending method of limits (Desc. MOL). Columns indicate method, minimum and maximum measured values, group mean, standard deviation (SD), variance and 95% prediction interval (PI), respectively.

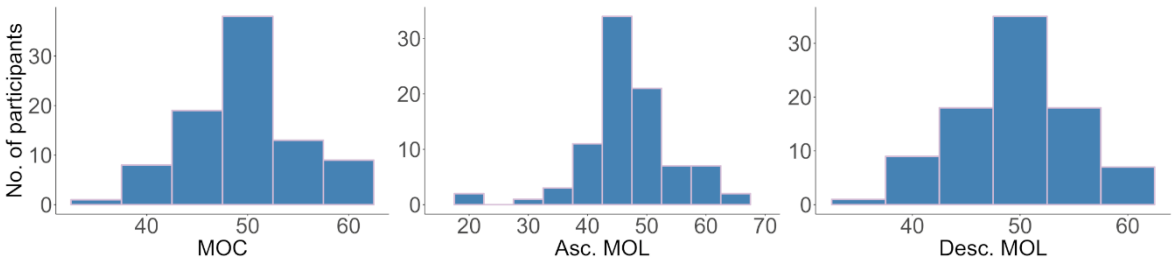

Fig 2.4. Distribution of CFF thresholds for the three different measurements. The method of constant stimuli and descending method of limits both followed a normal distribution (Shapiro-Wilk normality test: P = 0.12 and P = 0.57 respectively). Due to two influential extremely low values, the ascending method of limits does not follow a normal distribution (P < 0.05).

We found no difference in mean CFF-thresholds between males and females for any of the methods (P>0.05) (Fig 2.5).

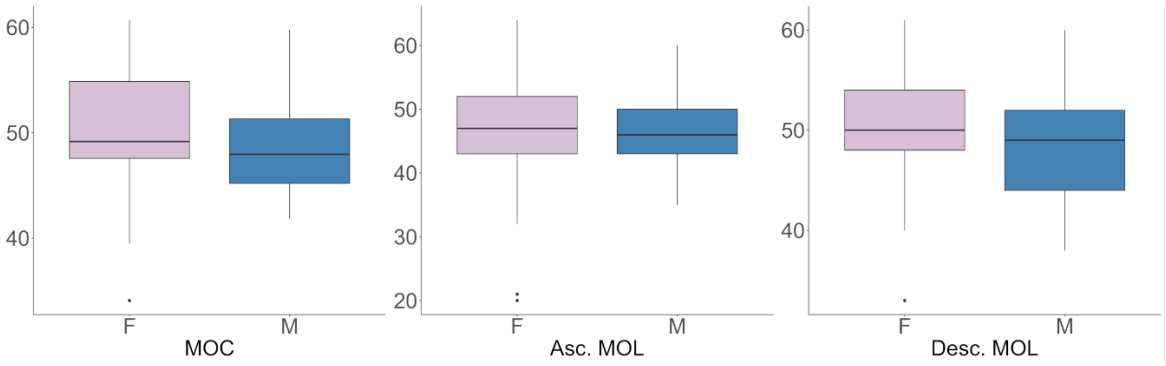

Fig 2.5. Boxplots of CFF-thresholds for each method, separated by sex. T=1.93 for MOC, t=0.54 for Asc. MOL and t=1.96 for Desc. MOL. M = males, F = females.

2.4.3 Test-retest variability

Of the 88 participants, 49 participants completed three sessions of CFF measurements. For each method, all three sessions were highly correlated with each other (Table 2.2). Within- and between individual variation in CFF thresholds for all three methods were analysed using mixed effects models, where the CFF threshold was used as the response variable, session as explanatory variable, sex as a fixed effect and participant as random effect. As we hypothesized that the magnitude of within-participant variation might not be equal between

participants, we performed the analyses using both random intercept and random slope models. The random slopes allow for different rates of change in CFF over the course of the three sessions. We used ANOVA to compare full (random slope and intercept) models against random-intercept-only models and against null models. To investigate possible effects of sex on CFF, best-fitting models were also compared against similar models that did not include the "sex" variable.

Table 2.2. Correlations between each session for each method.

Method	**S1 – S2**		**S1 – S3**		**S2 – S3**	
	R	*P*	*R*	*P*	*R*	*P*
MOC	0.9	<0.001	0.82	<0.001	0.9	<0.001
Asc. MOL	0.61	<0.001	0.43	<0.01	0.82	<0.001
Desc. MOL	0.83	<0.001	0.72	<0.001	0.86	<0.001

The level of correlation is indicated with Pearson's *r,* between session one and two (S1-S2), session one and three (S1-S3) and session two and three (S2-S3).

For all three methods, data was best explained with the inclusion of a random intercept and slope. For all three methods, full models were significantly different from random-intercept-only models and null-models, indicating that CFF thresholds within the same participants differed between sessions (Table 2.2. $P<0.01$ for all methods). Session correlated positively with CFF for all three methods, with 0.89 Hz for MOC, 1.22 Hz for ascending MOL and 1.3 for descending MOL, which accounted for about 10% of the variance for each method. About 80% of the variance in the multiple-measures data was explained by between-participant differences. The remaining 4 - 9% variance can be assumed to be due to within-individual differences (Table 2.3).

Table 2.3. Overall mean CFF, mean CFF difference between sexes and variance distribution for each method.

Method	Mean CFF	Female – male difference in Hz	Between-participant variance	Session variance	Residual variance
MOC	49.88	-2.56	17.20	1.88	1.8
Asc. MOL	46.32	-1.58	56.91	8.43	6.36
Desc. MOL	49.76	-3.03	26.73	3.37	3.17

2.4.4 Sex differences in within-individual variation

For the descending MOL, the model including sex was significantly different from the model where it was not included as a fixed variable ($P<0.05$) and for the MOC the two models were near-significantly different ($P=0.055$). For both models AIC values were lower with sex included as a fixed variable. For the ascending MOL, AIC values were similar and removing the variable "sex" did not have an effect on the model ($P=0.29$). Due to this possible effect of sex on the models, we conducted a post-hoc analysis of the multiple-measures data for each sex separately. We again created random slope fixed effects models with CFF threshold for each method as the response variable, session as explanatory variable, and participant as a random effect. This time, for all three methods, full models were no different from null-models for male participants (n = 20), indicating that for males, CFF-thresholds were relatively stable between sessions ($P=0.38$ for MOC, $P=0.17$ for asc. MOL and $P=0.31$ for desc. MOL). For females (n = 29) however, full models were significantly different from null models for each method ($P<0.001$ for MOC and desc. MOL, and $P<0.05$ for asc. MOL) (Fig 2.6). In males, CFF increased by about 0.4 Hz. between sessions on average, whereas in females it increased by about 1.6 Hz (Table 2.4).

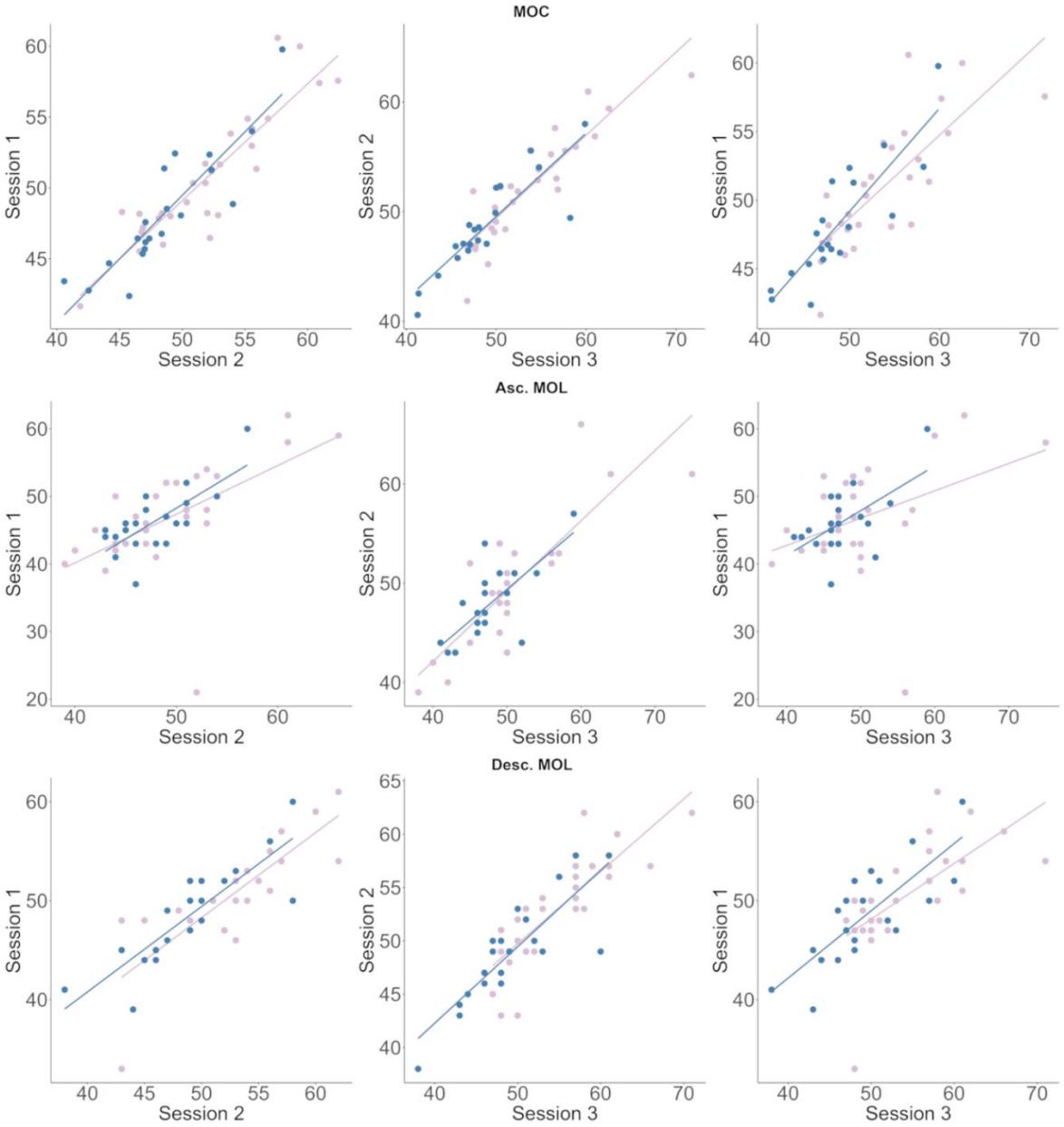

Fig 2.6. CFF test-retest variability for males and females. Correlation plots comparing CFF-thresholds between session one and two, session two and three and session one and three for the method of constant stimuli (top row), the ascending method of limits (middle row) and the descending method of limits (bottom row). Male CFF displayed in blue, female CFF displayed in purple.

Table 2.4. Model summaries of multiple-measures CFF per method for each sex.

Method	Mean CFF	Difference between sessions in Hz	Between-participant variance	Session variance	Residual variance
Male MOC	48.02	0.24	13.55	0.45	2.08
Male asc. MOL	45.93	0.63	22.67	1.78	4.23
Male desc. MOL	48.12	0.4	20.06	1.39	3.35
Female MOC	49.4	1.34	19.16	2.37	1.6
Female asc. MOL	45.49	1.64	78.86	12.6	7.83
Female desc. MOL	48.81	1.91	29.08	3.79	3.04

2.5 Discussion

With our current study, we have validated a quick, low-cost and portable method to test CFF thresholds. Results from all three methods followed a similar range and standard deviation (Table 2.1). The CFF threshold range discovered for the method of constant stimuli is also in agreement with the one found in Eisen-Enosh et al. (2017). Similar to our results, Eisen-Enosh et al. also reported a slightly lower test-retest repeatability for the method of limits than for the method of constant stimuli. This, according to our findings, may in most part be due to the ascending part of the measurement. Our results indicate that a shortened version of the method of constant stimuli can still provide an accurate result, while greatly reducing testing time. The ascending method of limits may be slightly more prone to extreme results. It is common in psychophysical paradigms to calculate a mean threshold from only an ascending- and a descending method of limits measurement (De Asís Fernández et al., 2019; Eisen-Enosh et al. 2017; Ginsburg et al., 1982), which may skew the results and may not represent an individual's true CFF threshold if one of the values turns out to be an outlier. CFF thresholds may potentially be made more robust by adding the shortened version of the method of constant stimuli.

Much of the existing literature relating to CFF compare measured thresholds to other physical and/or psychophysical attributes. Our study placed focus on variation in CFF thresholds both within- and between individuals of similar age. With this study, we have shown that there are considerable individual differences in CFF thresholds and that CFF is relatively stable over time. We found no significant difference in mean CFF thresholds between males and females,

which is in agreement with previous findings (Kaur et al., 2020; Liu et al., 2015; Misiak, 1947; Wilson, 1963). However, the results from our post-hoc analysis do show a clear difference between sexes in the test-retest repeatability of CFF. This could be an indication that CFF might be more stable in males than in females, but replication studies are needed to further explore this possibility.

As all participants in our study were within a small age range, had normal or corrected-to-normal visual acuity and all declared to be in general good health, the observed variation in CFF thresholds cannot be explained by variation in these factors. However, visual perception involves many physiological and psychological processes. It is therefore difficult to determine from where this variation might arise. For example, at the physical level, differences in the anatomy of the primary visual cortex can affect the processing of visual information (Himmelberg et al., 2022). At the higher level of psychological processing, the formation of a percept and subsequently, the generation of a decision about that percept, also influence whether an individual determines they are perceiving a stimulus as constant or not-constant. Additionally, natural variation in brain wave oscillations may result in a difference in visual integration window sizes in different individuals (Samaha & Postle, 2015).

The magnitude of the variation in CFF we found between individuals is quite large, and we calculated a prediction interval of roughly 21 Hz (± 10.6 Hz from the calculated mean). This amount of variation is comparable with the variation reported among closely related species that occupy different ecological niches, such as having habitats with different luminance levels (Jenssen & Swenson, 1974; McComb et al., 2010) or having a preference for faster or slower moving prey (Potier et al., 2020). This suggests that the spread of CFF thresholds in humans is in a range that could have important effects on function. It would therefore be interesting to explore how individual variation in visual temporal resolution in humans may translate to perception and behaviour in real-world scenarios, especially those requiring high-speed perception and action, such as athletic performance or competitive gaming.

Chapter 3

Individual peak alpha frequency correlates with visual temporal resolution, but only under specific task conditions

---

Author contributions

I co-conceived the idea, collected and analysed the data and wrote the manuscript. Redmond O'Connell, Kevin Mitchell and Andrew Jackson all contributed to the conception of the idea, secured funding and contributed to the analysis of the data and writing of the manuscript. Redmond O'Connell provided access to electroencephalogram testing facilities.

Status

This chapter has been published as:

Haarlem, C. S., Mitchell, K. J., Jackson, A. L., & Connell, R. G. O. (2024). Individual peak alpha frequency correlates with visual temporal resolution, but only under specific task conditions. *European Journal of Neuroscience*, *August*, 1–14.

3.1 Abstract

The study of alpha band oscillations in the brain is a popular topic in cognitive neuroscience. A fair amount of research in recent years has focused on the potential role these oscillations may play in the discrete sampling of continuous sensory information. In particular, the question of whether or not peak frequency in the alpha band is linked with the temporal resolution of visual perception is a topic of ongoing debate. Some studies have reported a correlation between the two, whereas others were unable to observe a link. It is unclear whether these conflicting findings are due to differing methodologies and/or low statistical power, or due to the absence of a true relationship. Replication studies are needed to gain better insight into this matter. In the current study, we replicated an experiment published in a 2015 paper by Samaha & Postle. Additionally, we expanded on this study by adding an extra behavioural task, the critical flicker fusion task, to investigate if any links with peak alpha frequency are generalizable across multiple measures for visual temporal resolution. We succeeded in replicating some, but not all of Samaha & Postle's findings. Our partial replication suggests that there may be a link between visual temporal resolution and peak alpha frequency. However, this relationship may be very small and only apparent for specific stimulus parameters. The correlations found in our study did not generalize to other behavioural measures for visual temporal resolution.

3.2 Introduction

The question of whether perception is discrete, continuous or a combination of both has been a subject of ongoing debate in the fields of sensory neuroscience, psychology and philosophy for many years (VanRullen & Koch, 2003; Herzog et al., 2016; Ruzzoli et al., 2019). Many different "flash fusion" paradigms have been developed based on the notion that our sensory system may sample information in discrete time windows: if two sensory stimuli, usually visual and/or auditory, are quickly flashed within the same time window, they are fused to form a single percept. If one of the stimuli falls outside of the window, they are segregated and two separate percepts are formed.

The rhythmic nature of brain activity is often proposed as a possible mechanism to support the idea of discrete sampling and is theorized to be a driving factor behind the integration and segregation of sensory information (Schroeder & Lakatos, 2009; Keitel et al., 2022; VanRullen & Koch, 2003). More specifically, the phase and frequency of neural oscillations are thought to determine the size of the temporal sampling window.

Neural oscillations are generally grouped into five distinct bands: delta (1 – 4 Hertz), theta (5 – 8 Hertz), alpha (8 – 13 Hertz), beta (13 – 30 Hertz) and gamma (30+ Hertz) (Başar et al., 2001; Ward, 2003; Keil & Senkowski, 2018). As alpha band oscillations are the dominant oscillations in the brain, they have been studied extensively and have been found to be affected by the activity of the visual system in multiple ways, with one of the most basic findings being that alpha power is high when eyes are closed, but suppressed when eyes are open (Adrian & Matthews, 1934; Klimesch, 2012). One popular theory is that alpha-band oscillations may play a role in the modulation of visual stimulus detection (Ergenoglu et al., 2004; Hanslmayr et al., 2005; Morrow & Samaha, 2022; Mathewson et al., 2009). Some studies have found that the phase and frequency of alpha oscillations may affect whether or not a near-threshold stimulus is perceived, with higher frequency alpha oscillations being correlated with a more finely tuned capacity to segregate visual asynchronous stimuli (Busch et al., 2009; Mathewson et al., 2009; Samaha & Postle, 2015). Other studies however, failed to replicate this effect (Buergers & Noppeney, 2022; Ruzzoli et al., 2019). It is unclear whether this failure to replicate is due to the absence of a true relationship or because the previously mentioned studies all differed in their task paradigms and analysis methods. As pointed out by Keitel et al. (2022), the lack of direct replications is one of the main issues this field suffers from, along with small effect sizes and low statistical power.

To address this issue, we carried out a replication of a visual perception experiment conducted by Samaha & Postle in 2015. In this experiment, a two-flash fusion task was used to investigate how alpha-band oscillations may affect the perception of near-threshold visual stimuli. The study found that both pre-stimulus and eyes-closed peak alpha frequency correlated with flash-fusion thresholds between subjects. Moreover, the study found that within subjects, instantaneous peak alpha was correlated with perceptual accuracy.

Samaha & Postle's 2015 study design is perfectly suited for a replication study for several reasons: first, the task itself is both easy to reproduce and easy to understand for participants. Second, the use of a stimulus with multiple gap lengths allows for the construction of psychometric functions similar to those of other measures for visual temporal resolution, making the results of different paradigms comparable. Third, Samaha & Postle's study design facilitates the exploration of possible correlations between temporal resolution and multiple aspects of peak alpha frequency: both at rest and during task performance, and both between- and within individuals. Lastly, the results of the original study reported a relatively large effect size. As the potential link between temporal resolution and brain rhythmicity has proven to be controversial in the field, it can be beneficial to conduct replications of studies that have observed large effects.

In the current study, we employed the two-alternative-forced choice gap detection task (hereafter: flash-fusion task) used by Samaha & Postle with a larger sample size, and carried out similar electroencephalogram (EEG) data analyses to compare flash-fusion thresholds in relation with peak alpha frequency for resting-state and pre-stimulus scenarios. We also replicated within-participant analyses to investigate potential correlations between instantaneous alpha frequency and perceptual accuracy, using methods developed by Cohen (2014).

Additionally, we hypothesized that, if natural variation in peak alpha frequency is indeed indicative of an individual's visual temporal resolution, it should correlate with different behavioural measures of visual perception speed. We therefore expanded the original study by also including a second visual perception speed task: the critical flicker fusion threshold task (hereafter: CFF task), which utilizes a continuously flickering stimulus to estimate individual temporal resolution thresholds.

3.3 Methods

3.3.1 Sample size and effect size analysis

To calculate the necessary minimum sample size for our replication, we used the effect sizes of the two main findings of the original study. Samaha & Postle reported an effect size of r = -0.503 for the observed correlation between eyes-closed data and peak alpha frequency, and r = -0.605 for the observed correlation between pre-stimulus data and peak alpha frequency. We aimed to have a statistical power of at least 90% (beta = 0.9). As our aim was to replicate the finding that higher peak alpha frequency is correlated with a lower flash-fusion threshold, we employed a one-sided hypothesis approach and a significance level of 5% (alpha = 0.05). We calculated the minimum sample size necessary for replication using the R package "pwr" (Champely, 2020). The results of the calculations suggested a minimum sample size of 31 participants for the eyes-closed data, and 20 participants for the pre-stimulus data.

3.3.2 Participants

We recruited 32 participants (17 female, age range 18 – 35 years) from Trinity College Dublin. All participants provided written, informed consent and all participants had normal or corrected-to-normal visual acuity. Participants were compensated for participating with either a € 10,- gift voucher per hour or with teaching credits forming part of their postgraduate research degree worth 1 ECTS per half hour of participation. The study was approved by the Ethics Committee of Trinity College Dublin's School of Psychology (approval

ID SPREC052022-01). One participant was excluded from analysis due to near chance performance on the flash-fusion task at all stimulus levels. Two participants showed no alpha-band peak in pre-stimulus EEG recordings and were excluded only from the pre-stimulus analyses.

3.3.3 Computerized flash-fusion task

We modelled the flash-fusion task after the one used in Samaha & Postle and followed a similar protocol (Fig 3.1). Participants were seated ~60 centimetres (cm) away from a computer monitor with a 100 Hertz (Hz) refresh rate. The task consisted of white disk stimuli appearing against a black background. Each trial started with a white fixation cross in the middle of the screen, at 0.98 degrees visual angle. The fixation cross reduced in luminance before stimulus onset to prepare participants. The duration of this period was drawn from a uniform distribution between 1000 and 1500 milliseconds (ms). The fixation cross remained present for the duration of the trial. Disk stimuli, at 1.23 degrees visual angle, were presented either to the left or to the right side, at 2.45 degrees visual angle (0.20 candela per square meter) of the fixation cross, with equal probability. Fifty percent of the trials were two-flash trials, in which a disk appeared for 40 ms, then disappeared for either 10, 20, 30, 40 or 50 ms, and then reappeared for 40 ms. The other fifty percent were one-flash trials, in which a disk appeared for durations that varied to match the stimulus onset to stimulus offset lengths for each stimulus type of the two-flash trials. 800 ms after stimulus offset the fixation cross increased in luminance to prompt participants to make a response. Participants held a mouse in both hands during the task and responded by clicking the left button with their left thumb to indicate when they perceived a single flash trial, or by clicking the right button with their right thumb to indicate when they perceived a two-flash trial. The next trial did not start until a response had been made and participants were instructed to focus on accuracy over speed. Participants completed 20 practice trials, followed by 600 test trials divided into 6 blocks. Each of the five inter-stimulus intervals thus appeared 120 times during test trials, with 60 trials being two-flash stimuli and 60 trials being one-flash stimuli. Participants took self-paced breaks in between each block.

Our task design deviated from Samaha & Postle's design in three minor ways: due to the physical set-up of equipment in our lab, participants were seated at ~60 cm away from the monitor, whereas in the original design this was ~70 cm. Because the original task design did not specify any specific colour values for the stimulus disks, or the amount with which fixation luminance decreased before stimulus onset, we were unable to replicate these variables exactly. We therefore opted to use white stimulus disks to optimize contrast, and we decreased the luminance of the fixation cross by 40% before stimulus onset.

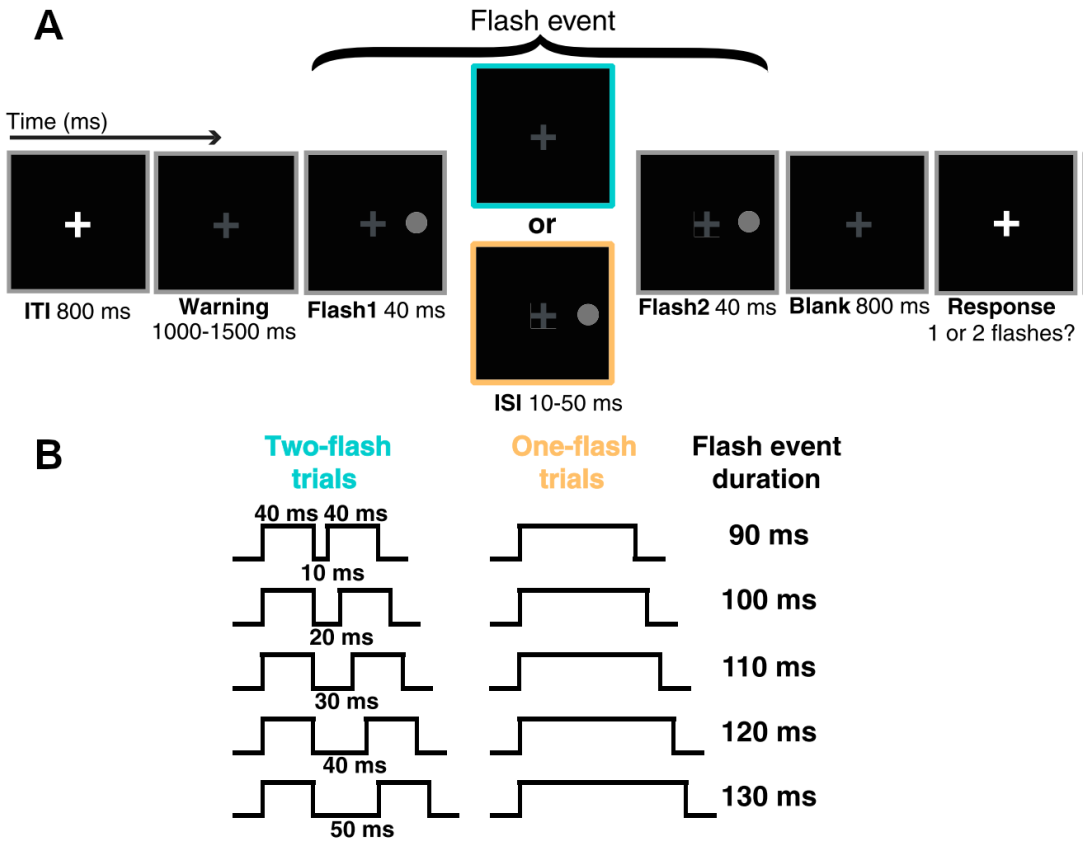

Figure 3.1. Task set-up and stimulus conditions. Reproduced from Samaha & Postle (2015). The image presented here has been altered from the original by removing a "confidence" step at the end of each trial, which was not analysed in the original study and therefore is not included here.

A: Depiction of a trial. The start of a trial was indicated with a white fixation cross, which reduced in luminance to prompt for an upcoming stimulus. Stimulus consisted of a single flash event in half of the trials and a double flash event in the other half. Flash events were presented either to the left or to the right of the fixation cross with equal probability.

B: Double flash events consisted of a white stimulus disk appearing for 40 ms, followed by a gap of 10 – 50 ms, after which the stimulus disk reappeared for another 40 ms. Lengths of single flash events were varied to match the duration of the double flash events.

3.3.4 Psychometric functions

We used the results from the flash-fusion task to create a psychometric function for each participant, using the Palamedes toolbox (Prins, N. & Kingdom, F.A.A., 2018) for MATLAB (The Mathworks Inc., 2022). Following the methods used in Samaha & Postle (2015), we employed a logistic function with four parameters: "guess rate," "threshold," "slope" and "lapse rate" to estimate the correct response rate for the different stimulus conditions. Guess rate was fixed

at 0.5. The other three parameters were estimated for each participant. Lapse rate was set to the limits of 0 – 0.06. We used goodness-of-fit testing to compare the deviance of the fit to the real data with deviance of the fit to 1,000 simulated datasets for each participant. No participant's fit exceeded the 95th percentile, indicating that all created psychometric functions fell within the expected range for the type of data and no function was deemed an outlier.

3.3.5 CFF threshold measurement

We measured critical flicker fusion thresholds using a novel measuring device and custom methods, the accuracy and robustness of which were validated in a separate, parallel study (Chapter 2, published as Haarlem et al., 2024b). The protocol for measuring CFF thresholds outlined below are reproduced from that study's methods section. All CFF thresholds measured in the current study were also included in the dataset used in Haarlem et al. (2024b).

The device consisted of an Arduino Uno R3 microprocessor and a 4500K white light-emitting diode (LED), housed in a black container. An opaque, black viewing tube was mounted on top of the container, to standardize viewing distance at ~16 cm and to eliminate almost all ambient light. Flicker frequency of the LED could be adjusted with a rotary encoder dial that either increased or decreased flicker rate in 1 Hz increments. We measured luminance and colour temperature with a ColorCal Mk II. Mean luminance of the LED was ~255 lux. The device was powered by a personal laptop, using a USBC cable. We measured the power input with a Tektronix TDS 210 oscilloscope to ensure stability. The precision and stability of the LED flash timings were measured using a photometer, both before the start of, and after completion of the study.

The protocol consisted of a measurement of 3 different quantifications of a participant's ability to perceive flashes and was based on a combination of two commonly used psychophysical experimental techniques: the method of limits and the method of constant stimuli. The protocol started with the method of limits: participants observed a constantly lit LED light through the viewing tube and were then instructed to turn the rotary encoder clockwise, to make the light source start flashing. Participants were then asked to keep rotating the dial to increase the flash frequency in 1 Hz increments until flashes could no longer be perceived and the light appeared steady. The frequency at which this occurred was recorded. The LED light source was then set to a flash frequency of 65 Hz, which is above the threshold at which humans are able to perceive light flashes at the described intensity. For the second measurement, participants were instructed to observe the light source again, but this

time they were asked to turn the dial counter-clockwise to decrease flash frequency, until they first observed flashing. The frequency at which this happened was again recorded.

The third step consisted of the method of constant stimuli: for each participant, we took the highest value measured with the method of limits, and created a series of 10 flash frequencies in 1 Hertz steps: 5 frequencies below the recorded threshold, and 4 frequencies above it. Each of the frequencies in the series was then multiplied by 5 to produce a set of 50 stimuli. We then randomized the entire set and presented it to the participant. Participants were then instructed to cycle through all of the 50 frequencies in the series, one by one, using the rotary encoder dial to instantiate the next stimulus in the set. Participants were asked to inform the experimenter for each stimulus whether they observed a steady light or not. The final critical flicker fusion threshold for the individual was determined by calculating the highest frequency in the series at which the user was able to perceive flashing 80% of the time.

Participants completed the CFF task roughly 30 minutes prior to the first eyes-closed EEG recording.

3.3.6 EEG-recording and processing

We recorded EEG from 128 scalp electrodes, using the Active Two Biosemi system, arranged according to the 10-5 system (Oostenveld & Praamstra, 2001). We recorded electrooculogram vertically, with one electrode just above the eyebrow and one approximately 3 cm below the eye. EEG was recorded with a sampling rate of 512 Hz.

We recorded eyes-closed resting state EEG for two minutes before participants started the computerized perceptual task, and again for two minutes after participants completed the task. Participants were asked to relax and sit still during this period. The four minutes of eyes-closed EEG recordings were then cut into 1-second, non-overlapping epochs for analysis. Epoched data was then detrended and we used spherical-spline interpolation to interpolate an average of 2.9% of electrodes due to high noise levels.

Pre-stimulus-EEG data was recorded during task performance and was epoched from -700 – 0 ms relative to stimulus onset. Epoched pre-stimulus data was then detrended and an average of 3.4% of electrodes was interpolated.

We used Matlab (Mathworks, 2022) for the pre-processing of all EEG-recordings, using custom Matlab scripts. Current source density (CSD) transformation is used in many EEG studies in order to reduce volume conduction effects and signal mixing (Kayser & Tenke, 2006; 2015). This step was not carried out in Samaha & Postle's original study. We therefore opted to analyse the data both with- and without applying CSD transformation in order to determine its impact.

For the CSD-transformed eyes-closed EEG data, we rejected epochs when voltages exceeded a CSD-transformed amplitude threshold of 500 microvolts per square meter ($\mu V\ m^2$) for both scalp and eye electrodes. An average of 47 (standard deviation (SD) 53.5) epochs were rejected per participant. For CSD-transformed pre-stimulus EEG data, we rejected epochs when voltages exceeded a threshold of 500 $\mu V\ m^2$ for scalp electrodes or 100 μV for eye electrodes (eye electrodes were not included in the CSD-transformation and therefore required a lower threshold). We rejected an average of 125 (SD 108.2) epochs per participant.

For the non-CSD-transformed eyes-closed EEG-data, we rejected epochs when voltages exceeded a threshold of 100 μV for scalp electrodes and 500 μV for eye electrodes. We rejected an average of 32 (SD 28) eyes-closed EEG-data epochs per participant. For non-CSD-transformed pre-stimulus EEG-data, we rejected epochs when voltages exceeded 100 μV for all electrodes. We rejected an average of 52 (SD 58.8) epochs of pre-stimulus EEG-data per participant.

Epochs were then multiplied by a hamming window and fast Fourier transformed with a frequency resolution of 0.1 Hz. Individual alpha peak frequency was defined as in Samaha & Postle and was extracted from the highest amplitude in the power spectrum within the frequency range 8 – 13 Hz. All participants showed a clear peak within this range at all scalp electrodes for eyes-closed data. Similar to the original study, not all electrodes showed a peak in the 8 – 13 Hz frequency range and no electrode showed a peak for all participants for pre-stimulus data. We therefore followed the original methodology and chose whichever electrode had the highest power amplitude within the alpha band range for each participant.

Because it has been shown that peak alpha frequency can change over time within an individual (Cohen, 2014), we computed instantaneous alpha to assess if pre-stimulus alpha frequency is higher prior to correct task responses compared to incorrect responses. Instantaneous alpha corresponds to the first temporal derivative of the phase angle time series. To calculate instantaneous alpha, we replicated Samaha & Postle's method, and chose the electrode that had the highest amplitude in the alpha band range for the pre-stimulus recordings at the group level, which we interpreted as the electrode that had the highest alpha amplitude for most participants: electrode Fp2. Following our same reasoning as with the previous analysis, we again also computed instantaneous alpha frequency for electrode PO8. We epoched the pre-stimulus EEG-recordings from -700 to 0 ms relative to stimulus onset, and then copied, flipped and appended each epoch to avoid edge artifacts. Using code developed by Cohen (2014), we then defined frequency boundaries of 8 – 13 Hertz, and applied a zero-phase bandpass filter with 15% transition zones. We extracted the analytic signal with a Hilbert transform and median filtered using default parameters set by Cohen: we applied the median filter ten times with different window sizes ranging from 10 to 400

ms, in steps of 10 ms. As Samaha & Postle only reported instantaneous frequency for the 500 ms prior to stimulus onset, we followed their method and only calculated instantaneous alpha for the timepoints ranging from -500 – 0 ms.

3.3.7 Statistical analysis

We used R (version 4.2.1; R Core Team 2022) and RStudio (version 2023.3.0.386; Posit Team 2023) to carry out the statistical analysis. All data was checked for the presence of significant outliers and we used linear models to assess linearity, distribution of residuals and homogeneity of variance. Unless otherwise stated, no statistically significant outliers were detected and all data met assumptions of linearity, homogeneity of variance and normal distribution of residuals, and two-tailed correlations were tested with Pearson's correlation coefficient (see Appendix A for full results of linear modelling). We used cluster-based permutation testing for the analysis of within-participant variation in peak alpha frequency (instantaneous alpha), using the "permutes" (Voeten, 2022) and "permuco" (Frossard, 2021) packages. 5000 permutations of randomly shuffled data were used to create a distribution of cluster sizes expected under the null- hypothesis. Clusters of real data that exceeded the 95th percentile of this null distribution were deemed statistically significant.

As an additional check for correlation robustness, we also carried out post-hoc correlation analyses for the main findings with the Matlab toolbox "Robust correlation" (Pernet et al., 2013). This toolbox calculates several alternative correlation methods, one of which being the "skipped-correlation," which protects against bivariate outliers by taking into account the structure of the data (Rousseeuw, 1984; Rousseeuw & Van Driessen, 1999; Verboven & Hubert, 2005). For the main findings, we reported the results from both correlation analysis methods. Note that the skipped-correlation method does not produce P-values, but calculates significance by thresholding T-values instead. Unless otherwise stated, we reported Pearson's r, and significance of the skipped-correlation method matches that of the results obtained in our R analysis.

3.4 Results

For all participants, alpha power was highest at occipital and parietal electrodes, both for the eyes-closed and pre-stimulus EEG data. Alpha power for pre-stimulus EEG-recording was substantially reduced compared to eyes-closed EEG recording (Fig 3.2).

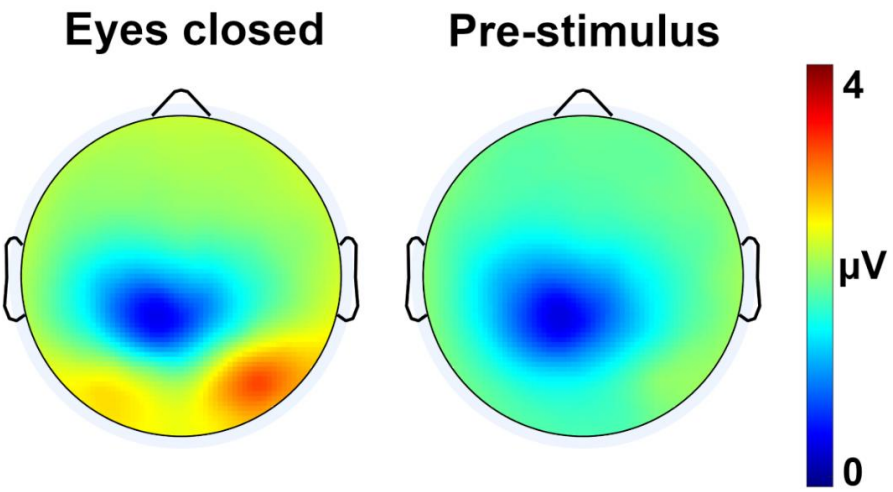

Figure 3.2. Topography of resting state alpha band (8 – 13 Hz) power, recorded from 128-electrode EEG. The topographies display data averaged over all participants. Alpha band power was highest in the occipital region for both eyes-closed EEG recording (left) and pre-stimulus EEG recording (right).

3.4.1 Effect of Current Source Density (CSD)-transforming on peak alpha frequency

We extracted peak alpha frequencies from the dataset both after applying CSD-transformation during EEG pre-processing and without applying CSD-transformation (see Methods). For resting state data, the two versions of the dataset were highly correlated ($r = 0.96$, $df = 29$, $P < 0.001$) and the mean difference between the two was 0.07 Hz ($t = 1.9$, $df = 30$, $P = 0.064$). Pre-stimulus CSD transformed data was also highly correlated with its non-CSD transformed counterpart ($r = 0.62$, $df = 28$, $P < 0.001$). The mean difference between these versions was 0.27 Hz. Though the two datasets did not differ from each other significantly ($t = 1.96$, $df = 29$, $P = 0.06$), a difference of 0.27 Hz in the alpha band range could potentially be meaningful. We therefore conducted all further correlation tests with both the CSD transformed and the non-CSD transformed versions of the data. Unless otherwise stated, we found no difference between the two versions of the data and only reported results from the non-CSD transformed dataset.

3.4.2 Flash fusion task

Psychometric functions

We fitted a psychometric function based on each participant's accuracy in the flash-fusion task (Fig 3.3) and calculated flash-fusion thresholds, defined as the interstimulus-interval at which accuracy is 75%.

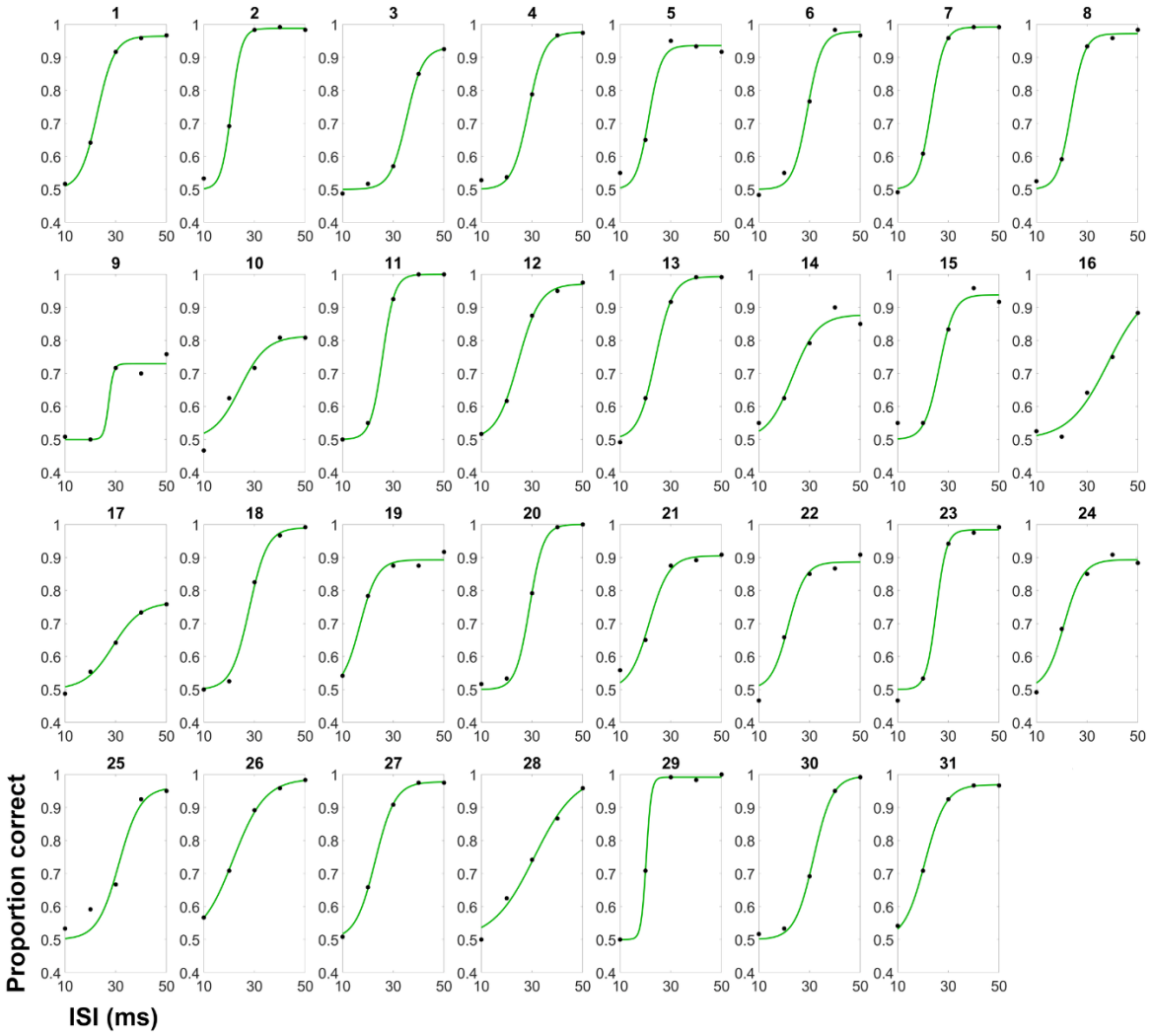

Figure 3.3. Psychometric functions fitted for each participant. Flash-fusion threshold corresponds to the inter-stimulus interval at which the participant performed with 75% accuracy.

Eyes-closed EEG analysis

Eyes-closed EEG data consisted of a 2-minute pre-task and a 2-minute post-task recording, which were highly correlated with each other ($r = 0.91$, 29 degrees of freedom (df), $P < 0.001$). Pre- and post-task recordings were therefore analysed as one dataset for each participant. We detected a moderate correlation in the expected direction between eyes-closed peak alpha frequency and flash-fusion thresholds (Fig 3.4, left) with both the Pearson correlation analysis method in R ($r = -0.43$, $df = 29$, $P = 0.016$) and the skipped-correlation

method in Matlab (r = -0.43, correlation coefficient confidence interval (CI) = [-0.685, -0.021], one outlier detected). We found no correlation between eyes-closed alpha power and flash-fusion thresholds with either analysis method (R analysis: r = 0.14, P = 0.438; skipped-correlation analysis: r = 0.240893, CI = [-0.11, 0.614], no outliers detected).

Pre-stimulus EEG analysis

Following the original study's protocol for pre-stimulus data, we calculated peak alpha frequency from the electrode that showed the highest amplitude in the alpha band range for each participant. We detected no significant correlations between peak alpha frequency and flash-fusion thresholds with the R analysis (r = -0.29, df = 28, P = 0.124) (Fig 3.4, middle) or the post-hoc skipped-correlation analysis (r = -0.2, CI = [-0.571, 0.292], no outliers detected). Pre-stimulus peak alpha power and flash-fusion thresholds were also not correlated (R analysis: r = 0.18, df = 29, P = 0.336; skipped-correlation analysis: r = 0.179416 CI = [-0.149, 0.489], one outlier detected).

Having initially failed to replicate Samaha & Postle's original result with the pre-stimulus dataset, we included a second analysis, post-hoc. Previous findings (Pfurtscheller et al., 1996; Busch et al., 2009; Ruzzoli et al., 2019) have indicated that high alpha power may be indicative of suboptimal performance or the absence of sensory processing, and a suppressed alpha power may be indicative of focused attention. Therefore, selecting the electrodes with highest amplitudes during task performance to extract peak alpha frequency may not be the most informative for pre-stimulus data. For our second analysis, we thus selected the electrode that had the highest amplitude in the alpha band in the *eyes-closed* data instead of the pre-stimulus data and used this same electrode to analyse peak alpha frequency in the pre-stimulus data. The electrode with the highest amplitude in the alpha-band for most participants was electrode PO8, located in the occipital region (Fig 3.5). The location of this electrode was close to the location of the electrode identified as having the highest power at the group level in Samaha & Postle's study (electrode O2). Two participants did not show a peak in the alpha band in pre-stimulus recordings for electrode PO8 and we therefore excluded these participants from the respective analyses. This time, we found a moderate correlation between flash-fusion thresholds and pre-stimulus peak alpha frequency (n = 29, df = 27, r = -0.42, P = 0.023, no outliers detected) (Fig 3.4, right). With our post-hoc skipped-correlation analysis, we found a correlation of a similar strength. However, using this method, the correlation was deemed not significant (r = 0.4, CI = [-0.693, 0.015], one outlier detected).

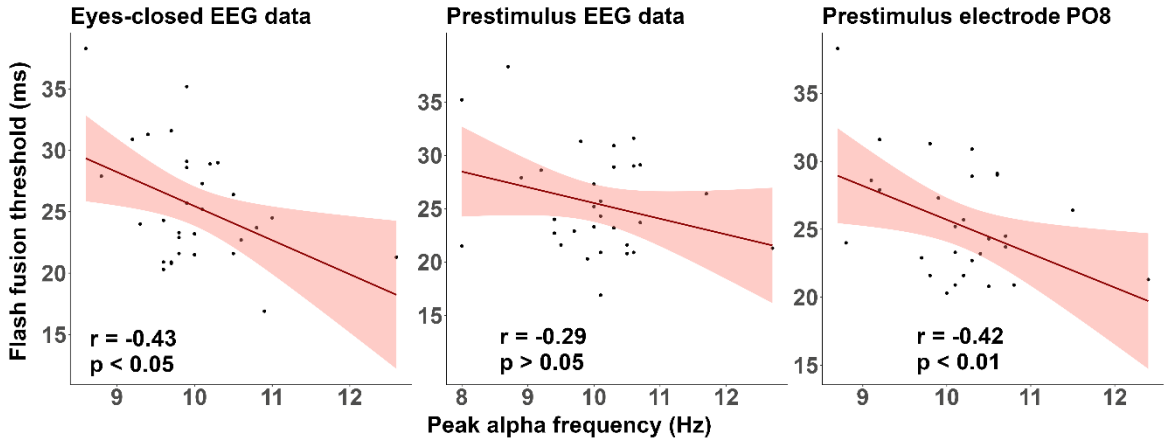

Figure 3.4. Correlations between flash fusion thresholds and peak alpha frequency. Left: we found a moderate correlation between flash fusion threshold and peak alpha frequency extracted from resting state EEG-recording. Middle: Peak alpha frequency extracted from the electrode that has the highest amplitude in the alpha band for pre-stimulus EEG-recording was not correlated with flash fusion thresholds. We found a moderate correlation between flash fusion threshold and peak alpha frequency extracted from electrode PO8 for pe-stimulus EEG-recording.

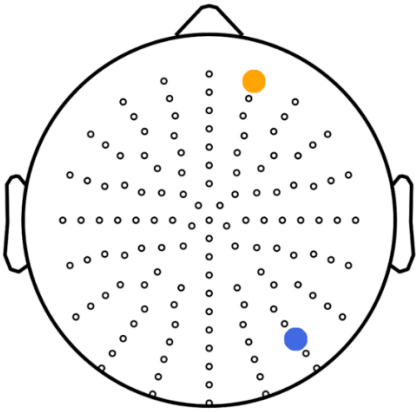

Figure 3.5. Electrode distribution. Topography shows the distribution and location of electrodes, arranged according to the 10-5 system. The two electrodes used for group level analyses are marked in blue (electrode PO8) and orange (electrode Fp2).

Intermediate stimulus comparisons

To ensure that the found correlation was not an artifact of the extracted thresholds, Samaha & Postle also conducted tests with the proportion of correct responses on the intermediate stimulus. The intermediate stimulus is defined as the median in the series of the tested stimuli with onset asynchronies of 10, 20, 30, 40 and 50 ms (i.e. the 30 ms stimulus). We replicated this analysis, and found a moderate correlation between the proportion correct and peak alpha frequency from eyes-closed EEG-recording (r = 0.33, df = 29, P = 0.035, one-

tailed). This correlation was not significant with the skipped-correlation analysis method (r = 0.27, CI = [-0.031, 0.535], one outlier detected). We found no statistically significant correlation between the proportion of correct responses and pre-stimulus peak alpha frequency, neither for the original method (R analysis: r = 0.28, df = 28, P = 0.07; skipped-correlation analysis: r = 0.06, CI = [-0.309, 0.382], three outliers detected) nor for peak alpha frequency extracted from electrode PO8 (R analysis: r = 0.28, df = 27, P = 0.07, one-tailed; skipped-correlation analysis: r = 0.06, CI = [-0.228, 0.343], two outliers detected).

Instantaneous alpha

We extracted instantaneous alpha, according to Cohen's method, as a within-participant measure for time resolved changes in peak alpha frequency between trials. We computed instantaneous alpha for the electrode used in the previous analysis, PO8 and, following the protocol of the original study, also for electrode Fp2, which had the highest amplitude in the alpha band for most participants in the pre-stimulus EEG data (see Fig 3.5 for the location of the electrode). We then compared pre-stimulus instantaneous alpha frequency between correct and incorrect responses. The mean instantaneous alpha extracted from electrode PO8 was 10.361 Hz (SD = 0.023) for correct responses and 10.363 Hz (SD = 0.025) for incorrect responses. For electrode Fp2, mean instantaneous alpha frequency for correct answers was 10.318 Hz (SD = 0.039). For incorrect answers it was 10.326 Hz (SD = 0.026). Cluster-based permutation testing revealed no time clusters with a statistically significant difference in instantaneous alpha between correct and incorrect answers for either electrode (Fig 3.6).

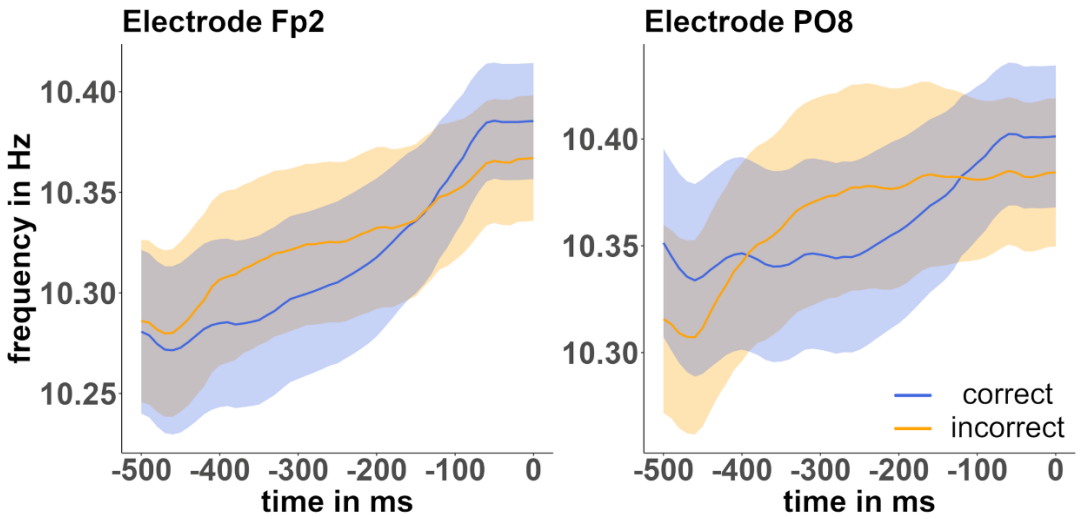

Figure 3.6. Within subject analysis of instantaneous alpha for correct (blue) versus incorrect (orange) responses. Left: instantaneous alpha extracted from electrode Fp2. Right: instantaneous alpha extracted from electrode PO8. Shaded regions indicate ± standard error of the mean.

3.4.3 CFF task

Eyes-closed EEG analysis

Participants completed the CFF task prior to EEG recording. Mean CFF was 50.01 Hz (SD = 6.32). We found no correlation between the task and eyes-closed peak alpha frequency (R analysis: r = 0.01, df = 29, P = 0.955; skipped-correlation analysis r = 0.01, CI = [-0.360, 0.434], no outliers detected). Quantile-quantile-plots showed a slight deviation from normality for the CFF task data. We therefore also conducted our correlation test using Spearman's rank correlation, but this did not significantly alter analysis results: Spearman's r = 0.04, P = 0.833. Peak alpha power also did not correlate with CFF (R analysis: Pearson's r = 0.14, df = 29, P = 0.348; skipped-correlation analysis: r = 0.17 CI = [-0.133371, 0.467874], no outliers detected).

Comparison of the two behavioural tasks

We compared the thresholds obtained with the CFF task with those obtained with Samaha & Postle's flash fusion paradigm. We found no correlation between the two (R analysis: r = -0.13, df = 29, P = 0.49; skipped-correlation analysis: r=-0.13, CI = [-0.455, 0.301], no outliers detected).

A summary of all main results is outlined in Table 3.1.

Table 3.1. Overview of main results. Overview of all the analyses performed in this study, comparing our findings with those of Samaha & Postle's (2015) where relevant. Significant correlations shown in bold.

Analysis	Current study	Samaha & Postle (2015)
Flash fusion task and eyes-closed peak alpha frequency	**r = -0.43** **P = 0.016**	**r = -0.503** **P = 0.023** (effect size and significance mentioned for a single electrode; O2)
Flash fusion task and eyes-closed peak alpha power	r = 0.14 P = 0.438	r not specified P > 0.19
Proportion of correct responses on intermediate stimulus and eyes-closed peak alpha frequency	**r = 0.33** **P = 0.035**	**r = 0.53** **P = 0.015**
Flash fusion task and pre-stimulus peak alpha frequency	r = -0.29 P = 0.124	**r = -0.605** **P = 0.004**
Flash fusion task and pre-stimulus peak alpha power	r = 0.18 P = 0.336	r = -0.093 P = 0.695
Proportion of correct responses on intermediate stimulus and pre-stimulus peak alpha frequency	r = 0.28 P = 0.07	**r = 0.4** **P = 0.044**
Flash fusion task and pre-stimulus peak alpha frequency extracted from electrode PO8	**r = 0.42** **P = 0.023**	-
Proportion of correct responses on intermediate stimulus and pre-stimulus peak alpha frequency extracted from electrode PO8	r = 0.28 P = 0.07	-
Pre-stimulus peak alpha frequency and within-individual perceptual accuracy	No significant difference between correct and incorrect responses	**Significant difference between correct and incorrect responses for certain time points**
Critical flicker fusion threshold and eyes-closed peak alpha frequency	r = 0.01 P = 0.955	-
Critical flicker fusion threshold and eyes-closed peak alpha power	r = 0.14 P = 0.348	-
Critical flicker fusion threshold and flash fusion task	r = -0.13 P = 0.49	-

3.5 Discussion

Though the study of alpha band oscillations in the brain and their potential effect on sensory perception is a popular area of research, conflicting results illustrate a need for more

replication studies. Our results add more insight into the possible role of peak frequency and amplitude of rhythmic brain patterns in sensory perception. Our study replicated some of the findings of Samaha & Postle, but not all.

Flash fusion task

Similar to the original study, we found a moderate correlation between peak alpha frequency from eyes-closed EEG data and flash-fusion thresholds. Following the original paper's methods for pre-stimulus EEG recording analysis, we analysed the electrode that showed the highest amplitude in the alpha band range for pre-stimulus EEG recording for each participant, and found no correlation between peak alpha frequency and flash fusion thresholds for pre-stimulus EEG recordings. However, regions with high alpha power during visual task performance might not be indicative of the areas where focused, fast temporal processing might be taking place. We therefore also analysed electrode PO8, which had the highest alpha band amplitude for most participants during eyes-closed EEG recording. For electrode PO8, we found a moderate correlation between pre-stimulus peak alpha frequency and flash fusion thresholds. This correlation was significant for our first analysis conducted in R, but not for our post-hoc skipped-correlation analysis method. Correlation strength remained similar. Consistent with Samaha & Postle's findings, flash-fusion thresholds were not correlated with either eyes-closed or pre-stimulus peak alpha power.

Intermediate stimulus

Similar to the original study, we found a correlation between the proportion of correct responses on the intermediate stimulus and peak alpha frequency from eyes-closed EEG data. This correlation was however not significant in our post-hoc, alternative correlation analysis. We did not replicate the correlation of $r = 0.4$ found in the original study for pre-stimulus EEG data. With $n = 20$ and $alpha = 0.05$, the original finding yielded a statistical power of 0.56. With our sample size, the effect size needed to match this power is 0.32. Our level of correlation, $r = 0.28$, came close to that of the original study, but it did not reach statistical significance. The low power and effect size of both the original and current results make it difficult to draw conclusions about any true relationships regarding peak alpha frequency and the proportion of correct responses on the intermediate stimulus. The lack of stronger correlations could suggest that a potential relationship between peak alpha frequency and temporal perception may be small and only apparent for near threshold stimuli. As the intermediate stimulus onset asynchrony is designed to be observable for most participants in more than 50% of the trials, it makes sense that correlations with a potential indicator for finely tuned temporal perception may be weak or even absent, as observing this stimulus would not require extremely fast visual processing. As such, there is a higher chance for

incorrect responses to be due to other factors than slower temporal processing, such as lack of attention or blinking.

Instantaneous alpha

Samaha & Postle reported a correlation between instantaneous alpha and response on the flash fusion task, with correct responses being linked with a higher instantaneous alpha. Such an effect was not observed in the present study. We analysed electrodes that had the highest alpha amplitudes at the group level for both eyes-closed (PO8) and pre-stimulus (Fp2) EEG-recording, and neither showed any time clusters within the -700 – 0 ms pre-stimulus window where instantaneous alpha frequency was significantly different for correct versus incorrect responses. Data from several other recent studies have also failed to support this link (Buergers & Noppeney, 2022; Ruzzoli et al., 2019). Though we have attempted to model our task as closely to Samaha & Postle's as possible, there were some differences in our methodology which could potentially account for the discrepant results. For instance, from Samaha & Postle's methods, it is not reported by how much the fixation cross decreased in luminance to prompt the participant of the upcoming stimulus. If this luminance shift was more drastic in our study, it could have caused a stronger phase reset effect, possibly nullifying any natural phase differences between trials (Harris, 2023).

CFF task and peak alpha frequency

We found no correlation between thresholds obtained with the CFF task and peak alpha frequency from eyes-closed EEG recording. This result illustrates how the choice of behavioural task may influence the results obtained in brain rhythmicity studies. As already touched upon by Buergers & Noppeney (2022), the effect alpha frequency may have on temporal perception may be very small and brittle, and may only be apparent for very specific stimulus parameters. A lack of correlation between the CFF task and peak alpha frequency may also be due to the continuous nature of the task stimulus. For example, alpha power is expected to reduce greatly during perception of a continuous stimulus, which in turn might affect alpha frequency as well, as the two are found to be intrinsically linked (Nelli et al., 2017). Additionally, previous literature has suggested that peak alpha frequency may only be indicative of perceptual sensitivity when the stimulus last for less than one alpha cycle (Keitel et al., 2022; Michail et al., 2022).

CFF and flash fusion task comparison

We also found no correlations between the thresholds obtained with the two different tasks. Though this may initially seem surprising, the flash fusion task fundamentally differs from the CFF task in several ways. For example, the former is essentially a two-alternative-forced

choice task, in which participants need to choose between two possible responses in each trial. This introduces a guess rate which may skew “true” flash-fusion thresholds. The responses may also be influenced by a pre-existing bias for one of the two options (Buergers & Noppeney; 2022). The flash fusion task also requires 600 trials for the proper fitting of a psychometric curve. This causes fatigue to become a significant factor and, though computationally corrected for during psychometric function fitting, introduces a certain lapse rate. The two tasks also differ in the number of different stimuli: the flash fusion task has five different fixed gap lengths, whereas no practical upper bound for flicker-fusion threshold exists in the CFF task, making the latter perhaps more suitable to assess inter-individual differences in the absolute maximum threshold, but less so for employing standardized tests to investigate brain activity correlates. Thresholds obtained with the CFF task may also not be directly comparable to those obtained with the flash fusion task due to a steady increase of mean luminance over time as flicker frequency increases in the former, which effectively increases flicker fusion thresholds up to a certain point. It is also important to note that Samaha & Postle’s flash fusion task was designed to assess possible correlates with alpha oscillations; which are a specific measure for visual attention and focus (Clayton et al., 2018; Pfurtscheller et al., 1996). The gap detection style task is very suitable to investigate the level of attention a participant pays to each stimulus. Any moment of inattention may mean that the gap in the stimulus is missed and a trial is considered incorrect. This is not the case for the critical flicker fusion task, in which the stimulus is always present, giving participants the opportunity to refocus and reconsider what they are perceiving throughout the whole task. The latter reason would not only explain the lack of correlation between the two behavioural task responses, but also between the CFF task and peak alpha frequency.

In conclusion, we have replicated some, but not all of the results from a previous study investigating the possible relationship between peak alpha frequency and visual temporal resolution. Our work adds to the ever-expanding body of research data aiming to tease apart the link between brainwave oscillations and visual perception. We have additionally shown that the choice of behavioural task is key in exploring these possible relationships.

Chapter 4

Quick eyes win the prize: Trained athletes have faster perception than non-athletes

---

Author contributions

I co-conceived the idea, created the testing paradigm, collected and analysed the data and wrote the manuscript. Redmond O'Connell, Kevin Mitchell and Andrew Jackson secured funding for the project and contributed to the conception of the idea, data collection and editing of the manuscript.

4.1 Abstract

Studies into the temporal processing abilities of different visual systems in the animal kingdom have suggested that temporal resolution may be linked with distinct ecological settings. Higher temporal resolution appears to be more common in fast-moving, highly manoeuvrable species, indicating that high visual processing rates may confer direct functional benefits in dynamic environments. As visual temporal resolution is found to vary substantially, not only among, but also within species, it is possible that these links are also observable among individuals. In this study, we tested this hypothesis by using high-level sports as a proxy for different ecological settings. We measured variation in temporal resolution using critical flicker fusion thresholds in two groups of highly trained athletes, one specialising in a visually dynamic sport, and the other specialising in a visually-non-dynamic sport. We found no significant difference in mean critical flicker fusion threshold between the two groups. However, both athlete groups had significantly higher thresholds than a non-athlete control group, suggesting that high visual temporal resolution may be linked with higher levels of cardiovascular fitness, rather than visual dynamics.

4.2 Introduction

All biological visual systems are constrained by the maximum rate with which information can be sampled and processed over time. This rate, also known as temporal resolution, is generally measured using the critical flicker fusion (CFF) threshold: the frequency at which a flickering light stimulus flickers so fast, that the flicker can no longer be perceived. This frequency can not only be quantified behaviourally, but also electrophysiologically, using electroretinogram, making CFF applicable across virtually all of the animal kingdom, from sea stars (Petie et al., 2016) to mammals (Healy et al., 2013; Inger et al., 2014; Lafitte et al. 2022). This has allowed researchers to compare the temporal resolution of visual systems among numerous species.

Previous works have found that CFF varies greatly in the animal kingdom. This variation can, at least in part, be attributed to specific aspects of a species' ecological setting. For example, highly agile and manoeuvrable species generally have high CFF thresholds, and animal species that track and hunt fast-moving prey items possess higher CFF thresholds than their close relatives that hunt slower prey (Autrum, 1950; Boström et al., 2016; Kingston et al., 2020; Potier et al., 2020). These observations suggest that a higher visual temporal resolution confers a direct behavioural benefit in highly dynamic environments.

Variation in CFF thresholds is present not only among, but also within species. Our recent research has shown that, in healthy humans of similar ages, this variation is quite substantial, yet stable (Chapter 2, published as Haarlem et al., 2024b). The magnitude of the variation in CFF thresholds we observed in humans is large enough to be comparable with the variation observed among different animal species that occupy significantly different ecological niches (Jenssen & Swenson 1974; McComb et al., 2010). This could suggest that the naturally present variation in visual temporal resolution within a species might have an important effect on function.

To study how individual variation in visual processing speed within a species may be linked with ecological function, humans are perfectly suited to serve as study species, as we have created multitudes of distinct settings in which individuals interact with their environment in ways that push certain aspects of their physiology to their limits. Elite sport is a prominent example of such a setting. To engage effectively in any type of sport, athletes must possess a combination of highly developed, situationally relevant, skills and traits. As such, a selection process occurs in which individuals who possess the most finetuned characteristics relevant to their respective sport, reach higher levels of performance and competition (Tucker & Collins, 2012). This selection pressure is at its strongest at the elite level. Consequently, elite athletes often exhibit markedly different neurophysiological, sensory or cognitive attributes compared to non-athletes or amateur athletes. For example, in a study with karate practitioners, researchers found that neural synchronization in the visual cortex after observing a visual stimulus was modulated differently between athletes and non-athletes. This difference was most extreme for the elite practitioners, with amateurs showing an intermediate modulation (Del Percio et al., 2007). In another study, elite fencers were found to have faster reaction times on a discriminative reaction task, as well as altered brainwave modulation associated with attention, stimulus discrimination, response selection and motor inhibition, compared to non-athletes (Di Russo et al., 2006). A recent large scale study involving athletes of multiple different types and expertise levels found that elite level athletes performed better on a battery of visual-motor tasks than athletes with less expertise. Interestingly, the same study also found that the type of sport played was correlated with different performance parameters: athletes practicing interceptive sports scored higher on visual sensitivity tasks, whereas athletes practicing strategic sports performed better on a spatial working memory task (Burris et al., 2019).

Here, we hypothesize that a link exists between athletic ability and visual temporal resolution, as quantified with CFF thresholds, and that this link is sport-specific. We predict that highly trained athletes who engage in visually dynamic sports possess higher CFF thresholds compared to highly trained athletes who engage in sports that are visually less

dynamic, due to a strong selection pressure favouring fast visual processing in the former. As physical fitness is correlated with improved nervous system functioning and cognitive performance (Chodzko-Zajko & Moore, 1994; Etnier et al., 1997; Ploughman, 2008), we additionally predict that physically fit athletes in general will also exhibit higher CFF thresholds than non-athletes. To test these hypotheses, we will measure CFF thresholds in three groups: highly trained athletes who engage in visually dynamic sports, highly trained athletes who engage in non-visually dynamic sports and a non-athlete control group.

To represent the athlete group engaging in visually dynamic sports, we focus on the sport of hurling, one of Ireland's national sports. Hurling is a 15 a-side stick-and-ball game played on a field of approximately 145 by 90 metres. The game shares some similarities with field hockey. It is one of the world's fastest field sports, and during a match the ball (sliotar), which is caught with the hands and struck with the stick (hurley), can reach speeds of up to 160 km/h (Murphy et al., 2012). Hurling is a highly dynamic game, requiring players to perform both offensive and defensive manoeuvres at high speeds and demanding a high degree of hand-eye coordination (Collins et al., 2022; Young et al., 2018). It is a men-only amateur sport (the female equivalent is named camogie and shares many similarities with hurling) and elite players compete at inter-county level.

We believe that trained rowers are perfectly suited to represent the athlete group engaging in non-visually dynamic sports. Rowing is a full-body, strength-endurance type sport, and thus requires exceptional physical fitness (Li et al., 2021; Mäestu et al., 2005). The sport is performed with athletes sitting facing the stern of the boat, with their backs towards the finish line, and rowing a pre-determined distance (Hosea & Hannafin, 2012; Li et al., 2021). Navigation of the boat is managed by an on-board coxswain, who uses auditory cues to direct the rowers. As such, rowers are not required to visually focus on a goal or stimulus. This defining characteristic means that the sport can be performed at elite level with visual impairments and even with 100% blindness (Rich et al., 2022; Schaffert et al., 2014). Rowing is popular worldwide, and elite athletes compete on international level.

4.3 Methods

4.3.1 Participant recruitment

The study was approved by the Ethics Committee of Trinity College Dublin's School of Psychology. All participants were aged 18 – 35, had normal or corrected-to-normal visual acuity and all participants provided written, informed consent. As the definitions of terms such as "elite" or "highly trained" are highly subjective and differ between sports, we

determined athlete performance level for each sample group based on the framework and suggestions from McKay et al., 2022 (Table 4.1). We only included athlete participants that most closely matched tier 3 of this framework, and we only included non-athletes that most closely matched tiers 0 or 1. Due to one of our target groups consisting of athletes from a men-only sport, we only recruited male participants for this study.

Table 4.1. Participant classification framework. Based on McKay et al., 2022. Tier 3 criteria were utilized for athlete participant recruitment, criteria for tiers 0 -1 were utilized to select the non-athlete control group.

Tier	Criteria for classification
Tier 5: World class	• Olympic or world medallists • Athletes achieving within 2% of world-record performance • Maximal or near-maximal training, within given sport norms • Exceptional skill level
Tier 4: Elite/International level	• Competing at international level • Division I athletes • Highly proficient in skills required to perform sport • May perform within ~7% of world leading performance
Tier 3: highly trained/national level	• Competing in national or state leagues/tournaments • Completing structured and periodized training • Developing towards maximal or nearly maximal norms for the given sport • Developing proficiency in skills required to perform the sport
Tier 2: trained/developmental	• Limited skill development • Training with intention to compete • Regularly train ~ 3 times a week • Identify with a specific sport
Tier 1: recreationally active	• Completing 150 – 300 minutes moderate-intensity activity or 75 – 150 minutes of vigorous-intensity activity per week • May participate in multiple sports/forms of activity • No specific focus or commitment to competition
Tier 0: sedentary	• No minimum activity guidelines

	• Occasional or incidental physical activity (walking to work, household activities)

Athlete participants

Athlete participant recruitment and data collection started in January 2024 and ended in October 2024. For the two athlete groups, we recruited participants that most closely matched McKay et al.'s (2022) criteria for tier 3 performance, defined as highly trained athletes who exhibit "proficiency in skills required to perform their sport at the highest level." McKay et al. also suggest that athletes in this tier "can be expected to provide reliable measures of performance in familiar tasks and are therefore well suited to both laboratory- and field-based research."

We recruited 10 hurlers and 12 rowers. Hurlers were recruited in Dublin, Ireland, through local Gaelic Athletic Associations (GAA's). All hurling participants were Senior Division II or III players and regularly competed at club level championships or higher. Mean training volume of the hurlers was 3.3 hours a week, and mean experience was 16.8 years (based on 9 players, as information for one participant was not available). Note: Senior is the highest classification within a local GAA, with lower classifications designated as either Intermediate or Junior. Senior Division I players have the potential to compete at inter-county level, which is the highest competitive level available within the sport and is thus comparable to international competition in other sports. Based on these categorizations, we estimated that Senior Division II and III players most closely match tier 3 of McKay et al.'s framework.

Rowers were recruited in the counties of Dublin and Wicklow, through local rowing clubs. All rowing participants regularly competed at national or international level, except for one participant who regularly competed at local level. Mean training volume for the rowing participants was 11.3 hours a week and mean experience was 6.3 years.

Non-athlete participants

For the non-athlete control group, we used CFF data available from a previous study (Haarlem et al., 2024b, ethics approval ID SPREC052022-01). From this dataset, we filtered out only male participants who fit tier 0 (sedentary) or 1 (recreationally active) of McKay et al.'s classification system. 25 individuals fit these criteria and were used in this study.

4.3.2 CFF measurement

We measured CFF thresholds using a custom measuring device and custom methods employed in two previous studies (Chapter 3, published as Haarlem et al., 2024a and Chapter

2, published as Haarlem et al., 2024b). CFF was measured with a 4500K white light-emitting diode (LED), with a mean luminance of ~255 lux. The LED was housed in an opaque black container, and an opaque black viewing tube was mounted on top of the container to standardize viewing distance at ~16 cm and to eliminate almost all ambient light. The flicker frequency of the LED was adjustable using a rotary encoder dial that either increased or decreased the flicker rate in 1-Hz increments. The device was powered with a personal laptop, using a USBC cable. Mean luminance and colour temperature were measured with a ColorCal Mk II, and stability of the power input was measured with a Tektronix TDS 210 oscilloscope, before the start of our previous two studies. The precision and stability of the LED flash timings were measured using a photometer, both before the start of our previous two studies, and before the start of the current study.

The protocol consisted of a measurement of three different quantifications of a participant's ability to perceive flashes and was based on a combination of two commonly used psychophysical experimental techniques: the method of limits and the method of constant stimuli. The protocol started with the method of limits: participants observed a constantly lit LED light through the viewing tube and were then instructed to turn the rotary encoder clockwise, to prompt the light source to start flashing at a rate of 1 Hz. Participants were then asked to keep rotating the dial to increase the flash frequency in 1-Hz increments until flashes could no longer be perceived and the light appeared steady. The frequency at which this occurred was recorded. The LED light source was then set to a flash frequency of 75 Hz, which is above the threshold at which humans are able to perceive light flashes at the described intensity. For the second measurement, participants were instructed to observe the light source again, but this time, they were asked to turn the dial counter-clockwise to decrease flash frequency in 1-Hz increments, until they first observed flashing. The frequency at which this happened was again recorded. The third step consisted of the method of constant stimuli: for each participant, we took the highest value measured with the method of limits and created a series of 10 flash frequencies in 1-Hz steps: five frequencies below the recorded threshold and four frequencies above it. Each of the frequencies in the series was then multiplied by 5 to produce a set of 50 stimuli. We then randomized the entire set and presented it to the participant. Participants were instructed to cycle through all of the 50 frequencies in the series, one by one, using the rotary encoder dial to instantiate the next stimulus in the set. Participants were asked to inform the experimenter for each stimulus whether they observed a steady light or not. The final critical flicker fusion threshold for the individual was determined by calculating the highest frequency in the series at which the user was able to perceive flashing 80% of the time. Only this final value was used in our statistical

analysis, as this threshold was found to be the most accurate in our previous study (Chapter 2, published as Haarlem et al., 2024b).

Athlete participants were tested either at rest or during light training sessions consisting of anaerobic exercises (i.e. light weight-lifting, technique drills). Previous studies have shown that moderate exercise has either no, or a minimal, effect on CFF threshold, with any noted variation still falling within the range of natural intra-individual variation observed in Haarlem et al. 2024b (Al-Nimer & Al-Kurashy, 2007; Clemente-Suarez & Diaz-Manzano, 2019; Davranche & Audiffren, 2004; Davranche & Pichon, 2005; Godefroy et al., 2002). However, aerobic exercise to the point of exhaustion may temporarily significantly affect CFF (Lambourne et al., 2010; Presland et al., 2005). We therefore avoided testing athlete participants during any type of aerobic- or high-intensity training. All non-athlete participants were tested at rest.

4.3.3 Statistical analysis

We performed statistical analyses using R (version 4.2.1; R Core Team, 2022) and RStudio (version 2023.3.0.386; Posit Team, 2023). We calculated CFF thresholds for the method of constant stimuli by creating a binomial generalized linear model for each participant, using the proportion of responses per frequency at which flicker was perceived as response variable and the frequency in Hertz as the explanatory variable. In these models, the range for y was set to 0–1, with 0.8 corresponding to an 80% correct score. We therefore calculated the x-value at which y = 0.8 (For an example see Fig 2.2 in Chapter 2).

We analysed our data using ANOVA, with CFF as our response variable and a factor named "Sport" as explanatory variable. The explanatory variable consisted of three levels; "hurling," representative for a visually dynamic sport, "rowing," representative for a non-visually dynamic sport and "general" to represent the control group. Normality of residuals was assessed visually with quantile-quantile plots of model residuals. Quantile-quantile plots were created using the car package (Fox & Weisberg, 2019). We utilized the post-hoc test Tukey's Honest Significant Differences to examine the differences in mean CFF thresholds between factor levels.

4.4 Results

The explanatory variable "Sport" had a significant effect on CFF thresholds (ANOVA, $f = 12.23$, $p < 0.001$). Mean CFF for the non-athlete control group was 47.87 Hz, with a standard deviation (SD) of ± 4.30 Hz. Mean CFF for the rowing group was 55.25 (SD ± 5.133) Hz and

the mean CFF for the hurling group was 53.25 (SD ± 4.56) Hz. Both the rowing and the hurling groups had significantly higher CFF thresholds than the "general" non-athlete control group, but there was no significant difference in mean CFF between the rowing and hurling groups (Table 4.2, Fig 4.1).

Table 4.2. Comparison of mean CFF thresholds of the three sample groups. Differences in mean CFF thresholds in Hz, for the sample groups "General" (n = 25), "Hurling" (n = 10) and "Rowing" (n = 12). Middle column shows 95% confidence intervals (CI) and last column indicates p-values, with significant values shown in bold.

Group comparison	Difference in Hz	95% CI	P-value
General - Hurling	5.38	[1.23, 9.53]	**0.0083**
General - Rowing	7.38	[3.48, 11.28]	**0.0001**
Hurling - Rowing	2.00	[-2.75, 6.75]	0.567

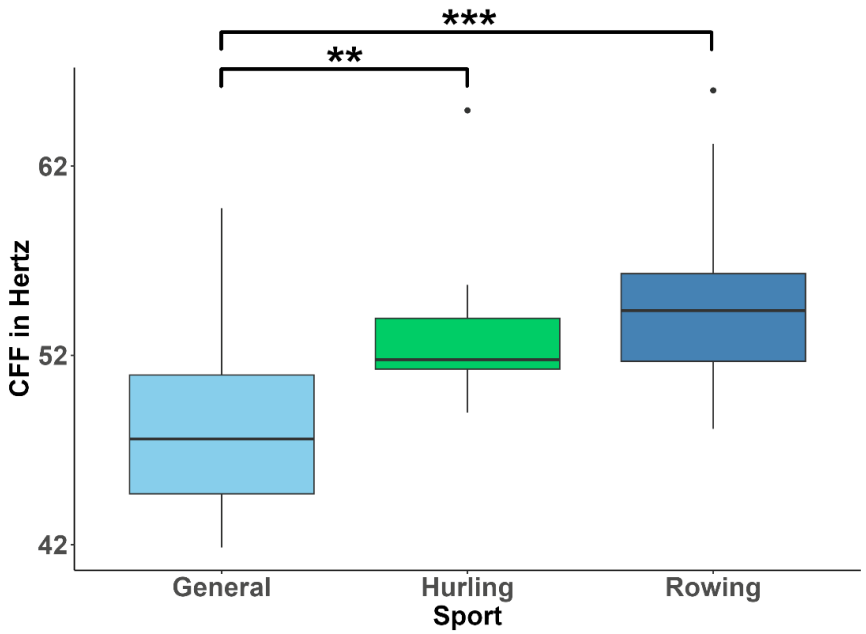

Figure 4.1. Boxplot of CFF thresholds for the three sample groups. CFF distributions for the non-athlete "General" group (n = 25) and the athlete groups "Hurling" (n = 10) and "Rowing" (n =12).

4.5 Discussion

Visually dynamic versus non-visually dynamic sports

We found no statistically significant difference in CFF thresholds between the athlete group engaging in a visually dynamic sport and the athlete group engaging in a non-visually dynamic sport. In fact, contrary to our prediction, mean CFF was marginally higher for the rowing group compared to the hurling group. Thus, the results of the current study do not support our hypothesis that CFF thresholds are higher in individuals trained in visually dynamic sports compared to non-visually dynamic sports. It must be noted however that the recruitment of highly trained athletes proved a difficult task, and as a result the sample sizes of both athlete groups are relatively small. A post-hoc power analysis using the pwr package for R (Champeley, 2020) indicated that, with the smallest sample group containing only 10 observations, and assuming a large effect size (f = 0.4), we achieved a statistical power of b = 0.44. While we speculate below on the possible causes for the results of our current study, we stress that with this level of statistical power, we were unable to draw any firm conclusions from our results with regards to our original hypothesis.

Previous studies have found that trained athletes perform better on specific cognitive tasks than non-athlete controls, and this observation has been made for many different aerobic sports (Burris et al., 2019; Chodzko-Zajko, 1994). Thus, it is possible that the results in the current study are mainly due to the level of cardiovascular fitness of athletes, rather than the specific type of sport played. This could also explain why mean CFF is slightly higher in our sample group of rowers compared to the hurlers. Though both athlete groups most closely matched tier 3 of McKay et al.'s (2022) framework, the specific requirements to perform the respective sports differ substantially, with rowing athletes likely placing more focus on cardiovascular fitness, while hurlers might place more emphasis on technique and hand-eye coordination. The marked difference in weekly training volume between the two groups may also be an indication of a higher level of cardiovascular fitness in the rowing group, with the mean volume being over three times higher in rowers.

More research needs to be conducted into the possible effect of cardiovascular fitness on CFF, so that this may be unlinked from any potential sport-specific variables of interest, such as the different levels of visual dynamics examined in the current study. One possibility to better account for the effects of physical fitness in follow up research would be to replace Division II and III hurlers with Division I players. These athletes likely have a higher training volume than hurlers competing in lower Divisions, and might therefore better match the cardiovascular fitness levels of highly-trained rowers. However, for the current study we were unfortunately unable to recruit hurlers of this level. Additionally, another focus group may be

identified for which visual dynamics plays an integral part of the ecological setting, but a high level of cardiovascular fitness does not. Such a group may consist of e-sports athletes or practitioners of shooting sports.

Athletes versus non-athletes

Mean CFF thresholds were significantly higher for the two athlete groups compared to the non-athlete group. This result suggests that physical fitness may play a role in visual processing rates. The relationship between fitness and cognitive function has been well-studied over the years, and researchers have found a host of differences between individuals of higher and lower levels of aerobic fitness in several cognitive and neurobiological traits. For example, physical fitness has been linked with increased neurogenesis, size differences in brain tissue, enhanced spatial memory, faster information processing, faster reaction times and better performance on specific tasks. These findings, along with many others, have been comprehensively highlighted in multiple review papers, such as those published by Chodzko-Zajko & Moore (1994), Etnier et al. (1997) and Gomez-Pinilla & Hillman (2013), which together summarize most of the research conducted on this topic to date. Though previous studies have investigated the immediate effect of aerobic exercise on CFF (Al-Nimer & Al-Kurashy, 2007; Clemente-Suarez & Diaz-Manzano, 2019; Davranche & Audiffren, 2004; Davranche & Pichon, 2005; Godefroy et al., 2002; Lambourne et al., 2010; Presland et al., 2005), potential associations with overall aerobic fitness or chronic exercise have, to our knowledge, not been explored specifically in the context of CFF thresholds. However, it is likely that visual temporal resolution (as measured with CFF) follows a similar trend of higher processing rates in more aerobically fit individuals.

Our finding that CFF thresholds are higher in the trained athlete groups compared to the non-athlete group is indeed interesting, but it is important to note the potential confounding factors that may be present in studies comparing highly-physically fit individuals with individuals who are either sedentary or only recreationally active. Physical fitness, as quantified by the amount and type of exercise an individual engages in, is only a single marker of overall health and may correlate with other markers of a healthy lifestyle. For example, physically fit individuals who regularly exercise may also be more likely to incorporate healthy diets, adopt healthier sleep schedules, practice more self-care and/or have lower rates of detrimental habits such as excessive drinking and/or smoking. Each of these factors may affect CFF thresholds on their own and can thus introduce collinearity with overall physical fitness in statistical analyses. It is also possible that individuals who naturally possess higher CFF thresholds are more likely to become high-performing athletes, rather than high CFF being a causal effect of athleticism. As research into individual variation in visual temporal resolution and CFF thresholds develops further, it is important to decouple

causal- from correlational relationships, and to identify which lifestyle factors may be most tightly linked with visual processing speed, while maintaining awareness of potential confounding factors.

Conclusions

Previous animal studies suggest that the temporal aspect of visual processing may be influenced by distinct ecological settings in which highly dynamic visual scenes may select for higher processing rates. Whether these ecological pressures may also drive variation in temporal processing within a species may be assessed by drawing comparisons with the diversity of ecological settings that humans have created, specifically in the form of sports. However, much is still unknown about individual variation in visual temporal resolution, and many physiological, anatomical and environmental factors may influence variation, making it difficult to isolate and examine specific variables. With our study, we have made a first attempt at assessing whether temporal resolution, as measured by CFF thresholds, varies in groups that experience different visual dynamics. Though we were unable to draw any direct conclusions regarding this hypothesis, we did make the original observation that CFF thresholds were significantly higher in trained athletes than in non-athletes. More research is warranted to assess if this observation is also seen in larger, and more varied samples. If so, this could suggest that CFF could potentially be used as a general screening tool for overall physical fitness level, and could possibly aid health and well-being diagnostics.

Chapter 5

Visual temporal resolution is linked with multiple aspects of a species' ecological profile

---

Author contributions

I conceived the idea, collected and analysed the data and wrote the manuscript. Kevin Healy contributed to the collection of data and Andrew Jackson contributed to the analysis of the data. Redmond O'Connell, Kevin Mitchell and Andrew Jackson all contributed to the writing of the manuscript and secured funding for the project.

Status

A version of this manuscript is in preparation for submission to the journal *Ecology Letters*.

5.1 Abstract

Visual perception varies widely in the animal kingdom and is closely tied to species ecology and evolution. The temporal processing capabilities of the visual system directly determine how much visual information a species has access to per timeframe, and may thus be a driving factor for the pace at which species can interact with their environment. How the temporal aspect of sensory perception may influence the occupation of specific ecological niches is still poorly understood, but recent, small-scale case studies have suggested that visual temporal resolution may be linked with species manoeuvrability and environmental dynamics. Here, we assess the relationship between different types of environmental dynamics and visual temporal resolution in the animal kingdom using a large-scale dataset. We collated critical flicker fusion thresholds, a quantification of visual temporal resolution, for over 200 animal species, along with multiple representations of different environmental dynamics. We found that high temporal resolution is found in species with more dynamic environmental interactions, such as those with active foraging strategies or the ability to fly. Species that may experience less dynamic visual ecologies, such as ambush predators, are found to have lower temporal resolution. Additionally, temporal resolution varies greatly in the animal kingdom, not only among, but also within taxa. These results suggest that the temporal processing abilities of species are linked with their distinct ecological profile, and that processing rates can both increase and decrease relatively quickly over evolutionary time, according to ecological demand.

5.2 Introduction

For most animal species, visual perception is a crucial facilitator of environmental interactions. Vision is used to navigate, manoeuvre, forage and reproduce, and as such, it is subject to strong selection pressures. However, sensory processing is costly, and natural selection tends to favour only the most efficient visual systems, which detect and process only information that is relevant for the species' respective ecology (Laughlin, 2001). As a result, the visual perception capabilities of different animal species are as diverse as the ecological niches they occupy. This diversity is apparent in many attributes of vision, such as spatial acuity, colour discrimination, depth perception and field of view, all of which vary widely between species (Land & Nilsson, 2012; Laughlin, 2001). Depending on the species, some attributes may even be absent entirely.

There is however one characteristic of visual perception that is ubiquitous in the animal kingdom, and that is that all visual processing must happen at a certain rate. This processing

rate arises from the dependence of all visual systems on the integration and summation of photon energy. Quanta of photon energy are summed over an integration period and only when a threshold is reached will the information be processed and perceived by the individual (Donner, 2021; Reeves, 1996). The quicker the threshold is reached, the higher the rate of visual processing. The maximum rate at which this processing occurs is known as temporal resolution. Visual temporal resolution can be generalized and quantified for any species using the critical flicker fusion (CFF) threshold, which is defined as the maximum rate at which a flickering light can no longer be perceived as such, and instead appears constant (Brozek & Keys, 1945; Misiak, 1947). This aspect of visual perception, as all the others, has been found to vary greatly between species (Healy et al., 2013; Inger et al., 2014; Lafitte et al., 2022). CFF can be quantified either with electroretinogram (ERG), by measuring the electrophysiological response of the retina to flickering light, or behaviourally, by assessing a trained or reflexive (such as the nystagmus reflex) response to flickering stimuli (Inger et al., 2014; Lafitte et al., 2022).

Visual temporal resolution is strongly dependent on the amount of light available in the environment (Kelly, 1961; Rider et al., 2019). This link can be observed at the species level, where visual processing rates are positively correlated with habitat light levels (Jenssen & Swenson, 1974; Lafitte et al., 2022; McComb et al., 2010). However, temporal perception across species varies over several orders of magnitude, and much of this variation is yet to be explained. It is likely that CFF is shaped, not solely by environmental light levels, but rather by a species' overall ecological profile, consisting of a combination of anatomical, physiological, behavioural and environmental factors.

For example, previous research has shown that CFF thresholds are positively correlated with a species' metabolic rate, and negatively with body mass (Healy et al., 2013). High metabolic rates directly facilitate faster neuronal processing (Atwell & Laughlin 2001; Bullmore & Sporns, 2012; Laughlin et al., 1998), whereas higher body mass is linked with reduced manoeuvrability (Dudley, 2002; Sato et al., 2007; Stockwell, 2001). The relationship observed in Healy et al. (2013) might thus suggest that CFF thresholds could be indicative of a species' ability to respond to highly dynamic environments. After all, fast visual processing is only useful if one has the physical capacity to act on fleeting information.

Small-scale studies that have examined CFF thresholds in closely related species appear to support this idea. For example, Boström et al. (2016) measured exceptionally high CFF thresholds in three highly manoeuvrable and fast-moving passerines, that often catch prey on the wing. Potier et al. (2020) compared CFF in three different raptor species and found that the two faster species had higher thresholds than the third, which moves more slowly and hunts slower prey.

Here, we hypothesize that variation in CFF thresholds in the animal kingdom is directly linked to the dynamics of a species' environmental interactions. We test this hypothesis by creating a large-scale dataset consisting of CFF thresholds of vertebrate and invertebrate species, collected from literature, and by correlating CFF with quantifications of multiple different proxies for species' environmental dynamics. We have chosen three different proxies to represent different aspects in which animal species visually interact with their environment: movement dimensionality, foraging dimensionality and foraging strategy.

Animal species locomoting and foraging in three dimensions (3D) likely have a more dynamic visual experience than those moving in two-dimensions (2D), due to a higher potential for environmental encounters in the form of obstacles, conspecifics, predators or prey items. We hypothesize that more visually dynamic environments select for faster visual processing rates, and that animal species that locomote in 3D possess higher CFF thresholds than species locomoting in 2D.

Some species may forage on a dimensional level that differs from their locomotion dimensionality. For example, some volant species (i.e. species that fly, and thus locomote in 3D) may only visually scan two-dimensional planes, such as the ground or plant surfaces, when foraging (Pawar et al., 2012). Foraging dimensionality may therefore result in different visual dynamics for different species. We hypothesize that animals that forage in three dimensions will have a more dynamic visual experience, and will have higher CFF thresholds than species foraging in two dimensions.

Lastly, different types of foraging strategies likely place specific demands upon a species' visual system. For instance, species that engage in high-speed chases experience highly dynamic visual percepts and would need to be able to process visual information very quickly. In contrast, ambush predators generally remain sessile, and this lack of self-generated motion results in a less dynamic visual experience (Fajen & Matthis, 2013; Harris et al., 2000; Warren, 1995). We hypothesize that active predators with prolonged pursuit or burst-pursuit style foraging strategies possess the highest CFF thresholds, and that species with an ambush foraging strategy have the lowest CFF thresholds. We hypothesize that grazing species possess intermediate CFF's.

5.3 Methods

5.3.1 Data collection

We collected CFF values of the visual systems of vertebrate and invertebrate animal species from literature, using Web of Science, Google Scholar and Google. For each source, we used the following search terms:

"CFF" OR "flicker fusion" OR "flicker frequenc*" OR "flicker threshold*" AND "ecolog*" OR "animal" OR "species"

We screened publications appearing in the search results both for direct mention of animal CFF values and for citations referencing additional animal CFF studies. When multiple CFF's were available for the same species, we only included the maximum value.

We included values from both behavioural and electroretinogram (ERG) measures, as previous studies have found no statistically significant differences between the two methodologies (Healy et al. 2013; Inger et al., 2014; Lafitte et al., 2022). For behavioural measures, we included both trained responses, such as those assessed with two-alternative-force-choice tasks, and reflexive responses, such as those assessed with eye- or head nystagmus. Though most CFF experiments were conducted with a flickering light source, some of the experiments in which the nystagmic reflex was assessed employed the rapid alternation of high- and low contrast bars or stripes to produce a flicker effect. All values were recorded in Hertz. Because the collected CFF thresholds spanned several orders of magnitude, we employed a log10 transformation of CFF-values in our models.

5.3.2 Environmental dynamics categorization

Movement dimensionality

To examine the effect of movement dimensionality on CFF thresholds, we categorized all the species for which CFF thresholds were available into one of three groups: volant (3D), terrestrial (2D) and aquatic. All species who utilized flight as the main mode of locomotion were categorized as volant. All species that spend the majority of their time on land were categorized as terrestrial. This included some species that have the ability to fly, but only rarely do so, such as the American cockroach and several mantid species. Though all aquatic species also locomote in either 3D or 2D, these species experience environmental light levels in a unique manner due to the medium they occupy, making them not directly comparable with the other groups. We therefore categorized these species as a separate group. The aquatic group comprised all species that spend most of their time under water.

Foraging dimensionality

To explore the potential effect of foraging dimensionality on CFF thresholds, we categorized each species according to Pawar et al.'s (2012) measure for consumer search space: species

that scan habitat volume (such as the air or the water column) were scored as having 3D foraging dimensionality, and species that scan habitat surfaces (such as the ground, plant surfaces or the benthos) were scored as having 2D foraging dimensionality.

Foraging strategy

To investigate if CFF thresholds correlate with foraging strategy, we categorized species based on methods adapted from Pawar et al. (2012). Species were classified as "active" foragers if both the forager and its food source actively locomote throughout the forager's focus habitat during foraging behaviour. This includes species that display typical pursuit predation, and species that engage in short burst-chase attempts to catch prey. Species that actively locomote during foraging, but whose food sources are sessile or moving passively throughout the focus species' habitat (such as plankton) were classified as "grazer." Lastly, species that remain sessile during foraging, but whose food sources actively locomote throughout the focus species' habitat were classified as "ambush" foragers.

5.3.3 General modelling variables

Environmental luminance levels

As previous research has shown that environmental luminance levels are strongly correlated with species' CFF, we included information for the luminance level in a species' ecological niche as a categorical variable using methods adapted from Healy et al. (2013). Diurnal species and species inhabiting clear/surface waters were classified as inhabiting high light levels, and nocturnal and crepuscular species and species inhabiting turbid or deep waters were classified as inhabiting low light levels. Habitat light levels per species were in the first instance chosen based on available scientific literature, using Google Scholar and Web of Science. In cases where no reference was available using these online databases, we searched other online catalogues, such as Animal Diversity Web, FishBase or online museum collections (see Appendix B, Table B.1 for full list of references).

Body length

Healy et al. (2013) found a correlation between species CFF and body mass, and we aimed to take this potential link into account in our models. However, for some species groups, such as Insecta, body mass records were not sufficiently available. We therefore opted to include the variable body length instead, which is expected to scale roughly as the one-third power of body mass (Dick & Clemente, 2017; Witting, 2023) and thus provides a suitable alternative. Mean body lengths in metres were collected from literature and included as a numerical variable. We searched for mean body length values using Google Scholar and Web of Science. Similar to our methodology for habitat light levels, in cases where references were not

available with these databases, we searched in other online catalogues (see Table B.1 in Supplementary info). Because the collected values spanned several orders of magnitude, we employed a log10 transformation of body length measures in our models.

Phylogeny

Lastly, to account for possible non-independence of data due to phylogenetic background, we included the taxonomic class of each species in the dataset. Note: a full, phylogenetically controlled analysis has been performed on the dataset in Haarlem et al., 2025 (in prep). However, the results of this more extensive analysis do not alter the main conclusions presented in this study.

5.3.4 Statistical analysis

We performed statistical analyses using R version 4.2.1 (R Core Team, 2022) and RStudio version 2023.3.0.386 (Posit Team, 2022). Normality of model residuals and homogeneity of variance were visually assessed with quantile-quantile plots and residual plots, using the "car" package (Fox & Weisberg, 2019). We analysed our dataset with linear mixed models, using the "lme4" package (Bates et al., 2015).

We included taxonomic class in our models as random term. Because vertebrates differ greatly from invertebrates, both in eye anatomy and overall physiology, we also included a random term to account for possible differences between vertebrate and invertebrate groups. Movement dimensionality, foraging dimensionality, foraging strategy, body length and light level were included in our models as fixed terms. We additionally assessed potential interaction effects by including interaction terms between all fixed variables.

Best fitting models were chosen according to Akaike's Information Criterion (AIC). We analysed the variance explained by each model by calculating two R^2 values, using the MuMIn package (Bartón, 2023): the marginal R^2 ($R^2_{glmm(m)}$), the value for the variance explained by the fixed variables and the conditional R^2 ($R^2_{glmm(c)}$), the value for the variance explained by both fixed and random variables.

5.4 Results

We collected CFF thresholds and information on environmental interaction dynamics for 229 animal species across 15 taxonomic classes. The largest group for which CFF thresholds were available was Insecta, with 60 observations. 43 observations were collected for Actinopterygii, 35 for Malacostraca, 21 for Reptilia and 20 for Chondrichthyes. The Mammalia and Aves classes each provided 17 observations. The fewest CFF thresholds were found for

the classes Amphibia, Annelida, Arachnida, Cephalopoda, Cnidaria, Echinodermata, Gastropoda and Hyperoartia, with only one to three observations each (Fig 5.1) (see Appendix B, Table B.1 for full dataset).

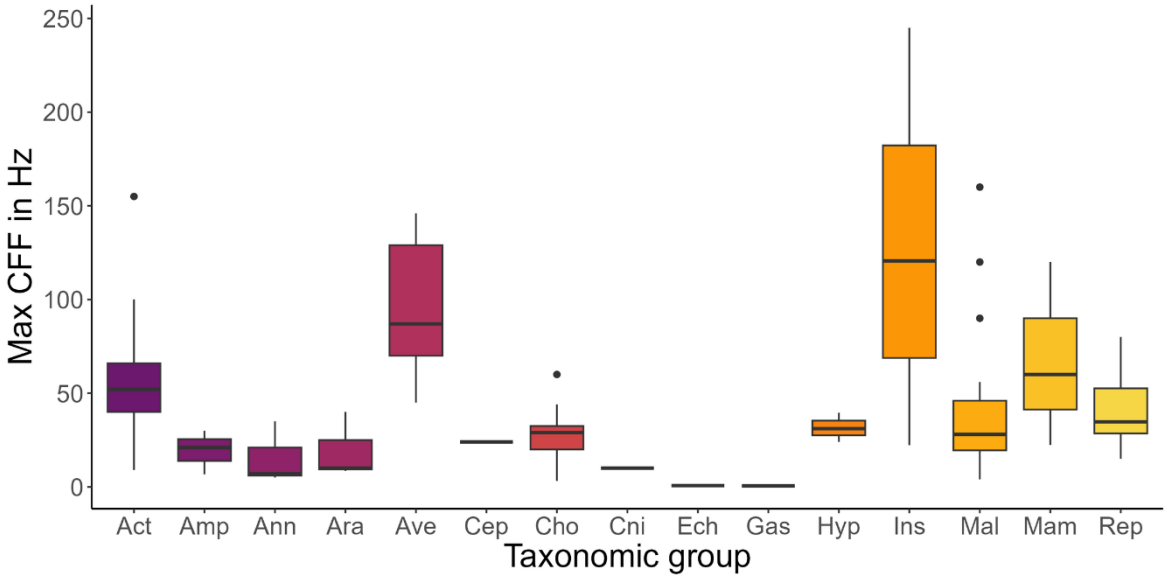

Figure 5.1. CFF distribution for different taxonomic classes. Act = Actinopterygii (n = 43), Amp = Amphibia (n = 3), Ann = Annelida (n = 3), Ara = Arachnida (n = 3), Ave = Aves (n = 17), Cep = Cephalopoda (n = 1), Cho = Chondrichthyes (n = 20), Cni = Cnidaria (n = 1), Ech = Echinodermata (n = 1), Gas = Gastropoda (n = 1), Hyp = Hyperoartia (n = 3), Ins = Insecta (n = 60), Mal = Malacostraca (n = 35), Mam = Mammalia (n = 17), Rep = Reptilia (n = 21).

As the number of CFF thresholds available for some of the taxonomic classes was extremely limited, these data may skew the effect of the random term and paint an inaccurate picture of the influence of phylogenetic class on variation in CFF thresholds. We therefore created our models with both the full dataset and with a reduced version of the dataset that excluded all taxonomic classes with three or fewer observations. The reduced dataset consisted of 213 CFF thresholds from seven classes and was only used to explore the potential effect of phylogeny on CFF. The full dataset was used to assess all other variables, as the additional data contained valid CFF measures for exploration of the fixed effects. Unless otherwise stated, all results presented below regarding fixed effects were analysed with the full dataset.

The most parsimonious model based on AIC value was made with the reduced dataset and included the fixed effects movement dimensionality, foraging strategy and luminance level (Table 5.1). According to this model, almost all explained variance in the data is explained by our fixed effects ($R_{glmm(m)}^2 = 0.57$, $R_{glmm(c)}^2 = 0.6$). In contrast, the same model made with the

full dataset including all 15 classes explains considerably more of the total variance ($R_{glmm(c)}^2$ = 0.90), but this time only a small portion is attributed to the fixed effects ($R_{glmm(m)}^2$ = 0.18) (Table 5.2). The random variable grouping vertebrates and invertebrates contained no variance and was dropped after the first model. The fixed variables foraging dimensionality and body length were not significant factors in any tested model, but removal of these variables did not substantially improve model fit.

Table 5.1. Coefficients of the most parsimonious model

Model 1			
Random effects	*Variance*	*Standard deviation*	
Class	0.00	0.06	
Residual	0.04	0.22	
Fixed effects	*Estimate*	*Standard error*	*t-value*
Intercept	1.68	0.05	33.78
MD - terrestrial	0.26	0.06	4.55
MD - volant	0.46	0.06	7.6
FS - ambush	-0.28	0.06	-4.45
FS - graze	-0.04	0.04	-1.09
Luminance - low	-0.22	0.03	-6.325

Model with response variable log10(max CFF); MD = movement dimensionality; FS = foraging strategy

Table 5.2. Comparison of model fits of the most parsimonious model made with the reduced dataset (M1) and the full dataset (M2)

Model	**Variable**	**P-value**	**AIC**	**$R_{glmm(c)}^2$**	**$R_{glmm(m)}^2$**
M1			-22.41	0.6	0.57
	Movement dimensionality	2.77×10^{-13}			
	Foraging strategy	2.84×10^{-5}			
	Luminance level	2.53×10^{-10}			
M2			25.15	0.90	0.18
	Movement dimensionality	7.18×10^{-6}			
	Foraging strategy	1×10^{-4}			
	Luminance level	1.16×10^{-9}			

Movement dimensionality

Movement dimensionality significantly affected CFF thresholds (ANOVA, P<0.001, Table 2). Mean CFF for the 3D group, represented by volant species, was 128.7 Hz, with a standard deviation (SD) of ± 61.61 Hz. Mean CFF for the 2D group, represented by terrestrial species was 61.25 (SD ± 41.34) Hz. Aquatic species had the lowest mean CFF, with 39.79 (SD ± 26.42) Hz. (Fig 5.2). All three groups significantly differed from the other two (Mann-Whitney test, U = 4195 for Aquatic:Terrestrial, U = 6261.5 for Aquatic:Volant, U = 2819 for Terrestrial:Volant, all Holm-Bonferroni corrected P-values <0.001).

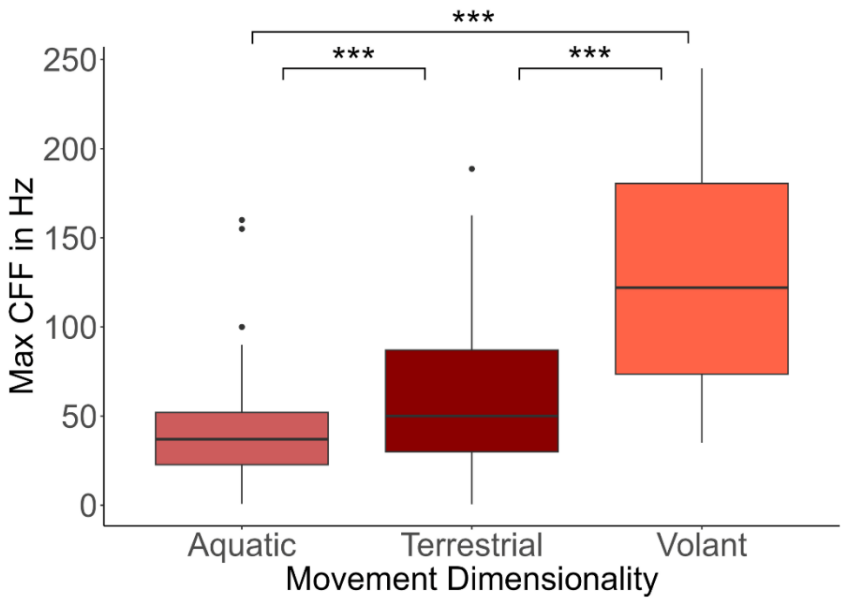

Figure 5.2. CFF distribution for the three different movement dimensionality groups. Distribution of CFF threshold for aquatic (n = 112), terrestrial (n = 57) and volant (n = 60) species. Mean CFF of all three groups were highly significantly different (P < 0.001) from those of the other groups.

Foraging strategy

Foraging strategy had a significant effect on CFF (ANOVA, P<0.001, Table 5.2). Active foragers did not differ significantly from grazers (Mann-Whitney U = 3845.5, Holm-Bonferroni corrected P = 0.93), with mean CFF thresholds of 67.31 (SD ± 43.56) Hz. and 77.35 (SD ± 62.24) Hz. respectively. Ambush foragers however had a mean CFF of 32.15 (± 18.01) Hz., significantly lower than both active foragers (Mann-Whitney U = 1433, Holm-Bonferroni corrected P<0.001) and grazers (Mann-Whitney U = 3412.5, Holm-Bonferroni corrected P<0.001) (Fig 5.3).

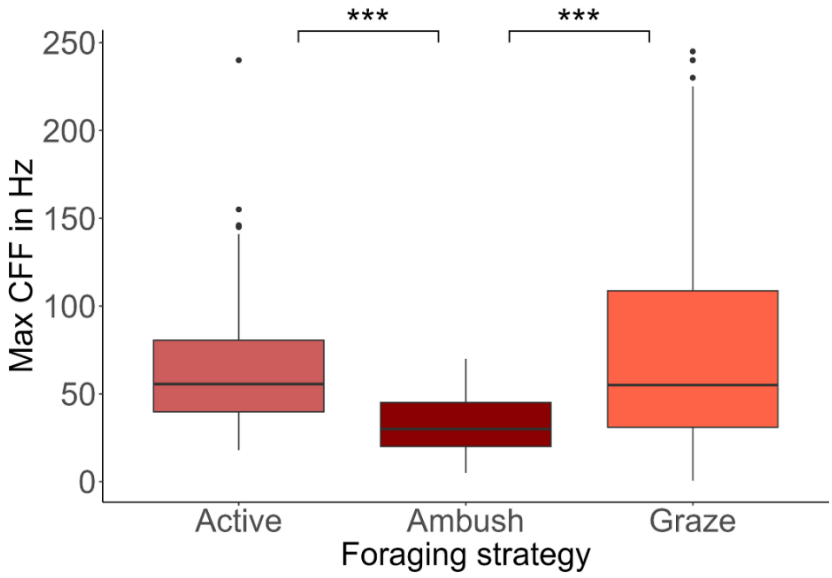

Figure 5.3. CFF distribution for different foraging strategies. Distribution of CFF thresholds for species with an active foraging strategy (n = 55), ambush foragers (n = 33) and grazers (n = 141). Ambush foragers had significantly lower CFF thresholds than both active and grazing foragers ($P < 0.001$ for each). CFF thresholds were not significantly different between active foragers and grazers.

Environmental luminance levels

Environmental luminance levels had the strongest effect on species' mean CFF (ANOVA, $P<0.001$, Table 5.2). Species inhabiting high-luminance habitats had a mean CFF of 88.24 (SD ± 57.78) and species inhabiting low-luminance habitats possessed a mean CFF of 44.62 (SD ± 42.71).

It is possible that the high CFF values found in volant species was due to the strong effect of the luminance variable (i.e. there could be a higher proportion of high-luminance species in the volant group compared to the other groups). To assess this possibility, we conducted a post-hoc analysis separating terrestrial and volant species into high-luminance and low-luminance groups. Both groups had a roughly equal number of volant and terrestrial species, and we found that volant species had significantly higher CFF thresholds than terrestrial species, both in the high-luminance group (Mann-Whitney U = 1201, Holm-Bonferroni corrected $P<0.001$) and in the low-luminance group (Mann-Whitney U = 338, Holm-Bonferroni $P<0.001$) (Fig 5.4).

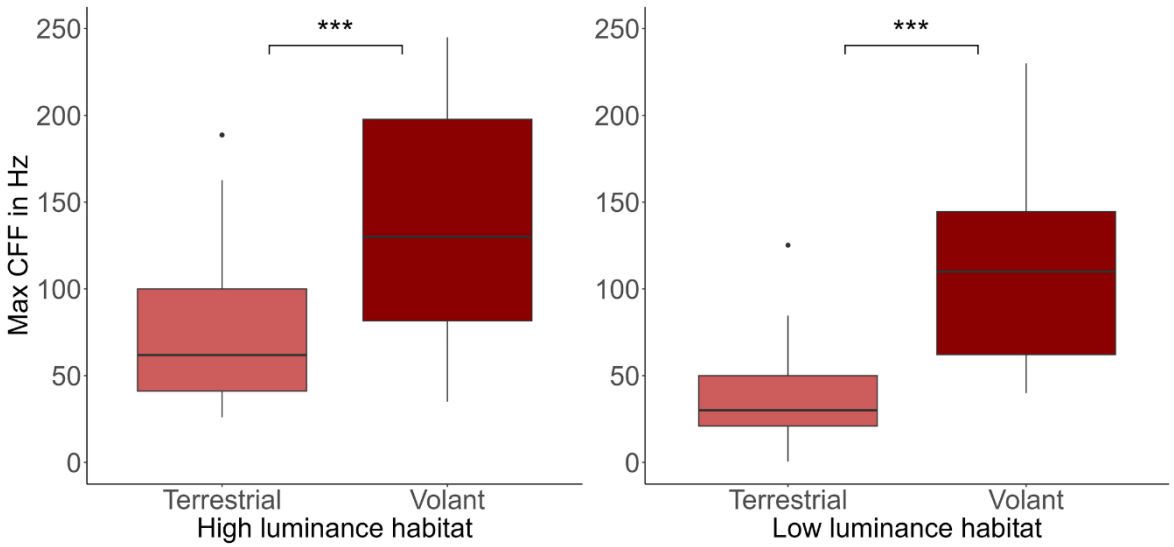

Figure 5.4. CFF comparison between volant and terrestrial species in both high- and low-luminance groups. Volant species have significantly higher CFF thresholds, regardless of the light levels in the habitat. The high luminance group consisted of 36 terrestrial species and 42 volant species. The low-luminance group consisted of 21 terrestrial species and 18 volant species.

5.5 Discussion

Movement dimensionality

Volant species possess substantially higher CFF thresholds than terrestrial species, which is consistent with previous findings made with smaller datasets (Böström et al., 2016; Inger et al., 2014; Lafitte et al., 2022). To the best of our knowledge, this is the first demonstration that CFF thresholds are higher for volant compared to terrestrial species both in high-luminance and in low-luminance habitats. In low-light conditions, where sensory information in the form of photon energy is scarce, the visual system is constrained by the necessary trade-off between high temporal resolution or high-spatial resolution. Visual systems require a minimum amount of information before it can process input. To reach this minimum information threshold, the system can either sample photon energy for short periods over a large area, resulting in low spatial resolution and high temporal resolution, or it can sample photon energy for longer periods over a smaller area, resulting in high spatial resolution but low temporal resolution (Donner, 2021; Reeves, 1996; Warrant, 1999). Most nocturnal species are theorized to be able to see in darkness by integrating the limited available light over relatively long periods (Donner, 2021; Laughlin & Weckström, 1993; Warrant, 1999; Warrant, 2008). Our finding that volant species possess high CFF thresholds even in low-

luminance habitats suggest that volancy places a strong demand on fast visual processing, even if this results in lower spatial acuity. Because the volant group is entirely comprised of only two phylogenetic classes, Aves and Insecta, it is not clear whether these higher CFF thresholds are truly due to the dimensionality aspect of volancy, or to other characteristics such as the velocity component linked with this mode of locomotion (O'Carroll et al., 1996) or shared evolutionary backgrounds and/or morphologies. One possibility to gain further insight into this is to assess whether 3D motion results in higher CFF thresholds in aquatic species as well. However, with the current dataset, we were unable to investigate this, as the number of aquatic species that move in a truly two-dimensional fashion is extremely limited. Additionally, aquatic species locomoting in two dimensions are generally benthic species inhabiting environments with very low luminance levels, which introduces a significant confounding factor. Aquatic species in general had the lowest CFF thresholds, which is most likely attributable to the different physical properties of light in water compared to air.

Foraging strategy

Foraging strategy had a highly significant effect on CFF thresholds. Active predators and grazers had similar CFF thresholds. Active predation by means of pursuit requires high-speed locomotion by both predator and prey and thus, a visual system capable of rapid integration of sensory information. During pursuit, the predator needs to maintain awareness of its own body in relation to its surroundings, as well as of the location of its prey. Escape behaviour of prey may consist of bursts of speed, along with rapid turns, which demand highly reactive sensory processing of both predator and prey (Moore & Biewener, 2015). It is therefore likely that fast visual perception has co-evolved in both active predator species and most grazing species.

Ambush predators had significantly lower CFF thresholds compared to the other two groups. As ambush predators are sessile during foraging, they do not experience the visual dynamics associated with self-generated motion, and need only to track motion induced by external sources. Ambush predators rely on rapid striking to capture prey, which is often the result of a fixed-action pattern, and as such, they also do not need to predict the prey's movement (Moore & Biewener, 2015). These adaptations make high temporal resolution less important and allow for a trade-off between a situationally more favourable high spatial resolution instead (Warrant, 1999).

Environmental luminance levels, body length and phylogeny

Consistent with previous studies, the strongest correlate with species' CFF in our models was environmental luminance level. Body length, as a measure for body size, was not a significant factor in any of our models. The effect of body size on CFF thresholds is presently unclear, as

Healy et al. (2013) found a negative relation, but Lafitte et al. (2022) found no relation. This discrepancy is possibly due to the larger datasets used, along with the inclusion of invertebrate species in both Lafitte et al. (2022) and the current study, as allometric relationships between physiological and ecological measures vary substantially both between invertebrates and vertebrates, and between different invertebrate taxonomic groups (Eberhard et al., 2011; Hendriks, 2007; Hirt et al., 2017).

For our most parsimonious model, we did not include the taxonomic classes that had three or fewer observations. In this model, almost all variance was explained by our fixed terms and almost none by the random term phylogeny. This result suggests that our measures for different environmental interaction dynamics have a larger effect on CFF thresholds in the animal kingdom than evolutionary relatedness. Though it is crucial that phylogeny is accounted for when comparing species traits, more data from multiple taxonomic classes is needed to fully explore the extent to which evolutionary relatedness may influence visual processing speed. It is also important to note that including phylogeny into statistical models as a random term does not take into account the varying degrees of relatedness of species. As such, it can provide relatively good exploratory insights, but additional phylogenetic analysis measures may need to be included if evolutionary relationships are the main focus of study.

Differences in methodology

Though previous studies have found no statistically significant effect of methodology on variation in CFF when comparing ERG with behavioural methods (Healy et al., 2013, Inger et al., 2014; Lafitte et al., 2022), it is important to note that CFF can be measured in many different ways, and no standardised methodology exists to assess visual temporal resolution among different animal species. Here, we have collated all available maximum CFF thresholds into a single dataset. Due to the lack of standardisation of methodologies, this does impose certain limitations on the type and strength of conclusions that can be drawn from analyses. However, the research that has been conducted over the last decades into the temporal processing abilities of different species remains highly valuable, and comparative analyses such as those carried out in the current study can provide an effective and practical way to identify significant ecological trends and patterns that may be linked with visual temporal processing in the animal kingdom, especially if the observed effects are relatively large.

Conclusions

We have compiled data on animal CFF threshold measurements and species-specific quantifications of several ecological parameters into what is to our knowledge the largest such dataset to date. Using this data, we have found that variation in CFF thresholds is correlated with multiple aspects of species' ecology. The range of CFF thresholds in the animal

kingdom spans several orders of magnitude, and our models did not indicate phylogenetic relatedness as a main driver for this variation. Our observations suggest that visual temporal processing is a highly flexible trait, both increasing and decreasing within- and across taxa over evolutionary time, depending on ecological demand. The high metabolic cost of fast sensory processing is likely a major constraint, maintaining high temporal resolution only in species occupying ecological niches that allow them to keep up with the high energy expenditure, and diminishing processing rates when species settle into metabolically cheaper niches. With our work, we have created a large-scale dataset which will be readily available for future research, and we have provided original insight into how a species' overall ecological profile directly links to its sensory processing abilities.

Chapter 6

Discussion

6.1 Overview

The world around us is rife with movement and changes, with forces and energies. In other words, we occupy a world full of information. To thrive in this world, it is crucial for individuals to make good use of the information available to them. This means not only collecting and processing input of varying types, but also doing so at an appropriate rate. A processing rate that is either too slow or too fast can mean you miss out on potentially valuable information about your environment, something that can have an immediate effect on fitness and survival. For animals that rely heavily on visual perception, the timely processing of visual information is thus of the utmost importance. It is therefore likely that different evolutionary selection pressures drive visual temporal processing towards an optimum, within the boundaries of a species' genetic limitations. What this optimum might be varies depending on the specific selection pressures acting on the species, or even the individual.

In this thesis, I examine visual temporal resolution with a holistic approach, investigating variation in this trait on multiple levels. The focal point of the first two data chapters is the naturally present variation among and within individuals of the same species, with healthy humans of similar ages as the focus group. In the last two data chapters, I explore several distinct ecological settings which may act as selective forces for visual temporal processing ability, both within and among species.

First, in chapter two, I show that temporal resolution varies considerably among individuals of the same species, yet is stable over time within individuals. As individual variation is necessary for natural selection to act on a trait, this finding highlights that visual temporal resolution indeed has the potential to be subject to selection pressures. The range of visual processing rates I've uncovered with this study is large enough to suggest that there may be real-world differences in how different individuals perceive certain situations. Next, in chapter three, I assess whether a specific neural oscillation may predict the rate of visual temporal processing within an individual. My results indicate a correlation between the two measures, though the link may be brittle and context-specific. The findings outlined in this chapter show a similar trend as those in chapter two, with the possible neural representative of temporal resolution again showing much greater variation among individuals than within

individuals. Additionally, the results of this chapter illustrate a potential neurobiological origin for natural within-species variation in temporal resolution, and emphasizes the direct metabolic cost of fast processing rates which may pose a constraint for the limits of variation.

In chapter four I measure visual temporal resolution in two groups of highly trained athletes, each of which occupies unique ecological settings with distinct visual dynamics, and compare them with a non-athlete control group. Though ultimately the sample sizes are insufficient to draw firm conclusions about the selective force of differing visual dynamics between the athlete groups, both athlete groups exhibit significantly higher temporal resolution than the non-athlete control. This result suggests that different degrees of cardiovascular fitness may be linked with variation in visual processing rates within a species. Lastly, in chapter five, I broaden my view to examine how different ecological variables may drive selection for different visual processing rates in the animal kingdom. I demonstrate that variation in temporal resolution among different species is linked with multiple ecological factors, such as habitat light levels, foraging strategy and the ability to fly. Moreover, I show that temporal resolution varies by several orders of magnitude, not only in the animal kingdom as a whole, but even among species within the same phyla. These findings indicate that the rate of visual processing is most likely influenced by numerous environmental, anatomical, physiological and behavioural factors which together make up a species' overall ecological profile, and that the trait has both increased and decreased, across and within taxa, depending on ecological demand.

The experimental results presented throughout this thesis have shed new light onto how visual processing rates vary, both within and among species, and how this variation may be linked with distinct ecological niches and environmental interactions. Though my work has filled several gaps in knowledge regarding the neurobiological, psychophysical and ecological background of this trait, the temporal aspect of sensory processing is a relatively understudied field, leaving many more unknowns to explore. Additionally, the findings made in each chapter of this thesis also give rise to several new questions. As such, many avenues are available for future research in this area.

6.2 Future directions

CFF measurement and individual variation

Visual temporal resolution is generally quantified using the critical flicker fusion threshold (CFF). For the experiments carried out in this thesis, I designed a novel CFF-measuring tool which is low-cost, easy to operate, portable and allows for an accurate CFF measurement in

under 10 minutes. The tool employs a shortened version of the "method of constant stimuli," the most accurate psychophysical method to measure CFF (Eisen-Enosh et al., 2017; Haarlem et al., 2024b). This tool makes it possible to measure CFF quickly, on a large scale and on-location. Though the research carried out in this thesis provides foundational insight into individual variation in visual temporal processing, much is still unclear about how and why this trait varies among individuals. For example, it is known that CFF declines with age (Brozek & Keys, 1945; Misiak, 1947; Wilson, 1963), and to eliminate this potential effect on CFF in my research, my experimental samples consisted only of individuals of similar ages, in the range of 18-35 years. However, to better understand how temporal processing ability is linked with both cognitive development and decline, measuring CFF thresholds in other age groups would be of great scientific value. Determining if and how CFF naturally fluctuates over the course of a lifetime could provide novel insights into the neurobiological development and deterioration of the trait.

Previous research has shown that CFF thresholds may temporarily be affected by certain physiological, psychological and chemical factors (Carmel et al., 2007; Hindmarch, 1982; Lambourne et al., 2010; Leigh, 1982; Presland et al., 2005; Smith & Misiak, 1976). As such, it would also be fruitful to investigate to what extent certain day-to-day activities may influence CFF in individuals, and whether these activities may have a cumulative effect. For instance, as perceptual load has been shown to affect flicker perception (Carmel et al., 2007), it is possible that our modern way of life, consisting of near-constant exposure to high intensity visual stimuli, high luminance digital images and high frequency flicker, may profoundly affect our temporal processing ability. Similarly, the regular use of consumables which may have stimulatory, depressing or sedating effects, either as part of our daily diets, or taken as supplements, medication or for recreation, may also alter CFF thresholds throughout the day, and may have an effect on how we perceive the world from moment to moment (Leigh, 1982; Hindmarch, 1982; Smith & Misiak, 1976).

Real-world perception and functional benefits

As more becomes known about individual variation in visual processing rates, possibly the most compelling question to answer is how this variation is reflected in real-world situations. Though the fact that some individuals can perceive flickering lights at frequencies where others cannot is in itself a real-life demonstration of differing visual experiences, in the context of practical, day-to-day situations, this observation is fairly abstract. Flicker consists only of the intermittent presence of photon energy and as such, it conveys very little information about an overall visual scene. Still, as I have shown in chapter five, visual temporal resolution is tightly linked with multiple ecological variables, suggesting that there are likely functional advantages to possessing specific rates of visual processing. The

correlations I have established with active foraging strategies and volancy, along with previous observations linking CFF with manoeuvrability (Boström et al., 2016; Potier et al., 2020) indicate that CFF may be associated with the ability to quickly react in dynamic environments. As such, it is expected that visual processing rate will also be linked with particular cognitive and behavioural variables such as physical reaction time, motion detection ability and decision making. Though some studies have started to look into this (Prabu Kumar et al., 2020; Tikkinen et al., 2016; Umeton et al., 2017), the research in this area is currently very limited.

It would be relatively straight-forward to correlate CFF with other individual measures of fast-paced behaviour. However, the potential relationship between CFF and an individual's overall ability to respond quickly and accurately in dynamic environments could probably be most thoroughly examined with tools that are capable of assessing links with multiple cognitive and behavioural processes at once, such as the neurally-informed computational model for perceptual decision making created by Kelly et al. (2021). This model could be employed to take into account multiple components of an individual's sensory environment during perception, and can draw links between CFF and neurophysiological variables such as evidence accumulation, urgency, decision formation and motor preparation. The utilization of a computational model such as this could provide extensive and comprehensive insight into the role that CFF plays in the overall perception of, and interaction with, dynamic environments.

Genetics, heritability and trainability

The finding that visual temporal resolution varies significantly within a healthy population leads to the question from where this variation originates. To what extent is perception speed an innate trait, and to what extent is it shaped by environmental influences? Twin studies are a widely used classical method used to tease apart the relative contribution of genetics and the environment to traits in the human population (Boomsma et al., 2002; Evans & Martin, 2000). As such, they could offer an effective approach to increase our understanding of the potential genetic basis of variation in visual temporal resolution and may determine the level of heritability and stability of the trait. Assessing variability in sensory experience through twin studies is not a new concept, and has been employed in the past to study multiple sensory modalities, including visual perception (Knaapila et al., 2012; Norbury et al., 2007; Paramei et al., 2004; Polk et al., 2007; Wise et al., 2007).

Though the research conducted in this thesis suggests that CFF thresholds are relatively stable over time within individuals, it is not known how rigid temporal resolution is over long periods, and whether certain interventions or environmental influences may induce long-

term or permanent changes in visual processing rates. This is particularly relevant in the context of potential functional benefits and drawbacks of possessing a certain temporal resolution. As future research in this area advances, one question will inevitably arise: can we train our perception speed? If the trait proves to be sensitive to manipulation, this could present the possibility to correct "poor" temporal resolution, or for individuals to alter their temporal processing to better suit specific professions or elite sports. Should the trait turn out to be rigid and untrainable, the measurement of CFF thresholds could still provide valuable information as a screening or selection tool in these same situations.

Answering questions relating to the genetic basis of temporal resolution and the heritability, stability and trainability of perception speed, would require large-scale experimental setups and substantial sample sizes. As such, this type of research is well-suited for a citizen science approach. By providing access to a standardized CFF measuring paradigm to the general public, in combination with surveys and questionnaires, large amounts of data could be collected to investigate correlations, not only between variation in CFF and genetic relatedness, but also geographical location, cultural background, physical fitness levels, profession and much more. This research could then inform which particular lifestyle factors and ecological variables may impact the temporal aspect of sensory processing, and could provide an indication of how this trait has evolved over time within a species.

Inter-species research, evolution and ecology

The critical flicker fusion threshold is not a new concept in science, and the parameter has been used to assess the temporal processing abilities of both human and animal visual systems since as early as the 1930's. The works of William John Crozier and Ernst Wolf in particular have contributed significantly to our current knowledge of the visual perception speed of different animal species (see Appendix B, Table B.1 for a selection of their publications). However, it was not until relatively recently that scientists have started to draw parallels between visual temporal resolution and the many different environmental, physiological and behavioural aspects that make up a species' ecological niche. We are continually gaining greater understanding of how evolutionary pressures drive sensory processing, and how variation in sensory processing creates specific ecological niches. Understanding sensory niches is crucial in all manner of animal research, from behavioural studies to conservation works. Knowledge of the visual temporal processing abilities of animal species may be specifically useful in the context of urbanisation and artificialization of the natural world, where more and more species are exposed to artificial flickering lights, which may affect behaviour. Studies such as those conducted by Inger et al. (2014) and Lafitte et al. (2022), which assess the ecological effects of artificial flickering lights on animal species, provide valuable information which may be used in mediation and conservation efforts.

Moreover, awareness of species' sensory temporal processing would also be beneficial in animal research with certain model species, particularly in the fields of neuroscience and comparative psychology. In these fields, the behaviour and cognition of model animal species are studied to draw comparisons with human behaviour and psychology, and as such, it is essential to understand an animal's subjective experience as accurately and precisely as possible.

In summary, temporal resolution is an intriguing, but relatively understudied aspect of visual processing. Particularly in terms of individual variation, much is still unclear about what governs this trait within an individual, how it contributes to sensory experiences and how it is driven by natural selection and evolution. As we learn more about variation in temporal resolution and its relationships with the environment, more questions arise regarding functionality, limits and limitations and the existence of distinct temporal perception niches. My thesis has provided new and original data to address some of these questions, and places previous research in new context. It also highlights the many more unknowns in this area and thus opens up novel avenues for future research in many fields of science.

Bibliography

Adrian, E. D., & Matthews, B. H. C. (1934). The Berger rhythm: potential changes from the occipital lobes in man. *Brain*, *57*, 355–385.

Al-Nimer, M. S. M., & Al-Kurashy, H. M. K. (2007). Gender differences in psychomotor performance after six minutes cycling exercise. *Journal of Medical Sciences*, *7*(8), 1345–1349.

Attwell, D., & Laughlin, S. B. (2001). An energy budget for signaling in the grey matter of the brain. *Journal of Cerebral Blood Flow and Metabolism*, *21*(10), 1133–1145. https://doi.org/10.1097/00004647-200110000-00001

Autrum, H. (1950). Die Belichtungspotentiale und das Sehen der Insekten (Untersuchungen an Calliphora und Dixippus). *Zeitschrift Für Vergleichende Physiologie*, *32*(3), 176–227. https://doi.org/10.1007/BF00344524

Barth, F. G., & Schmid, A. (Eds.).(2001). *Ecology of Sensing*. Springer-Verlag. https://doi.org/10.1007/978-3-662-22644-5

Bates, D., Maechler, M., Bolker, B., & Walker, S. (2015). Fitting linear mixed-effects models using lme4. *Journal of Statistical Software, 67*(1), 1-48. https://doi.org/10.18637/jss.v067.i01

Bartoń K. (2023). *MuMIn: Multi-Model Inference* (Version 1.47.5) [R package]. https://CRAN.R-project.org/package=MuMIn

Başar, E., Başar-Eroglu, C., Karakaş, S., & Schürmann, M. (2001). Gamma, alpha, delta, and theta oscillations govern cognitive processes. *International Journal of Psychophysiology*, *39*(2–3), 241–248. https://doi.org/10.1016/S0167-8760(00)00145-8

Beatty, D. D. (1966). A study of the succession of visual pigments in Pacific salmon (Oncorhynchus). *Canadian Journal of Zoology, 44*(3), 429–455. https://doi.org/10.1139/z66-045

Beatty, D. D. (1975). Visual pigments of the American eel Anguilla rostrata. *Vision Research, 15*(7), 771–776. https://doi.org/10.1016/0042-6989(75)90254-0

Boomsma, D., Busjahn, A., & Peltonen, L. (2002). Classical twin studies and beyond. *Nature Reviews Genetics*, *3*(11), 872–882. https://doi.org/10.1038/nrg932

Boström, J. E., Dimitrova, M., Canton, C., Håstad, O., Qvarnström, A., & Ödeen, A. (2016). Ultra-rapid vision in birds. *PLoS ONE*, *11*(3), 3–9. https://doi.org/10.1371/journal.pone.0151099

Brozek, J., & Keys, A. (1945). Changes in flicker-fusion frequency with age. *Journal of Consulting Psychology*, *9*(2), 87–90. https://doi.org/https://doi.org/10.1037/h0053488

Buergers, S., & Noppeney, U. (2022). The role of alpha oscillations in temporal binding within and across the senses. *Nature Human Behaviour*, *6*(5), 732–742. https://doi.org/10.1038/s41562-022-01294-x

Bullmore, E., & Sporns, O. (2012). The economy of brain network organization. *Nature Reviews Neuroscience*, *13*(5), 336–349. https://doi.org/10.1038/nrn3214

Burris, K., Liu, S., & Appelbaum, L. (2019). Visual-motor expertise in athletes: Insights from semiparametric modelling of 2317 athletes tested on the Nike SPARQ Sensory Station. *Journal of Sports Sciences*, *38*(3), 320–329. https://doi.org/10.1080/02640414.2019.1698090

Busch, N. A., Dubois, J., & VanRullen, R. (2009). The phase of ongoing EEG oscillations predicts visual perception. *Journal of Neuroscience*, *29*(24), 7869–7876. https://doi.org/10.1523/JNEUROSCI.0113-09.2009

Carmel, D., Saker, P., Rees, G., & Lavie, N. (2007). Perceptual load modulates conscious flicker perception. *Journal of Vision*, *7*(14), 1–13. https://doi.org/10.1167/7.14.14

Champely, S. (2020). *pwr: Basic Functions for Power Analysis* (Version 1.3-0) [R package]. https://CRAN.R-project.org/package=pwr

Chodzko-Zajko, W. J., & Moore, K. A. (1994). Physical fitness and cognitive functioning in aging. *Exercise and Sport Sciences Reviews*, *22*(1), 195–220.

Clayton, M. S., Yeung, N., & Cohen Kadosh, R. (2018). The many characters of visual alpha oscillations. *European Journal of Neuroscience*, *48*(7), 2498–2508. https://doi.org/10.1111/ejn.13747

Clemente-Suárez, V. J. (2017). The application of cortical arousal assessment to control neuromuscular fatigue during strength training. *Journal of Motor Behavior*, *49*(4), 429–434. https://doi.org/https://doi.org/10.1080/00222895.2016.1241741

Clemente-Suárez, V. J., & Diaz-Manzano, M. (2019). Evaluation of central fatigue by the critical flicker fusion threshold in cyclists. *Journal of Medical Systems*, *43*(61), 1–5. https://doi.org/https://doi.org/10.1007/s10916-019-1170-3

Cohen, M. X. (2014). Fluctuations in oscillation frequency control spike timing and coordinate neural networks. *Journal of Neuroscience, 34*(27), 8988–8998. https://doi.org/10.1523/JNEUROSCI.0261-14.2014

Collins, K., Reilly, T., Malone, S., Keane, J., & Doran, D. (2022). Science and hurling: A review. *Sports*, *10*(8), 1–20. https://doi.org/10.3390/sports10080118

Curran, S., & Wattis, J. (2000). Critical flicker fusion threshold: A potentially useful measure for the early detection of Alzheimer's disease. *Human Psychopharmacology*, *15*(2), 103–112. https://doi.org/10.1002/(SICI)1099-1077(200003)15:2<103::AID-HUP149>3.0.CO;2-7

Davranche, K., & Audiffren, M. (2004). Facilitating effects of exercise on information processing. *Journal of Sports Sciences*, *22*(5), 419–428. https://doi.org/10.1080/02640410410001675289

Davranche, K., & Pichon, A. (2005). Critical flicker frequency threshold increment after an exhausting exercise. *Journal of Sport & Exercise Psychology*, *26*, 515–520. https://doi.org/https://doi.org/10.1123/jsep.27.4.515

De Asís Fernández, F., González-Mohino, F., & González-Ravé, J. M. (2019). Assessment of sensory sensitivity through critical flicker fusion frequency thresholds after a maximum voluntary apnoea. *Diving and Hyperbaric Medicine*, *49*(3), 186–191. https://doi.org/https://doi.org/ 10.28920/dhm49.3.186-191

Del Percio, C., Brancucci, A., Vecchio, F., Marzano, N., Pirritano, M., Meccariello, E., Padoa, S., Mascia, A., Giallonardo, A. T., Aschieri, P., Lino, A., Palma, E., Fiore, A., Di Ciolo, E., Babiloni, C., & Eusebi, F. (2007). Visual event-related potentials in elite and amateur athletes. *Brain Research Bulletin*, *74*(1–3), 104–112. https://doi.org/10.1016/j.brainresbull.2007.05.011

Dick, T. J. M., & Clemente, C. J. (2017). Where Have All the Giants Gone? How Animals Deal with the Problem of Size. *PLoS Biology, 15*(1), 1–10. https://doi.org/10.1371/journal.pbio.2000473

Di Russo, F., Taddei, F., Apnile, T., & Spinelli, D. (2006). Neural correlates of fast stimulus discrimination and response selection in top-level fencers. *Neuroscience Letters*, *408*(2), 113–118. https://doi.org/10.1016/j.neulet.2006.08.085

Donner, K. (2021). Temporal vision: Measures, mechanisms and meaning. *Journal of Experimental Biology*, *224*(15), 1–15. https://doi.org/10.1242/jeb.222679

Dudley, R. (2002). Mechanisms and implications of animal flight maneuverability. *Integrative and Comparative Biology*, *42*(1), 135–140. https://doi.org/10.1093/icb/42.1.135

Eberhard, W. G., & Wcislo, W. T. (2011). Grade changes in brain-body allometry. morphological and behavioural correlates of brain size in miniature spiders, insects and other invertebrates. In *Advances in Insect Physiology* (1st ed., Vol. 40). Elsevier Ltd. https://doi.org/10.1016/B978-0-12-387668-3.00004-0

Eisen-Enosh, A., Farah, N., Burgansky-Eliash, Z., Polat, U., & Mandel, Y. (2017). Evaluation of critical flicker-fusion frequency measurement methods for the investigation of visual temporal resolution. *Scientific Reports*, *7*(1). https://doi.org/https://doi.org/10.1038/s41598-017-15034-z

Emery, K. J., & Webster, M. A. (2019). Individual differences and their implications for color perception. *Current Opinion in Behavioral Sciences*, *30*, 28–33. https://doi.org/10.1016/j.cobeha.2019.05.002

Ergenoglu, T., Demiralp, T., Bayraktaroglu, Z., Ergen, M., Beydagi, H., & Uresin, Y. (2004). Alpha rhythm of the EEG modulates visual detection performance in humans. *Cognitive Brain Research*, *20*(3), 376–383. https://doi.org/10.1016/j.cogbrainres.2004.03.009

Etnier, J., Salazar, W., Landers, D. M., Petruzzello, S. J., Han, M., & Nowell, P. (1997). The influence of physical fitness and exercise upon cognitive functioning: A meta-analysis. *Journal of Sport and Exercise Psychology*, *19*(3), 249–277.

Evans, D. M., & Martin, N. G. (2000). The validity of twin studies. *GeneScreen*, *1*(2), 77–79. https://doi.org/10.1046/j.1466-9218.2000.00027.x

Fajen, B. R., & Matthis, J. S. (2013). Visual and non-visual contributions to the perception of object motion during self-motion. *PLoS ONE*, *8*(2). https://doi.org/10.1371/journal.pone.0055446

Fernald, R. D. (2006). Casting a genetic light on the evolution of eyes. *Science*, *313*(5795), 1914–1918. https://doi.org/10.1126/science.1127889

Fox, J., & Weisberg, S. (2019). *An R Companion to Applied Regression* (3rd ed.). Sage, Thousand Oaks CA.

Frossard J. & Renaud, O. (2021). Permutation tests for regression, ANOVA, and comparison of signals: The permuco package. *Journal of Statistical Software, 99*(15), 1-32. https://doi.org/10.18637/jss.v099.i15

Fuentes, J. P., Villafaina, S., Collado-Mateo, D., de la Vega, R., Gusi, N., & Clemente-Suárez, V. J. (2018). Use of biotechnological devices in the quantification of psychophysiological workload of professional chess Players. *Journal of Medical Systems*, *42*(3). https://doi.org/https://doi.org/10.1007/s10916-018-0890-0

Gescheider, G. A. (1984). *Psychophysics: Method, Theory and Application* (2nd ed.). Psychology Press.

Ginsburg, N., Jurenovskis, M., & Jamieson, J. (1982). Sex differences in critical flicker frequency. *Perceptual and Motor Skills*, *54*(3 Pt 2), 1079–1082. https://doi.org/10.2466/pms.1982.54.3c.1079

Godefroy, D., Rousseu, C., Vercruyssen, F., Crémieux, J., & Brisswalter, J. (2002). Influence of physical exercise on perceptual response in aerobically trained subjects. *Perceptual and Motor Skills*, *94*(1), 68–70. https://doi.org/10.2466/pms.2002.94.1.68

Gomez-Pinilla, F., & Hillman, C. (2013). The influence of exercise on cognitive abilities. *Comprehensive Physiology*, *3*(1), 403–428. https://doi.org/10.1002/cphy.c110063

Grothe, B., & Klump, G. M. (2000). Temporal processing in sensory systems. *Current Opinion in Neurobiology*, *10*(4), 467–473. https://doi.org/10.1016/S0959-4388(00)00115-X

Haarlem, C.S., Hynes, C., Jackson, A.L., Mitchell, K.J., O'Connell, R.G., Healy, K. (2025). Pace of ecology drives temporal perception across the Animal Kingdom. [Manuscript in preparation]

Haarlem, C. S., Mitchell, K. J., Jackson, A. L., & O'Connell, R. G. (2024a). Individual peak alpha frequency correlates with visual temporal resolution, but only under specific task conditions. *European Journal of Neuroscience*, *August*, 1–14. https://doi.org/10.1111/ejn.16519

Haarlem, C. S., O'Connell, R. G., Mitchell, K. J., & Jackson, A. L. (2024b). The speed of sight: Individual variation in critical flicker fusion thresholds. *PLoS ONE*, *19*(4 April), 1–13. https://doi.org/10.1371/journal.pone.0298007

Halpern, S. D., Andrews, T. J., & Purves, D. (1999). Interindividual variation in human visual performance. *Journal of Cognitive Neuroscience*, *11*(5), 521–534. https://doi.org/10.1162/089892999563580

Hanslmayr, S., Klimesch, W., Sauseng, P., Gruber, W., Doppelmayr, M., Freunberger, R., & Pecherstorfer, T. (2005). Visual discrimination performance is related to decreased alpha amplitude but increased phase locking. *Neuroscience Letters*, *375*(1), 64–68. https://doi.org/10.1016/j.neulet.2004.10.092

Harris, A. M. (2023). Phase resets undermine measures of phase-dependent perception. *Trends in Cognitive Sciences*, *27*(3), 224–226. https://doi.org/10.1016/j.tics.2022.12.008

Harris, L. R., Jenkin, M., & Zikovitz, D. C. (2000). Visual and non-visual cues in the perception of linear self motion. *Experimental Brain Research*, *135*(1), 12–21. https://doi.org/10.1007/s002210000504

Healy, K., McNally, L., Ruxton, G. D., Cooper, N., & Jackson, A. L. (2013). Metabolic rate and body size are linked with perception of temporal information. *Animal Behaviour*, *86*(4), 685–696. https://doi.org/10.1016/j.anbehav.2013.06.018

Hecht, S., & Shlaer, S. (1936). Intermittent stimulation by light: V. the relation between intensity and critical frequency for different parts of the spectrum. *Journal of General Physiology*, *19*(6), 965–977. https://doi.org/10.1085/jgp.19.6.965

Hecht, S., & Verrijp, C. D. (1933). The influence of intensity, color and retinal location on the fusion frequency of intermittent illumination. *Proc Natl Acad Sci USA*, *19*(5), 522–535. https://doi.org/10.1073/pnas.19.5.522

Hemelryck, W., Rozloznik, M., Germonpré, P., Balestra, C., & Lafère, P. (2013). Functional comparison between critical flicker fusion frequency and simple cognitive tests in subjects breathing air or oxygen in normobaria. *Diving and Hyperbaric Medicine*, *43*(3), 138–142.

Hendriks, A. J. (2007). The power of size: A meta-analysis reveals consistency of allometric regressions. *Ecological Modelling*, *205*(1–2), 196–208. https://doi.org/10.1016/j.ecolmodel.2007.02.029

Herzog, M. H., Kammer, T., & Scharnowski, F. (2016). Time slices: What is the duration of a percept? *PLoS Biology*, *14*(4). https://doi.org/10.1371/journal.pbio.1002433

Himmelberg, M. M., Winawer, J., & Carrasco, M. (2022). Linking individual differences in human primary visual cortex to contrast sensitivity around the visual field. *Nature Communications*, *13*(1), 1–13. https://doi.org/10.1038/s41467-022-31041-9

Hindmarch, I. (1982). Critical flicker fusion frequency (CFF): The effects of psychotropic compounds. *Pharmacopsychiatry*, *15*(S 1), 44–48. https://doi.org/10.1055/s-2007-1019549

Hirt, M. R., Jetz, W., Rall, B. C., & Brose, U. (2017). A general scaling law reveals why the largest animals are not the fastest. *Nature Ecology and Evolution*, *1*(8), 1116–1122. https://doi.org/10.1038/s41559-017-0241-4

Hosea, T. M., & Hannafin, J. A. (2012). Rowing injuries. *Sports Health*, *4*(3), 236–245. https://doi.org/10.1177/1941738112442484

Inger, R., Bennie, J., Davies, T. W., & Gaston, K. J. (2014). Potential biological and ecological effects of flickering artificial light. *PLoS ONE*, *9*(5), 98631. https://doi.org/10.1371/journal.pone.0098631.t001

Jeffery, W. R. (2005). Adaptive evolution of eye degeneration in the Mexican blind cavefish. *Journal of Heredity*, *96*(3), 185–196. https://doi.org/10.1093/jhered/esi028

Jenssen, T. A., & Swenson, B. (1974). An ecological correlate of critical flicker-fusion frequencies for some Anolis lizards. *Vision Research, 14*(10), 965–970. https://doi.org/10.1016/0042-6989(74)90164-3

Kaur, V., Walia, L., & Singh, R. (2020). Critical flicker fusion frequency: Effect of age, gender, sleep and display Screens. *International Journal of Contemporary Medical Research [IJCMR]*, *7*(6), 9–12. https://doi.org/10.21276/ijcmr.2020.7.6.20

Kayser, J., & Tenke, C. E. (2006). Principal components analysis of Laplacian waveforms as a generic method for identifying ERP generator patterns: I. Evaluation with auditory oddball tasks. *Clinical Neurophysiology*, *117*(2), 348–368. https://doi.org/10.1016/j.clinph.2005.08.034

Kayser, J., & Tenke, C. E. (2015). On the benefits of using surface Laplacian (Current Source Density) methodology in electrophysiology. *International Journal of Psychophysiology*, *97*(3), 171–173. https://doi.org/10.1016/j.ijpsycho.2015.06.001

Keil, J., & Senkowski, D. (2018). Neural oscillations orchestrate multisensory processing. *Neuroscientist*, *24*(6), 609–626. https://doi.org/10.1177/1073858418755352

Keitel, C., Ruzzoli, M., Dugué, L., Busch, N. A., & Benwell, C. S. Y. (2022). Rhythms in cognition: The evidence revisited. *European Journal of Neuroscience*, *55*(11–12), 2991–3009. https://doi.org/10.1111/ejn.15740

Kelly, D. H. (1961). Visual responses to time-dependent stimuli. I. Amplitude sensitivity measurements. *Journal of the Optical Society of America*, *51*(4), 422–429.

Kelly, S. P., Corbett, E. A., & O'Connell, R. G. (2021). Neurocomputational mechanisms of prior-informed perceptual decision-making in humans. *Nature Human Behaviour*, *5*(4), 467–481. https://doi.org/10.1038/s41562-020-00967-9

Kingston, A. C. N., Chappell, D. R., & Speiser, D. I. (2020). A snapping shrimp has the fastest vision of any aquatic animal: Fast vision in snapping shrimp. *Biology Letters*, *16*(6). https://doi.org/10.1098/rsbl.2020.0298rsbl20200298

Klimesch, W. (2012). Alpha-band oscillations, attention, and controlled access to stored information. *Trends in Cognitive Sciences*, *16*(12), 606–617. https://doi.org/10.1016/j.tics.2012.10.007

Knaapila, A., Hwang, L. D., Lysenko, A., Duke, F. F., Fesi, B., Khoshnevisan, A., James, R. S., Wysocki, C. J., Rhyu, M. R., Tordoff, M. G., Bachmanov, A. A., Mura, E., Nagai, H., & Reed, D. R. (2012). Genetic analysis of chemosensory traits in human twins. *Chemical Senses*, *37*(9), 869–881. https://doi.org/10.1093/chemse/bjs070

Kowalko, J. (2020). Utilizing the blind cavefish Astyanax mexicanus to understand the genetic basis of behavioral evolution. *Journal of Experimental Biology*, *223*. https://doi.org/10.1242/jeb.208835

Lafitte, A., Sordello, R., Legrand, M., Nicolas, V., Obein, G., & Reyjol, Y. (2022). A flashing light may not be that flashy: A systematic review on critical fusion frequencies. *PloS ONE*, *17*(12), e0279718. https://doi.org/10.1371/journal.pone.0279718

Lambourne, K., Audiffren, M., & Tomporowski, P. D. (2010). Effects of acute exercise on sensory and executive processing tasks. *Medicine and Science in Sports and Exercise*, *42*(7), 1396–1402. https://doi.org/10.1249/MSS.0b013e3181cbee11

Land, M. F., & Nilsson, D.-E. (2012). *Animal Eyes* (2nd ed.). Oxford University Press.

Lappin, J. S., Tadin, D., Nyquist, J. B., & Corn, A. L. (2009). Spatial and temporal limits of motion perception across variations in speed, eccentricity, and low vision. *Journal of Vision*, *9*(1), 1–14. https://doi.org/10.1167/9.1.30

Laughlin, S. B. (2001). The Metabolic Cost of Information- a Fundamental Factor in Visual Ecology. *Ecology of Sensing*, 169–185. https://doi.org/10.1007/978-3-662-22644-5_9

Laughlin, S. B., De Ruyter van Steveninck, R. R., & Anderson, J. C. (1998). The metabolic cost of neural information. *Nature Neuroscience*, *1*(1), 36–41.

Laughlin, S. B., & Weckström, M. (1993). Fast and slow photoreceptors - a comparative study of the functional diversity of coding and conductances in the Diptera. *Journal of Comparative Physiology A*, *172*(5), 593–609. https://doi.org/10.1007/BF00213682

Leigh, G. (1982). The combined effects of alcohol consumption and cigarette smoking on critical flicker frequency. *Addictive Behaviors*, *7*(3), 251–259. https://doi.org/10.1016/0306-4603(82)90052-1

Li, Y., Koldenhoven, R. M., Jiwan, N. C., Zhan, J., & Liu, T. (2021). Intra-trunk and arm coordination displayed by Olympic rowing athletes. *Sports Biomechanics*, *23*(5), 655–669. https://doi.org/10.1080/14763141.2021.1883728

Liu, M., Yan, Y., Xue, Q., & Gong, L. (2015). The research and analysis of factors affecting critical flicker frequency. *Procedia Manufacturing*, *3*, 4279–4286. https://doi.org/10.1016/j.promfg.2015.07.417

Lloyd, V. V. (1952). A comparison of critical fusion frequencies for different areas in the fovea and periphery. *The American Journal of Psychology*, *65*(3), 346–357. https://doi.org/https://doi.org/10.2307/1418757

Maciejewska, K., Greń, A., & Wieczorek, A. (2020). The effect of acute, moderate intensity indoor cycling on the temporal resolution of human vision system, measured by critical fusion frequency. *Physiological Reports*, *8*(21). https://doi.org/https://doi.org/10.14814/phy2.14618

Mackie, J. B., & Beck, E. C. (1965). Relations among age, intelligence, and critical flicker fusion. *Perception and Motor Skills*, *21*, 875–878. https://doi.org/10.2466/pms.1965.21.3.875

Mäestu, J., Jürimäe, J., & Jürimäe, T. (2005). Monitoring of performance and training in rowing. *Sports Medicine*, *35*(7), 597–617.

Mankowska, N. D., Marcinkowska, A. B., Waskow, M., Sharma, R. I., Kot, J., & Winklewski, P. J. (2021). Critical flicker fusion frequency: A narrative review. *Medicina (Lithuania)*, *57*(10), 1–9. https://doi.org/10.3390/medicina57101096

Mark, H. J., Meier, P., & Pasamanick, B. (1958). Variability of critical flicker fusion in brain injured children. *Archives of Neurology and Psychiatry*, *80*(682–688). https://doi.org/https://doi.org/10.1001/archneurpsyc.1958.02340120018003

Mathewson, K. E., Gratton, G., Fabiani, M., Beck, D. M., & Ro, T. (2009). To see or not to see: Prestimulus α phase predicts visual awareness. *Journal of Neuroscience*, *29*(9), 2725–2732. https://doi.org/10.1523/JNEUROSCI.3963-08.2009

McComb, D. M., Frank, T. M., Hueter, R. E., & Kajiura, S. M. (2010). Temporal resolution and spectral sensitivity of the visual system of three coastal shark species from different light environments. *Physiological and Biochemical Zoology*, *83*(2), 299–307. https://doi.org/10.1086/648394

McKay, A. K. A., Stellingwerff, T., Smith, E. S., Martin, D. T., Mujika, I., Goosey-Tolfrey, V. L., Sheppard, J., & Burke, L. M. (2022). Defining training and performance caliber: A participant classification framework. *International Journal of Sports Physiology and Performance*, *17*(2), 317–331. https://doi.org/10.1123/ijspp.2021-0451

Michail, G., Toran Jenner, L., & Keil, J. (2022). Prestimulus alpha power but not phase influences visual discrimination of long-duration visual stimuli. *European Journal of Neuroscience*, *55*(11–12), 3141–3153. https://doi.org/10.1111/ejn.15169

Misiak, H. (1947). Age and sex differences in critical flicker frequency. *Journal of Experimental Psychology*, *37*(4), 318–332. https://doi.org/https://doi.org/10.1037/h0061531

Moore, T. Y., & Biewener, A. A. (2015). Outrun or outmaneuver: Predator-prey interactions as a model system for integrating biomechanical studies in a broader ecological and evolutionary context. *Integrative and Comparative Biology*, *55*(6), 1188–1197. https://doi.org/10.1093/icb/icv074

Morrow, A., & Samaha, J. (2022). No evidence for a single oscillator underlying discrete visual percepts. *European Journal of Neuroscience*, *55*(11–12), 3054–3066. https://doi.org/10.1111/ejn.15362

Murphy, J. C., Gissane, C., & Blake, C. (2012). Injury in elite county-level hurling: A prospective study. *British Journal of Sports Medicine*, *46*(2), 138–142. https://doi.org/10.1136/bjsm.2010.072132

Muth, T., Schipke, J. D., Brebeck, A. K., & Dreyer, S. (2023). Assessing critical flicker fusion frequency: which confounders? A narrative review. *Medicina*, *59*(800), 1–12. https://doi.org/10.3390/medicina59040800

Nelli, S., Itthipuripat, S., Srinivasan, R., & Serences, J. T. (2017). Fluctuations in instantaneous frequency predict alpha amplitude during visual perception. *Nature Communications*, *8*(1). https://doi.org/10.1038/s41467-017-02176-x

Niven, J. E., & Laughlin, S. B. (2008). Energy limitation as a selective pressure on the evolution of sensory systems. *Journal of Experimental Biology*, *211*(11), 1792–1804. https://doi.org/10.1242/jeb.017574

Norbury, T. A., MacGregor, A. J., Urwin, J., Spector, T. D., & McMahon, S. B. (2007). Heritability of responses to painful stimuli in women: A classical twin study. *Brain*, *130*(11), 3041–3049. https://doi.org/10.1093/brain/awm233

O'Carroll, D. C., Bidwell, N. J., Laughlin, S. B., & Warrant, E. J. (1996). Insect motion detectors matched to visual ecology. *Nature, 382*(6586), 63–66. https://doi.org/10.1038/382063a0

Oostenveld, R., & Praamstra, P. (2001). The five percent electrode system for high-resolution EEG and ERP measurements. *Clinical Neurophysiology*, *112*(4), 713–719. https://doi.org/10.1016/S1388-2457(00)00527-7

Paramei, G. V., Bimler, D. L., & Mislavskaia, N. O. (2004). Colour perception in twins: individual variation beyond common genetic inheritance. *Clinical and Experimental Optometry*, *87*(4–5), 305–312. https://doi.org/10.1111/j.1444-0938.2004.tb05059.x

Parkin, C., Kerr, J. S., & Hindmarch, I. (1997). The effects of practice on choice reaction time and critical flicker fusion threshold. *Human Psychopharmacology*, *12*, 65–70.

Pawar, S., Dell, A. I., & Savage, V. M. (2012). Dimensionality of consumer search space drives trophic interaction strengths. *Nature*, *486*(7404), 485–489. https://doi.org/10.1038/nature11131

Pernet, C. R., Wilcox, R., & Rousselet, G. A. (2013). Robust correlation analyses: False positive and power validation using a new open source matlab toolbox. *Frontiers in Psychology*, *3*(JAN), 1–18. https://doi.org/10.3389/fpsyg.2012.00606

Petie, R., Hall, M. R., Hyldahl, M., & Garm, A. (2016). Visual orientation by the crown-of-thorns starfish (Acanthaster planci). *Coral Reefs*, *35*(4), 1139–1150. https://doi.org/10.1007/s00338-016-1478-0

Pfurtscheller, G., Stancák, A., & Neuper, C. (1996). Event-related synchronization (ERS) in the alpha band - An electrophysiological correlate of cortical idling: A review. *International Journal of Psychophysiology*, *24*(1–2), 39–46. https://doi.org/10.1016/S0167-8760(96)00066-9

Ploughman, M. (2008). Exercise is brain food: The effects of physical activity on cognitive function. *Developmental Neurorehabilitation*, *11*(3), 236–240. https://doi.org/10.1080/17518420801997007

Polk, T. A., Park, J., Smith, M. R., & Park, D. C. (2007). Nature versus nurture in ventral visual cortex: A functional magnetic resonance imaging study of twins. *Journal of Neuroscience*, *27*(51), 13921–13925. https://doi.org/10.1523/JNEUROSCI.4001-07.2007

Posit team (2023). *RStudio: Integrated Development Environment for R* (Version 2023.3.0.386). Posit Software, PBC, Boston, MA. http://www.posit.co/

Potier, S., Lieuvin, M., Pfaff, M., & Kelber, A. (2020). How fast can raptors see? *Journal of Experimental Biology*, *223*(1). https://doi.org/10.1242/jeb.209031

Prabu Kumar, A., Omprakash, A., Kuppusamy, M., Maruthy, K. N., Sathiyasekaran, B. W. C., Vijayaraghavan, P. V., & Padmavathi, R. (2020). How does cognitive function measured by the reaction time and critical flicker fusion frequency correlate with the academic performance of students? *BMC Medical Education*, *20*(1), 1–12. https://doi.org/10.1186/s12909-020-02416-7

Presland, J. D., Dowson, M. N., & Cairns, S. P. (2005). Changes of motor drive, cortical arousal and perceived exertion following prolonged cycling to exhaustion. *European Journal of Applied Physiology*, *95*(1), 42–51. https://doi.org/10.1007/s00421-005-1395-3

Prins, N. & Kingdom, F. A. A. (2018). Applying the model-comparison approach to test specific research hypotheses in psychophysical research using the palamedes toolbox. *Frontiers in psychology, 9*(1250). https://doi.org/10.3389/fpsyg.2018.01250

R Core Team (2022). *R: A language and environment for statistical computing* (Version 4.2.1). R Foundation for Statistical Computing, Vienna, Austria. https://www.R-project.org/

Reeves, A. (1996). Temporal resolution in visual perception. In W. Prinz & B. Bridgeman (Eds.), *Handbook of Perception and Action* (1st ed.). Academic Press Ltd. https://doi.org/10.1016/S1874-5822(96)80004-1

Regal, D. M. (1981). Development of critical flicker frequency in human infants. *Vision Research*, *21*(4), 549–555. https://doi.org/https://doi.org/10.1016/0042-6989(81)90100-0

Rich, J., Lieberman, L. J., Beach, P., & Perreault, M. (2022). "Moving freely in space with power and not be afraid": An interpretative phenomenological analysis of the experiences of elite rowers with visual impairment. *International Journal of Environmental Research and Public Health*, *19*(21). https://doi.org/10.3390/ijerph192114059

Rider, A. T., Bruce Henning, G., & Stockman, A. (2019). Light adaptation controls visual sensitivity by adjusting the speed and gain of the response to light. *PLoS ONE*, *14*(8), 1–34. https://doi.org/10.1371/journal.pone.0220358

Rousseeuw, P. J. (1984). Least median of squares regression. *Journal of the American Statistical Association*, *79*(388), 871–880. https://doi.org/10.1080/01621459.1984.10477105

Rousseeuw, P. J., & Van Driessen, K. (1999). A Fast Algorithm for the Minimum Covariance Determinant Estimator. *Technometrics 212*(23).

Ruzzoli, M., Torralba, M., Morís Fernández, L., & Soto-Faraco, S. (2019). The relevance of alpha phase in human perception. *Cortex*, *120*, 249–268. https://doi.org/10.1016/j.cortex.2019.05.012

Samaha, J., & Postle, B. R. (2015). The speed of alpha-band oscillations predicts the temporal resolution of visual perception. *Current Biology*, *25*(22), 1–6. https://doi.org/10.1016/j.cub.2015.10.007

Sato, K., Watanuki, Y., Takahashi, A., Miller, P. J. O., Tanaka, H., Kawabe, R., Ponganis, P. J., Handrich, Y., Akamatsu, T., Watanabe, Y., Mitani, Y., Costa, D. P., Bost, C. A., Aoki, K., Amano, M., Trathan, P., Shapiro, A., & Naito, Y. (2007). Stroke frequency, but not swimming speed, is related to body size in free-ranging seabirds, pinnipeds and cetaceans. *Proceedings of the Royal Society B: Biological Sciences*, *274*(1609), 471–477. https://doi.org/10.1098/rspb.2006.0005

Schaffert, N., & Mattes, K. (2015). Effects of acoustic feedback training in elite-standard Para-rowing. *Journal of Sports Sciences*, *33*(4), 411–418. https://doi.org/10.1080/02640414.2014.946438

Schroeder, C. E., & Lakatos, P. (2009). Low-frequency neuronal oscillations as instruments of sensory selection. *Trends in Neurosciences*, *32*(1), 9–18. https://doi.org/10.1016/j.tins.2008.09.012

Smith, C. U. M. (2008). *Biology of Sensory Systems* (2nd ed.). John Wiley & Sons, Ltd. https://doi.org/10.1016/s0166-2236(00)01615-5

Smith, J. M., & Misiak, H. (1976). Critical flicker frequency (CFF) and psychotropic drugs in normal human subjects-A review. *Psychopharmacology*, *47*(2), 175–182. https://doi.org/10.1007/BF00735818

Stockwell, E. F. (2001). Morphology and flight manoeuvrability in New World leaf-nosed bats (Chiroptera: Phyllostomidae). *Journal of Zoology*, *254*(4), 505–514. https://doi.org/10.1017/S0952836901001005

The MathWorks Inc. (2022). *MATLAB* version 9.11.0.1837725 (R2021b), Natick, Massachusetts: The MathWorks Inc. https://www.mathworks.com

Tikkinen, J., Wuorimaa, T., & Siimes, M. (2016). A comparison of simple reaction time, visual discrimination and critical flicker fusion frequency in professional divers at elevated pressure. *Diving and Hyperbaric Medicine*, *46*(2).

Tucker, R., & Collins, M. (2012). What makes champions? A review of the relative contribution of genes and training to sporting success. *British Journal of Sports Medicine*, *46*(8), 555–561. https://doi.org/10.1136/bjsports-2011-090548

Umeton, D., Read, J. C. A., & Rowe, C. (2017). Unravelling the illusion of flicker fusion. *Biology Letters*, *13*(2). https://doi.org/10.1098/rsbl.2016.0831

VanRullen, R., & Koch, C. (2003). Is perception discrete or continuous? *Trends in Cognitive Sciences*, *7*(5), 207–213. https://doi.org/10.1016/S1364-6613(03)00095-0

Verboven, S., & Hubert, M. (2005). LIBRA: A MATLAB library for robust analysis. *Chemometrics and Intelligent Laboratory Systems*, *75*(2), 127–136. https://doi.org/10.1016/j.chemolab.2004.06.003

Voeten, C. C. (2022). *permutes: Permutation Tests for Time Series Data* (Version 2.6) [R package]. https://CRAN.R-project.org/package=permutes

Ward, L. M. (2003). Synchronous neural oscillations and cognitive processes. *Trends in Cognitive Sciences*, *7*(12), 553–559. https://doi.org/10.1016/j.tics.2003.10.012

Warrant, E. J. (1999). Seeing better at night: Life style, eye design and the optimum strategy of spatial and temporal summation. *Vision Research*, *39*(9), 1611–1630. https://doi.org/10.1016/S0042-6989(98)00262-4

Warrant, E. J. (2008). Seeing in the dark: Vision and visual behaviour in nocturnal bees and wasps. *Journal of Experimental Biology*, *211*(11), 1737–1746. https://doi.org/10.1242/jeb.015396

Warren, W. H. (1995). Self-motion: Visual perception and visual control. In *Perception of Space and Motion* (pp. 263–325). Academic Press, Inc. https://doi.org/10.1016/b978-012240530-3/50010-9

Wilson, T. (1963). Flicker fusion frequency, age and intelligence. *Gerontologia*, *7*, 200–208. https://doi.org/https://doi.org/10.1159/000211196

Wise, P. M., Hansen, J. L., Reed, D. R., & Breslin, P. A. S. (2007). Twin study of the heritability of recognition thresholds for sour and salty taste. *Chemical Senses*, *32*(8), 749–754. https://doi.org/10.1093/chemse/bjm042

Witting, L. (2023). On the natural selection of body mass allometries. *Acta Oecologica, 118*, 1-13. https://doi.org/10.1016/j.actao.2023.103889

Yokoyama, S., & Yokoyama, R. (1996). Adaptive evolution of photoreceptors and visual pigments in vertebrates. Annual Review of Ecology and Systematics, 27, 543–567. https://doi.org/10.1146/annurev.ecolsys.27.1.543

Young, D., Mourot, L., & Coratella, G. (2018). Match-play performance comparisons between elite and sub-elite hurling players. *Sport Sciences for Health*, *14*(1), 201–208. https://doi.org/10.1007/s11332-018-0441-6

Appendix A | Supplementary material for chapter 3

Linear modelling results

Linear models were created to assess the structure of the data before any correlation analyses. Analyses were conducted with base R (version 4.2.1, R Core Team 2021) and RStudio (version 2023.3.0.386, Posit Team 2023) functions, as well as functions from the "car" package (Fox & Weinberg, 2019). The following assumptions were tested for each model:

- Linearity of the data, with the function "ResidualPlots" and Tukey's one-degree-of-freedom test, for which the null hypothesis represents a linear relationship (P-values listed in tables as "Tukey").
- Homoscedasticity of residuals, with Non-Constant Error Variance testing, using the function "ncvTest," for which the null-hypothesis represents homoskedasticity (P-values listed in tables as "ncv").
- Normality of residuals, assessed visually with Quantile-Quantile plots and numerically with Shapiro tests (P-values listed in tables as "Shapiro").
- Absence of outliers, with the function "InfluenceIndexPlots," which returns values for: 1) Cook's Distance, as a measure for individual point influence (listed in tables as "Cook"), 2) hat value, as a measure for leverage of fitted values (listed in tables as "Hat") and 3) Bonferroni p-value, as a measure for individual point significance (listed in tables as "Bonf").

Additionally, post-hoc correlation analyses were performed on all models using the Matlab (version 2.11.0.1837725, The Mathworks Inc, 2022) toolbox "Robust correlations" (Pernet et al., 2013), which has the capacity to run correlation analyses both before and after automatic outlier removal. Unless stated otherwise, we observed no difference between the correlation tests performed in R and those performed in Matlab.

A1. Eyes-closed EEG recording

Eyes-closed EEG-data was recorded for two minutes prior to starting the flash-fusion task and for two minutes after task completion. To assess how these two recordings compare with each other, and how the corresponding peak alpha frequency of each recording correlates with flash-fusion thresholds, we created the following three linear models:

Model 1: flash-fusion threshold ~ peak alpha frequency extracted from CSD-transformed pre-task EEG recording

Model 2: flash-fusion threshold ~ peak alpha frequency extracted from CSD-transformed post-task EEG recording

Model 3: flash-fusion threshold ~ peak alpha frequency extracted from mean of CSD-transformed pre-task and post-task EEG recording

All three models indicated a correlation between flash-fusion threshold and peak alpha frequency (Table a1). Peak alpha frequency extracted from pre-task EEG recording was highly correlated with peak alpha frequency extracted from post-task EEG recording (Pearson's r = 0.91, P = 1.602e-12), and all models resulted returned similar analysis results. Therefore, all further eyes-closed alpha analyses were conducted using the mean of the pre-task and post-task EEG recordings.

Table A.1. Results from analyses of linear models 1, 2 and 3. P-values printed in bold indicate a significant result.

Model	Tukey	ncv	Shapiro	Cook	Hat	Bonf	Model P
1	0.178	0.119	0.834	< 0.5	0.05 – 0.3	> 0.05	**0.022**
2	0.290	0.249	0.25	< 0.3	0.1 – 0.4	> 0.05	**0.019**
3	0.199	0.214	0.422	< 0.5	0.1 – 0.4	> 0.05	**0.018**

The next set of models was constructed to test if eyes-closed alpha peak frequency was correlated with the critical flicker fusion threshold, if either of the behavioural tasks were correlated with eyes-closed alpha peak amplitude and if Current-Source Density (CSD) transformation had an effect on the main results of the previously created linear models. The following models were created:

Model 4: Critical flicker fusion threshold ~ peak alpha frequency extracted from mean of CSD-transformed pre-task and post-task EEG recording

Model 5: Flash-fusion threshold ~ peak alpha amplitude extracted from mean of CSD-transformed pre-task and post-task EEG recording

Model 6: Critical flicker fusion threshold ~ peak alpha amplitude extracted from mean of CSD-transformed pre-task and post-task EEG recording

Model 7: Flash-fusion threshold ~ peak alpha frequency extracted from non-CSD-transformed mean of pre-task and post-task EEG recording

Model 8: Flash-fusion threshold ~ peak alpha amplitude extracted from non-CSD-transformed mean of pre-task and post-task EEG recording

Model 9: Critical flicker fusion threshold ~ peak alpha frequency extracted from non-CSD transformed mean of pre-task and post-task EEG recording

Model 10: Critical flicker fusion threshold ~ peak alpha amplitude extracted from non-CSD transformed mean of pre-task and post-task EEG recording

Residuals were not normally distributed for models 4, 5, 8 and 9. No significant outliers were observed (Table a2). We therefore conducted correlation tests using both Spearman's and Pearson's r. Neither revealed a significant correlation between the two tested variables for models 4, 8 and 9. Results from model 5 indicated a significant correlation between flash-fusion threshold and eyes-closed CSD-transformed peak alpha amplitude, only for Spearman's correlation test (r = 0.383, P = 0.033). This correlation was not statistically significant in our post-hoc analysis using the "Robust correlations" toolbox in Matlab, the difference most likely being due to its automatic outlier detection functionality, which uses three different methods for outlier detection and removal. We observed a significant correlation between the variables tested in model 7.

Table A.2. Results from analyses of linear models 4 – 10. Significant values printed in bold. Correlation column shows P-value for the highest R.

Model	Tukey	ncv	Shapiro	Cook	Hat	Bonf	Model P	Correlation
4	0.205	0.098	**0.039**	< 0.5	0.0 – 0.4	> 0.05	0.963	Pearson r = -0.009 Spearman r = 0.004
5	0.666	0.143	**0.010**	< 0.4	0.0 – 0.15	> 0.05	0.192	Pearson r = 0.241 Spearman r = **0.384** P = **0.033**
6	0.572	0.465	0.142	< 0.14	0.04 – 0.18	> 0.05	0.311	Pearson r = 0.188
7	0.182	0.182	0.203	< 0.5	0.04 – 0.5	> 0.05	**0.016**	Pearson r = -0.428
8	0.514	0.105	**0.037**	< 0.5	0.0 – 0.15	> 0.05	0.438	Pearson r = 0.145 Spearman r = 0.267 P = 0.146
9	0.241	0.227	**0.033**	< 0.5	0.0 – 0.5	> 0.05	0.955	Pearson r = 0.011 Spearman r = -0.04 P = 0.833
10	0.961	0.681	0.107	< 0.5	0.0 – 0.15	> 0.05	0.348	Pearson r = 0.174

A2. Pre-stimulus EEG-recording

Pre-stimulus EEG-data was recorded during behavioural task performance. To assess how pre-stimulus peak alpha frequency and amplitude correlate with flash-fusion thresholds and critical flicker fusion thresholds, the following linear models were created:

Model 11: Flash-fusion threshold ~ peak alpha frequency extracted from CSD-transformed pre-stimulus EEG-recording

Model 12: Flash-fusion threshold ~ peak alpha amplitude extracted from CSD-transformed pre-stimulus EEG-recording

Model 13: Critical flicker fusion ~ peak alpha frequency extracted from CSD-transformed pre-stimulus EEG-recording

Model 14: Critical flicker fusion ~ peak alpha amplitude extracted from CSD-transformed pre-stimulus EEG-recording

Residuals of models 13 and 14 were not normally distributed (Table a3). However, no significant outliers were detected. We therefore tested for correlations with both Spearman's and Pearson's r. We observed no significant correlations between the variables of any of the tested models.

Table A.3. Results from analyses of linear models 11 – 14. Significant values printed in bold. Correlation column shows P-value for largest R.

Model	Tukey	ncv	Shapiro	Cook	Hat	Bonf	Model P	Correlation
11	0.398	0.063	0.509	< 0.7	0.0 – 0.4	> 0.05	0.234	Pearson r = -0.22
12	0.324	0.824	0.085	< 0.2	0.0 – 0.4	> 0.05	0.276	Pearson r = 0.202
13	0.149	0.380	**0.017**	< 0.5	0.0 – 0.4	> 0.05	0.686	Pearson r = 0.076 Spearman r = 0.026 P = 0.889
14	0.836	0.775	**0.039**	< 0.3	0.0 – 0.4	> 0.05	0.541	Pearson r = 0.114 Spearman r = 0.106 P = 0.572

To assess the possible effect of Current Source Density transformation on the data, we analysed the same variables on non-CSD transformed EEG-data. For this, we created the following linear models:

Model 15: Flash-fusion threshold ~ peak alpha frequency extracted from non-CSD-transformed pre-stimulus EEG-recording

Model 16: Flash-fusion threshold ~ peak alpha amplitude extracted from non-CSD-transformed pre-stimulus EEG-recording

Model 17: Critical flicker fusion ~ peak alpha frequency extracted from non-CSD-transformed pre-stimulus EEG-recording

Model 18: Critical flicker fusion ~ peak alpha amplitude extracted from non-CSD-transformed pre-stimulus EEG-recording

Residuals of model 17 were not normally distributed (Table a4). However, no significant outliers were detected. We therefore tested for correlations with both Spearman's and Pearson's r. We found no significant correlations between variables of any of the tested models.

Table A.4. Results from analyses of linear models 15 – 18. Significant values printed in bold. Correlation column shows P-value for the highest R.

Model	Tukey	ncv	Shapiro	Cook	Hat	Bonf	Model P	Correlation
15	0.512	0.073	0.717	< 0.5	0.0 – 0.3	> 0.05	0.124	Pearson r = -0.29
16	0.414	0.699	0.210	< 0.2	0.0 – 0.5	> 0.05	0.336	Pearson r = 0.182
17	0.205	0.474	**0.039**	< 0.5	0.0 – 0.4	> 0.05	0.131	Pearson r = 0.282 Spearman r = 0.285 P = 0.127
18	0.876	0.936	0.061	< 0.4	0.0 – 0.4	> 0.05	0.66	Pearson r = 0.084

A3. Analysis of individual electrode PO8 with pre-stimulus EEG data

Linear models were created to assess possible correlations between flash-fusion thresholds / critical flicker fusion thresholds and pre-stimulus peak alpha frequency extracted only from electrode PO8. Again we tested both CSD-transformed and non-CSD-transformed versions of the data. The following models were created:

Model 19: Flash-fusion threshold ~ peak alpha frequency extracted from CSD-transformed pre-stimulus EEG-recording of electrode PO8

Model 20: Critical flicker fusion ~ peak alpha frequency extracted from CSD-transformed pre-stimulus EEG-recording of electrode PO8

Model 21: Flash-fusion threshold ~ peak alpha frequency extracted from non-CSD-transformed pre-stimulus EEG-recording of electrode PO8

Model 22: Critical flicker fusion ~ peak alpha frequency extracted from non-CSD-transformed pre-stimulus EEG-recording of electrode PO8

Residuals of model 22 were not normally distributed (Table a5). However, no significant outliers were detected. We therefore tested for correlations with both Spearman's and Pearson's r. We observed significant correlations for the variables tested in models 19 and 21.

Table A.5. Results from analyses of linear models 19 – 22. Significant values printed in bold. Correlation column shows p-value for the highest R.

Model	Tukey	ncv	Shapiro	Cook	Hat	Bonf	Model	Correlation
19	0.369	0.241	0.164	< 0.5	0.0 – 0.4	> 0.05	**0.007**	Pearson r = **-0.49**
20	0.172	0.902	0.053	< 0.5	0.0 – 0.4	> 0.05	0.097	Pearson r = 0.314
21	0.158	0.185	0.651	< 0.5	0.0 -0.4	> 0.05	**0.023**	Pearson r = **-0.421**
22	0.211	0.471	**0.0438**	< 0.5	0.0 – 0.4	> 0.05	0.224	Pearson r = 0.233 Spearman r = 0.183 P = 0.341

A4. Analysis of performance of intermediate stimulus

For the analysis of correlations between peak alpha frequency and the proportion of correct responses on the intermediate stimulus of the flash-fusion task, the following linear models were created:

Model 23: Proportion correct ~ peak alpha frequency extracted from mean of CSD-transformed pre-task and post-task EEG recording

Model 24: Proportion correct ~ peak alpha frequency extracted from mean of non-CSD-transformed pre-task and post-task EEG recording

Model 25: Proportion correct ~ peak alpha frequency extracted from CSD-transformed pre-stimulus EEG-recording

Model 26: Proportion correct ~ peak alpha frequency extracted from non-CSD-transformed pre-stimulus EEG-recording

Model 27: Proportion correct ~ peak alpha frequency extracted from CSD-transformed pre-stimulus EEG-recording of electrode PO8

Model 28: Proportion correct ~ peak alpha frequency extracted from non-CSD-transformed pre-stimulus EEG-recording of electrode PO8

All models met the assumptions for linear regression (Table a6). We found significant correlations between the variables tested in models 23 and 24.

Table A.6. Results from analyses of linear models 23 – 28. Significant values printed in bold.

Model	Tukey	ncv	Shapiro	Cook	Hat	Bonf	Model P	Correlation
23	0.777	0.35	0.781	< 0.2	0.0 – 0.4	> 0.05	0.06	Pearson r = **0.34** P = **0.03** one-tailed
24	0.779	0.235	0.751	< 0.2	0.0 – 0.5	> 0.05	0.069	Pearson r = **0.33** P = **0.035** one-tailed
25	0.992	0.382	0.267	< 0.2	0.0 – 0.4	> 0.05	0.227	Pearson r = 0.22 P = 0.113 one-tailed
26	0.658	0.234	0.07	< 0.4	0.0 – 0.4	> 0.05	0.14	Pearson r = 0.28 P = 0.07 one-tailed
27	0.516	0.279	0.438	< 0.2	0.0 – 0.4	> 0.05	0.14	Pearson r = 0.28 P = 0.07 one-tailed
28	0.807	0.296	0.312	< 0.3	0.0 – 0.4	> 0.05	0.138	Pearson r = 0.28 P = 0.069 one-tailed

A5. Comparison between the two behavioural paradigms

To analyse if performance on the flash-fusion task is correlated with performance on the critical flicker fusion task, we created the following model:

Model 29: Flash-fusion threshold ~ critical flicker fusion threshold

Residuals of model 29 were not normally distributed (Table a7). However, no significant outliers were detected. We therefore tested for correlations with both Spearman's and Pearson's r. We found no correlations between performance on the flash-fusion task and performance on the critical flicker fusion task.

Table A.7. Results from analyses of linear models 29. Significant values printed in bold. Correlation column shows p-value for largest R.

Model	Tukey	ncv	Shapiro	Cook	Hat	Bonf	Model P	Correlation
29	0.563	0.564	**0.029**	< 0.4	0.0 – 0.3	> 0.05	0.49	Pearson's r = -0.129 Spearman's r = -0.024 P = 0.898

Appendix B | Supplementary material for chapter 5

Animal CFF dataset and references

Below is the full dataset used in the analysis in chapter 5, along with all references for max CFF values, habitat light levels and body length values found in literature and online catalogues.

Table B.1. Animal CFF dataset.

	Species	Common name	Class	Max CFF	CFFRef	Forag strat	Forag dim	Move dim	Luminance	LumRef	Body length	BLRef
1	Acanthochromis polyacanthus	Spiny chromis	Actinopterygii	89.0	3	Graze	3D	Aquatic	High	57	0.14	57
2	Amia calva	Bowfin	Actinopterygii	38.0	9	Ambush	3D	Aquatic	High	58	0.53	57
3	Anguilla anguilla	European eel	Actinopterygii	14.0	8	Ambush	2D	Aquatic	Low	57	0.5	57
4	Betta splendens	Siamese fighting fish	Actinopterygii	45.1	2	Active	3D	Aquatic	High	56	0.065	57
5	Carassius auratus	Goldfish	Actinopterygii	67.2	8	Graze	3D	Aquatic	High	8	0.1	57
6	Carassius gibelio	Prussian carp	Actinopterygii	33.0	14	Graze	3D	Aquatic	High	61	0.27	132
7	Centropomus undecimalis	Common snook	Actinopterygii	40.0	16	Active	3D	Aquatic	High	57	0.5	56
8	Centropristis striata	Black sea bass	Actinopterygii	52.0	17	Active	3D	Aquatic	High	57	0.3	57
9	Chaetodipterus faber	Atlantic spadefish	Actinopterygii	60.0	17	Graze	2D	Aquatic	High	57	0.5	57
10	Cynoscion nebulosus	Spotted seatrout	Actinopterygii	60.0	24	Active	3D	Aquatic	High	57	0.36	57
11	Cynoscion regalis	Weakfish	Actinopterygii	42.0	24	Active	3D	Aquatic	High	57	0.5	57
12	Dicentrarchus labrax	European sea bass	Actinopterygii	155.0	25	Active	3D	Aquatic	High	56	1	56
13	Enneacanthus gloriosus	Blue-spotted sunfish	Actinopterygii	50.0	26	Graze	3D	Aquatic	High	65	0.075	85
14	Fundulus heteroclitus	Mummichog	Actinopterygii	52.0	29	Graze	3D	Aquatic	High	66	0.06	66
15	Gasterosteus aculeatus	Threespined stickleback	Actinopterygii	67.0	2	Active	3D	Aquatic	High	57	0.05	57
16	Gnathonemus petersii	Elephantnose fish	Actinopterygii	45.0	31	Graze	2D	Aquatic	Low	57	0.18	96
17	Lagodon rhomboides	Pinfish	Actinopterygii	44.0	16	Active	3D	Aquatic	High	57	0.18	57
18	Leiostomus xanthurus	Spot	Actinopterygii	55.0	24	Graze	2D	Aquatic	High	56	0.25	57

	Lepidocybium											
19	flavobrunneum	Escolar	Actinopterygii	9.0	36	Ambush	3D	Aquatic	Low	57	1.5	57
20	Leuresthes tenuis	California grunion	Actinopterygii	60.0	33	Active	3D	Aquatic	High	57	0.19	57
21	Lutjanus griseus	Grey snapper	Actinopterygii	47.0	16	Active	3D	Aquatic	Low	57	0.4	57
22	Micropogonias undulatus	Atlantic croaker	Actinopterygii	59.0	24	Active	2D	Aquatic	Low	57	0.3	57
23	Morone saxatilis	Striped bass	Actinopterygii	74.0	24	Active	3D	Aquatic	High	57	1.2	57
24	Mugil cephalus	Striped mullet	Actinopterygii	100.0	33	Graze	3D	Aquatic	High	57	0.5	57
25	Oncorhynchus mykiss	Rainbow trout	Actinopterygii	27.0	8	Active	3D	Aquatic	Low	57	0.6	57
26	Oryzias latipes	Japanese rice fish	Actinopterygii	37.2	8	Graze	3D	Aquatic	Low	8	0.023	111
27	Paralabrax nebulifer	Sand bass	Actinopterygii	50.0	33	Active	3D	Aquatic	High	57	0.67	57
28	Paralichthys dentatus	Summer flounder	Actinopterygii	52.0	24	Ambush	3D	Aquatic	High	56	0.61	57
29	Perca flavescens	Yellow perch	Actinopterygii	40.0	42	Active	3D	Aquatic	High	56	0.18	56
30	Poecilia reticulata	Guppy	Actinopterygii	67.0	2	Graze	3D	Aquatic	High	57	0.028	57
31	Pomatomus saltatrix	Bluefish	Actinopterygii	56.0	24	Active	3D	Aquatic	High	57	0.6	57
32	Pterois spp	Lionfish	Actinopterygii	88.0	45	Active	3D	Aquatic	Low	56	0.165	45
33	Rachycentron canadum	Cobia	Actinopterygii	65.0	24	Active	3D	Aquatic	High	58	1.1	57
34	Salmo salar	Salmon	Actinopterygii	72.0	2	Active	3D	Aquatic	High	57	1.1	57
35	Salvelinus fontinalis	Brook trout	Actinopterygii	71.0	48	Active	3D	Aquatic	High	57	0.45	56
36	Sciaenops ocellatus	Red drum	Actinopterygii	54.0	24	Active	3D	Aquatic	High	58	1	57
37	Sebastolobus altivelis	Longspine thornyhead	Actinopterygii	10.0	33	Ambush	2D	Aquatic	Low	57	0.33	57
38	Serranus scriba	Painted comber	Actinopterygii	25.0	14	Ambush	3D	Aquatic	Low	68	0.203	119
39	Tautoga onitis	Tautog	Actinopterygii	48.0	17	Graze	2D	Aquatic	High	57	0.54	57
40	Thunnus albacares	Yellowfin tuna	Actinopterygii	100.0	33	Active	3D	Aquatic	High	58	0.88	121

41	Thunnus obesus	Bigeye tuna	Actinopterygii	37.0	52	Active	3D	Aquatic	Low	52	1.8	57
42	Xiphias gladius	Swordfish	Actinopterygii	22.0	2	Active	3D	Aquatic	Low	71	3	57
43	Xiphophorus hellerii	Green swordtail	Actinopterygii	43.0	2	Graze	3D	Aquatic	High	57	0.028	57
44	Ambystoma tigrinum	Tiger salamander	Amphibia	30.0	8	Ambush	2D	Terrestrial	Low	56	0.25	56
45	Rana clamitans	Green frog	Amphibia	21.0	2	Ambush	2D	Terrestrial	Low	56	0.1	56
46	Rhinella marina	Cane toad	Amphibia	6.7	2	Ambush	2D	Terrestrial	Low	56	0.194	56
47	Acromegalomma vesiculosum	Fan worm	Annelida	35.0	6	Graze	3D	Aquatic	High	6	0.12	83
48	Harmothoe imbricata	Scale worm	Annelida	5.0	32	Ambush	2D	Aquatic	Low	32	0.065	149
49	Lepidonotus squamatus	Scale worm	Annelida	7.0	32	Graze	2D	Aquatic	Low	32	0.05	149
50	Cupiennius salei	Tiger bromeliad spider	Arachnida	8.6	22	Ambush	2D	Terrestrial	Low	22	0.032	81
51	Lycosa baltimoriana	Wolf spider	Arachnida	10.0	2	Ambush	2D	Terrestrial	Low	2	0.016	140
52	Maevia inclemens	Jumping spider	Arachnida	40.0	2	Active	2D	Terrestrial	High	2	0.007	82
53	Asio flammeus	Short-eared owl	Aves	70.0	8	Active	2D	Volant	Low	56	0.38	56
54	Athene noctua	Little owl	Aves	50.0	2	Ambush	2D	Volant	Low	56	0.22	126
55	Bubo virginianus	Great horned owl	Aves	45.0	8	Ambush	2D	Volant	Low	56	0.546	56
56	Calypte anna	Anna's hummingbird	Aves	85.0	13	Graze	3D	Volant	High	56	0.1	56
57	Columba livia	Rock pigeon	Aves	143.0	2	Graze	2D	Volant	High	56	0.28	136
58	Cyanistes caeruleus	Blue tit	Aves	131.0	23	Active	2D	Volant	High	23	0.12	126
59	Falco cherrug	Saker falcon	Aves	102.0	28	Active	2D	Volant	High	56	0.475	56
60	Falco peregrinus	Peregrine falcon	Aves	129.0	28	Active	3D	Volant	High	56	0.47	56
61	Ficedula albicollis	Collared flycatcher	Aves	141.0	23	Active	3D	Volant	High	23	0.13	137
62	Ficedula hypoleuca	Pied flycatcher	Aves	146.0	23	Active	3D	Volant	High	23	0.13	56

63	Gallus gallus	Domestic chicken	Aves	87.0	8	Graze	2D	Terrestrial	High	8	0.7	56
64	Melopsittacus undulatus	Budgerigar	Aves	74.7	8	Graze	2D	Volant	High	56	0.19	56
65	Molothrus ater	Brown-headed cowbird	Aves	114.7	28	Active	2D	Volant	High	56	0.19	56
66	Parabuteo unicinctus	Harris hawk	Aves	81.0	28	Active	2D	Volant	High	56	0.61	56
67	Passer domesticus	House sparrow	Aves	55.0	41	Graze	2D	Volant	High	56	0.145	126
68	Sturnus vulgaris	Starling	Aves	100.0	8	Active	2D	Volant	High	56	0.215	56
69	Taeniopygia guttata	Zebrafinch	Aves	55.0	51	Graze	2D	Volant	High	56	0.1	56
70	Sepia officinalis	Cuttlefish	Cephalopoda	24.0	49	Ambush	3D	Aquatic	Low	56	0.45	56
71	Carcharhinus acronotus	Blacknosed shark	Chondrichthyes	18.0	8	Active	3D	Aquatic	Low	57	1.57	57
72	Carcharhinus plumbeus	Sandbar shark	Chondrichthyes	21.0	15	Active	3D	Aquatic	Low	57	2.6	56
73	Chiloscyllium punctatum	Brown banded bamboo shark	Chondrichthyes	44.0	19	Active	2D	Aquatic	Low	58	1.09	57
74	Galeocerdo cuvier	Tiger shark	Chondrichthyes	38.0	15	Active	3D	Aquatic	Low	57	5	57
75	Haploblepharus edwardsii	Puffadder shyshark	Chondrichthyes	29.0	19	Active	2D	Aquatic	Low	57	0.59	57
76	Hemiscyllium ocellatum	Epaulette shark	Chondrichthyes	40.0	19	Graze	2D	Aquatic	High	57	0.83	57
77	Heterodontus francisci	Horned shark	Chondrichthyes	20.0	33	Graze	2D	Aquatic	Low	57	0.97	57
78	Heterodontus portusjacksoni	Port Jackson shark	Chondrichthyes	28.0	19	Graze	2D	Aquatic	Low	57	1.37	57
79	Leucoraja erinacea	Little skate	Chondrichthyes	30.0	8	Graze	2D	Aquatic	Low	57	0.5	57
80	Mustelus canis	Smooth dogfish	Chondrichthyes	13.0	15	Graze	2D	Aquatic	Low	57	1	57
81	Mustelus manazo	Star spotted dogfish	Chondrichthyes	10.0	19	Graze	2D	Aquatic	Low	57	1.41	57
82	Mustelus mustelus	Smooth hounds	Chondrichthyes	29.0	19	Active	2D	Aquatic	Low	57	1	57
83	Negaprion brevirostris	Lemon shark	Chondrichthyes	37.0	8	Active	3D	Aquatic	Low	57	2.4	57

84	Platyrhinoidis triseriata	Thornback ray	Chondrichthyes	60.0	33	Active	2D	Aquatic	High	57	0.695	57
85	Raja ocellata	Winter skate	Chondrichthyes	30.0	46	Graze	2D	Aquatic	Low	57	0.93	57
86	Rhinobatos productus	Shovelnose guitarfish	Chondrichthyes	30.0	33	Graze	2D	Aquatic	Low	57	1.345	57
87	Scyliorhinus canicula	Smallspotted catfish	Chondrichthyes	3.2	14	Graze	2D	Aquatic	Low	58	1	58
88	Sphyrna lewini	Scalloped hammerhead shark	Chondrichthyes	27.3	8	Active	3D	Aquatic	Low	57	4.3	57
89	Sphyrna tiburo	Bonnethead shark	Chondrichthyes	31.0	2	Graze	3D	Aquatic	Low	57	0.8	57
90	Squalus acanthias	Spiny dogfish	Chondrichthyes	20.0	15	Active	3D	Aquatic	Low	58	1	57
91	Tripedalia cystophora	Box jellyfish	Cnidaria	10.0	54	Graze	3D	Aquatic	High	54	0.013	146
92	Acanthaster planci	Crown of thorns starfish	Echinodermata	0.7	1	Graze	2D	Aquatic	High	56	0.3	56
93	Achatina fulica	Giant African land snail	Gastropoda	0.6	4	Graze	2D	Terrestrial	Low	56	0.3	56
94	Lampetra fluviatilis	River lamprey	Hyperoartia	24.0	35	Active	3D	Aquatic	Low	57	0.35	57
95	Mordacia mordax	Shortheaded lamprey	Hyperoartia	39.6	38	Active	3D	Aquatic	Low	38	0.375	57
96	Mordacia praecox	Precocious lamprey	Hyperoartia	31.1	38	Graze	2D	Aquatic	Low	38	0.375	57
97	Acherontia styx	Lesser death's head hawkmoth	Insecta	140.0	5	Graze	2D	Volant	Low	5	0.06	61
98	Acraea terpsicore	Tawny coster	Insecta	183.0	5	Graze	2D	Volant	High	5	0.02	125
99	Agrius convolvuli	Convolvus hawkmoth	Insecta	110.0	5	Graze	2D	Volant	Low	5	0.045	122
100	Anisoptera	Dragon fly	Insecta	240.0	2	Active	3D	Volant	High	2	0.057	82
101	Antheraea pernyi	Chinese tussar moth	Insecta	70.0	2	Graze	2D	Volant	Low	2	0.04	77
102	Apis mellifera	Honeybee	Insecta	240.0	2	Graze	2D	Volant	High	2	0.015	56
103	Ariadne ariadne	Angled castor	Insecta	205.0	5	Graze	2D	Volant	High	5	0.017	125
104	Atta sexdens rubropilosa	Leaf cutting ant	Insecta	22.3	2	Graze	2D	Terrestrial	Low	2	0.013	127

105	Bombus morio	Bumblebee	Insecta	69.4	2	Graze	2D	Volant	High	2	0.019	128
106	Calliphoridae	Blowfly	Insecta	240.0	2	Graze	2D	Volant	High	2	0.009	129
107	Camponotus rufipes	Ant	Insecta	23.5	2	Graze	2D	Terrestrial	Low	2	0.011	130
108	Carausius morosus	Stick insect	Insecta	40.0	2	Graze	2D	Terrestrial	High	2	0.085	133
109	Catopsilia pomona	Lemon emigrant	Insecta	180.0	5	Graze	2D	Volant	High	5	0.02	125
110	Catopsilia pyranthe	Mottled emigrant	Insecta	194.0	5	Graze	2D	Volant	High	5	0.018	125
111	Cephonodes hylas	Coffee bee hawkmoth	Insecta	128.0	5	Graze	2D	Volant	High	5	0.022	125
112	Chauliognathus marginatus	Soldier beetle	Insecta	45.0	18	Graze	2D	Terrestrial	High	18	0.01	134
113	Cicindela chinensis	Tiger beetle	Insecta	45.0	21	Active	2D	Terrestrial	High	64	0.02	135
114	Danaus chrysippus	African monarch	Insecta	211.0	5	Graze	2D	Volant	High	5	0.012	125
115	Daphnis nerii	Oleander hawkmoth	Insecta	116.0	5	Graze	2D	Volant	Low	5	0.045	125
116	Delias eucharis	Common jezebel	Insecta	225.0	5	Graze	2D	Volant	High	5	0.021	125
117	Drosophila hydei	Fruit fly	Insecta	80.0	2	Graze	2D	Volant	High	2	0.001	84
118	Erebus macrops	Common owl moth	Insecta	110.0	5	Graze	2D	Volant	Low	5	0.04	125
119	Eristalis tenax	Drone fly	Insecta	58.8	2	Graze	2D	Volant	High	2	0.014	134
120	Eudocima materna	Dot-underwing moth	Insecta	139.0	5	Graze	2D	Volant	Low	5	0.029	87
121	Euploea core	Common crow	Insecta	208.0	5	Graze	2D	Volant	High	5	0.033	125
122	Gangara thyrsis	Giant redeye	Insecta	173.0	5	Graze	2D	Volant	Low	5	0.07	92
123	Glossina morsitans	Tsetse fly	Insecta	145.0	2	Active	2D	Volant	High	2	0.011	56
124	Hasora chromus	Common banded awl	Insecta	149.0	5	Graze	2D	Volant	Low	5	0.016	125
125	Hemianax papuensis	Dragon fly	Insecta	55.6	2	Active	3D	Volant	High	2	0.1	124
126	Hippotion spp	Sphinx moth	Insecta	146.0	5	Graze	2D	Volant	Low	5	0.028	98
127	Hypolimnas bolina	Blue moon butterfly	Insecta	199.0	5	Graze	2D	Volant	High	5	0.025	125

128	Junonia Lemonias	Lemon pansy	Insecta	203.0	5	Graze	2D	Volant	High	5	0.017	125
129	Locusta migratoria	Migratory locust	Insecta	65.0	2	Graze	2D	Volant	High	2	0.046	141
130	Macroglossum spp	Hawkmoth	Insecta	182.0	5	Graze	2D	Volant	High	5	0.02	104
131	Melanitis leda	Common evening brown	Insecta	230.0	5	Graze	2D	Volant	Low	5	0.023	125
132	Melipona quadrifasciata	Tropical bee	Insecta	67.1	2	Graze	2D	Volant	High	2	0.01	142
133	Moduza procris	Commander	Insecta	199.0	5	Graze	2D	Volant	High	5	0.02	125
134	Musca domestica	House fly	Insecta	83.3	2	Graze	2D	Volant	High	2	0.006	56
135	Myrmecia croslandi	Bull ant	Insecta	188.7	39	Graze	2D	Terrestrial	High	39	0.012	107
136	Myrmecia gulosa	Bull ant	Insecta	151.6	39	Graze	2D	Terrestrial	High	39	0.019	108
137	Myrmecia midas	Bull ant	Insecta	84.6	39	Graze	2D	Terrestrial	Low	39	0.016	109
138	Myrmecia pyriformis	Bull ant	Insecta	73.3	39	Graze	2D	Terrestrial	Low	39	0.021	107
139	Myrmecia tarsata	Bull ant	Insecta	162.6	39	Graze	2D	Terrestrial	High	39	0.02	107
140	Myrmecia vindex	Bull ant	Insecta	125.2	39	Graze	2D	Terrestrial	Low	39	0.021	109
141	Oecophylla smaragdina	Green weaver ant	Insecta	132.0	62	Active	2D	Terrestrial	High	62	0.007	143
142	Papilio demoleus	Lime swallowtail	Insecta	110.0	5	Graze	2D	Volant	High	5	0.029	112
143	Papilio polytes	Common mormon	Insecta	245.0	5	Graze	2D	Volant	High	5	0.026	125
144	Papilio xuthus	Asian swallowtail	Insecta	107.0	40	Graze	2D	Volant	High	5	0.045	113
145	Pareronia hippia	Indian wanderer	Insecta	165.0	5	Graze	2D	Volant	High	5	2.68	114
146	Periplaneta americana	American cockroach	Insecta	42.5	2	Graze	2D	Terrestrial	Low	2	0.043	56
147	Photinus pyralis	Firefly	Insecta	40.0	18	Graze	2D	Volant	Low	18	0.012	56
148	Polistes canadensis	Red paper wasp	Insecta	42.5	2	Active	2D	Volant	Low	2	0.021	144
149	Pseudomyrmex phyllophilus	Ant	Insecta	108.7	2	Graze	2D	Terrestrial	High	2	0.005	116

150	Psilogramma increta	Plain grey hawkmoth	Insecta	171.0	5	Graze	2D	Volant	Low	5	0.051	125
151	Rhynchophorus ferrugineus	Red palm weevil	Insecta	100.0	47	Graze	2D	Terrestrial	High	61	0.026	117
152	Saturnia pavonia	Emperor moth	Insecta	75.0	2	Graze	2D	Volant	Low	2	0.014	122
153	Tenodera Australasiae	Purple-winged mantis	Insecta	55.3	2	Ambush	3D	Terrestrial	High	2	0.085	124
154	Trigona spinipes	Tropical bee	Insecta	59.5	2	Graze	2D	Volant	Low	2	0.005	145
155	Udaspes folus	Grass demon	Insecta	105.0	5	Graze	2D	Volant	High	5	0.019	125
156	Xenos peckii	Twisted-wing fly	Insecta	35.0	55	Graze	2D	Volant	High	70	0.004	70
157	Acanthephyra purpurea	Oplophorid shrimp	Malacostraca	18.0	2	Graze	3D	Aquatic	Low	2	0.017	72
158	Alpheus heterochaelis	Snapping shrimp	Malacostraca	160.0	7	Graze	3D	Aquatic	Low	56	0.03	56
159	Ancylomenes pedersoni	Pedersons cleaner shrimp	Malacostraca	48.0	10	Graze	2D	Aquatic	High	10	0.02	75
160	Asellus aquaticus	Water louse	Malacostraca	51.3	12	Graze	2D	Aquatic	High	60	0.007	78
161	Bathynectes longipes	Crab	Malacostraca	14.0	2	Graze	2D	Aquatic	Low	2	0.051	123
162	Booralana tricarinata	Isopod	Malacostraca	4.0	2	Graze	2D	Aquatic	Low	2	0.053	79
163	Cambarus spp	American crayfish	Malacostraca	53.0	2	Graze	2D	Aquatic	Low	2	0.059	80
164	Eugonatonotus crassus	Caridean shrimp	Malacostraca	24.0	2	Graze	3D	Aquatic	Low	2	0.08	88
165	Eumunida picta	Squat lobster	Malacostraca	11.0	2	Ambush	3D	Aquatic	Low	2	0.05	89
166	Euphausia gibboides	Euphausiid shrimp	Malacostraca	24.0	2	Graze	3D	Aquatic	Low	2	0.02	90
167	Funchalia villosa	Penaeid shrimp	Malacostraca	24.0	2	Graze	3D	Aquatic	Low	2	0.06	91
168	Gastroptychus spinifer	Squat lobster	Malacostraca	10.0	2	Graze	2D	Aquatic	Low	2	0.019	93
169	Gelasimus dampieri	Fiddler crab	Malacostraca	90.0	30	Graze	2D	Aquatic	High	30	0.015	138
170	Glyptonotus antarcticus	Isopod	Malacostraca	11.0	2	Graze	2D	Aquatic	Low	2	0.09	95
171	Heterocarpus ensifer	Pandalid shrimp	Malacostraca	16.0	2	Graze	3D	Aquatic	Low	2	0.081	97

172	Janicella spinicauda	Oplophorid shrimp	Malacostraca	31.0	2	Graze	3D	Aquatic	Low	2	0.02	101
173	Jasus edwardsii	Red rock lobster	Malacostraca	55.0	2	Graze	2D	Aquatic	Low	2	0.208	150
174	Ligia occidentalis	Rock louse	Malacostraca	120.0	2	Graze	2D	Terrestrial	High	2	0.025	139
175	Lysmata amboinensis	Pacific cleaner shrimp	Malacostraca	42.0	10	Graze	2D	Aquatic	High	10	0.034	102
176	Macrobrachium rosenbergii	Palaemonide shrimp	Malacostraca	44.0	2	Graze	2D	Aquatic	High	2	0.12	103
177	Meganyctiphanes norvegica	Euphausiid shrimp	Malacostraca	23.0	2	Graze	3D	Aquatic	Low	2	0.033	105
178	Munidopsis erinacea	Squat lobster	Malacostraca	12.0	2	Graze	2D	Aquatic	Low	2	0.014	106
179	Nematobrachion boopis	Euphausiid shrimp	Malacostraca	33.0	2	Graze	3D	Aquatic	Low	2	0.02	105
180	Nematobrachion flexipes	Euphausiid shrimp	Malacostraca	44.0	2	Graze	3D	Aquatic	Low	2	0.02	101
181	Nematobrachion sexspinosus	Euphausiid shrimp	Malacostraca	56.0	2	Graze	3D	Aquatic	Low	2	0.02	101
182	Nematoscelis megalops	Euphausiid shrimp	Malacostraca	28.0	2	Graze	3D	Aquatic	Low	2	0.025	110
183	Oplophorus gracilirostris	Oplophorid shrimp	Malacostraca	32.0	2	Graze	3D	Aquatic	Low	2	0.08	101
184	Pagurus spp	Hermit crab	Malacostraca	53.0	2	Graze	2D	Aquatic	Low	56	0.08	56
185	Pasiphaea multidentata	Glass shrimp	Malacostraca	21.0	2	Graze	3D	Aquatic	Low	2	0.11	140
186	Plesionika rossignoli	Pandalid shrimp	Malacostraca	14.0	2	Graze	3D	Aquatic	Low	2	0.07	115
187	Sergestes arcticus	Sergestid shrimp	Malacostraca	21.0	2	Graze	3D	Aquatic	Low	2	0.065	148
188	Sergia filictum	Sergestid shrimp	Malacostraca	25.0	2	Graze	3D	Aquatic	Low	2	0.05	101
189	Stylocheiron maximum	Euphausiid shrimp	Malacostraca	36.0	2	Graze	3D	Aquatic	Low	2	0.02	101
190	Systellaspis debilis	Oplophorid shrimp	Malacostraca	21.0	2	Graze	3D	Aquatic	Low	2	0.012	120
191	Urocaridella antonbruunii	Red white cleaner shrimp	Malacostraca	40.0	10	Graze	2D	Aquatic	High	10	0.04	147
192	Canis lupus familiaris	Dog	Mammalia	80.0	8	Active	2D	Terrestrial	High	8	0.57	131

193	Cavia porcellus	Guinea pig	Mammalia	50.0	8	Graze	2D	Terrestrial	Low	56	0.23	56
194	Erinaceus europaeus	European hedgehog	Mammalia	30.0	27	Graze	2D	Terrestrial	Low	27	0.25	86
195	Felis catus	Domestic cat	Mammalia	55.0	8	Ambush	2D	Terrestrial	Low	56	0.76	56
196	Homo sapiens	Human	Mammalia	60.7	34	Active	2D	Terrestrial	High	56	1.65	99
197	Macaca mulatta	Rhesus macaque	Mammalia	95.0	8	Graze	2D	Terrestrial	High	56	0.54	56
198	macaca nemestrina	Southern pig-tailed macaque	Mammalia	89.0	37	Graze	3D	Terrestrial	High	56	0.51	56
199	Mus musculus	Mouse	Mammalia	41.3	2	Graze	2D	Terrestrial	Low	56	0.08	56
200	Neotamias amoenus	Yellow-pine chipmunk	Mammalia	100.0	8	Graze	2D	Terrestrial	High	56	0.21	56
201	Pagophilus groenlandicus	Harp seal	Mammalia	32.7	8	Active	3D	Aquatic	Low	56	1.75	56
202	Rattus norvegicus	Brown rat	Mammalia	39.0	8	Graze	2D	Terrestrial	Low	56	0.4	56
203	Sciurus vulgaris	Eurasian red squirrel	Mammalia	103.0	27	Graze	2D	Terrestrial	High	27	0.23	118
204	Spermophilus lateralis	Ground squirrel	Mammalia	120.0	8	Graze	2D	Terrestrial	High	56	0.265	56
205	Tamiasciurus hudsonicus	American red squirrel	Mammalia	60.0	8	Graze	2D	Terrestrial	High	56	0.33	56
206	Trichosurus vulpecula	Brushtail possum	Mammalia	22.4	53	Graze	2D	Terrestrial	Low	56	0.45	56
207	Tupaia belangeri	Northern tree shrew	Mammalia	60.0	2	Graze	2D	Terrestrial	High	69	0.165	56
208	Tupaia glis	Common tree shrew	Mammalia	90.0	8	Graze	2D	Terrestrial	High	56	0.195	56
209	Anolis auratus	Anole lizard	Reptilia	41.5	2	Ambush	2D	Terrestrial	High	59	0.038	74
210	Anolis beckeri	Anole lizard	Reptilia	26.1	2	Ambush	2D	Terrestrial	High	59	0.058	73
211	Anolis carolinensis	Anole lizard	Reptilia	34.6	2	Ambush	2D	Terrestrial	High	59	0.06	56
212	Anolis cristatellus	Anole lizard	Reptilia	70.0	2	Ambush	2D	Terrestrial	High	59	0.066	56
213	Anolis grahami	Anole lizard	Reptilia	34.7	2	Ambush	2D	Terrestrial	High	59	0.053	76
214	Anolis gundlachi	Anole lizard	Reptilia	55.0	2	Ambush	2D	Terrestrial	High	59	0.057	73
215	Anolis limifrons	Anole lizard	Reptilia	28.5	2	Ambush	2D	Terrestrial	High	59	0.043	73

216	Anolis lineatopus	Anole lizard	Reptilia	26.0	11	Ambush	2D	Terrestrial	High	59	0.052	76
217	Anolis pulchellus	Anole lizard	Reptilia	63.0	2	Ambush	2D	Terrestrial	High	59	0.041	73
218	Anolis sagrei	Anole lizard	Reptilia	34.4	2	Ambush	2D	Terrestrial	High	59	0.05	73
219	Anolis valencienni	Anole lizard	Reptilia	33.4	2	Ambush	2D	Terrestrial	High	59	0.058	76
220	Caretta caretta	Loggerhead sea turtle	Reptilia	40.0	8	Graze	3D	Aquatic	High	8	0.925	56
221	Chelonia mydas	Green sea turtle	Reptilia	40.0	8	Graze	2D	Aquatic	High	8	1.1	56
222	Chrysemis picta	Painted turtle	Reptilia	31.0	20	Graze	3D	Aquatic	High	63	0.15	63
223	Dermochelys coriacea	Leatherback sea turtle	Reptilia	15.0	8	Graze	3D	Aquatic	High	8	1.525	56
224	Gekko gecko	Tokay gecko	Reptilia	20.0	8	Ambush	2D	Terrestrial	Low	56	0.138	94
225	Iguana iguana	Green iguana	Reptilia	80.0	8	Graze	2D	Terrestrial	High	56	0.3	100
226	Phrynosoma cornutum	Horned lizard	Reptilia	42.4	43	Ambush	2D	Terrestrial	High	56	0.13	43
227	Pseudemys scripta	Pond slider	Reptilia	52.6	44	Graze	2D	Aquatic	High	67	0.18	67
228	Sphaerodactylus inaguae	Inagua gecko	Reptilia	26.5	50	Ambush	2D	Terrestrial	Low	50	0.07	50
229	Sphenodon punctatus	Tuatara	Reptilia	55.4	2	Ambush	2D	Terrestrial	Low	56	0.5	56

Abbreviations in columns: Max CFF = CFF in Hertz, CFFRef = reference number for CFF values, Forag strat = foraging strategy, Forag dim = foraging dimensionality, Mov dim = movement dimensionality, LumRef = reference number for luminance level, Body length = body length in meters, BLRef = reference number for body length. Note: butterfly body lengths were estimated relative to referenced wingspan.

(1) Petie et al., 2016; (2) Rospars & Meyer-Vernet, 2021; (3) Chung et al., 2014; (4) Bobkova et al., 2004; (5) Chatterjee et al., 2020; (6) Bok et al., 2019; (7) Kingston et al., 2020; (8) Healy et al., 2013; (9) Gramoni et al., 1970; (10) Caves et al., 2016; (11) Jenssen & Swenson, 1974; (12) Crozier & Wolf, 1939a; (13) Goller et al., 2019; (14) Milosevic et al., 2009; (15) Kalinoski et al., 2014; (16) McComb et al., 2013; (17) Horodysky et al., 2013; (18) Stowasser et al., 2015; (19) Ryan et al., 2017; (20) Graf, 1972; (21) Mizutani & Toh 1995; (22) Fenk & Schmid, 2011; (23) Boström et al., 2016; (24) Horodysky et al., 2010; (25) Brill et al., 2019; (26) Crozier & Wolf, 1938; (27) Horsten & Winkelman, 1962; (28) Potier et al., 2020; (29) Crozier & Wolf, 1940; (30) Brodrick et al., 2022; (31) Pusch et al., 2013; (32) Garm et al., 2021; (33) Bullock et al., 1990; (34) Haarlem et al., 2024; (35) Dreyfert et al., 1979; (36) Landgren et al., 2014; (37) Stavros & Kiorpes, 2008; (38) Warrington et al., 2017; (39) Ogawa et al., 2022; (40) Nakagawa et al., 1994; (41) Crozier & Wolf, 1944; (42) Ubels et al., 2018; (43) Crozier & Wolf, 1941a; (44) Crozier & Wolf, 1939b; (45) Hasenei et al., 2020; (46) Green & Siegel, 1975; (47) Ilić et al., 2016; (48) Ali & Kobayashi, 1968; (49) Nelson, 2003; (50) Crozier & Wolf, 1939c; (51) Crozier & Wolf, 1941b; (52) Fritsches et al., 2005; (53) Signal et al., 2001; (54) O'Connor et al., 2010; (55) Buschbeck et al., 2003; (56) Myers et al., 2024; (57) Froese & Pauly, 2024; (58) Florida Museum of Natural History, 2024; (59) Loew et al., 2002; (60) Horváth et al., 2023; (61) CABI, 2024; (62) Ogawa et al., 2023; (63) Rowe & Dalgarn, 2010; (64) Lafitte et al., 2022; (65) Snyder & Peterson, 1999; (66) Weisberg et al., 1981; (67) Cagle, 1950; (68) Mršulja & Rakić, 1974; (69) Meijer et al., 1990; (70) James et al., 2016; (71) Abecassis et al., 2012; (72) Sivertson & Holthuis., 1956; (73) Uetz et al., 2024; (74) Fleishman, 1988; (75) Mascaró et al., 2012; (76) Johnson & Wade, 2010; (77) Li et al., 2017; (78) Hargeby et al., 2005; (79) Camp & Heard, 1988; (80) Holdich, 2002; (81) Weihmann, 2013; (82) VanDyk, 2024; (83) WoRMS Editorial Board, 2024; (84) Pitnick & Markow, 1994; (85) Graham, 1989; (86) Haigh, 2011; (87) Hill & Matyot, 2001; (88) Chan & Yu, 1988; (89) Nizinski et al., 2023; (90) Décima et al., 2010; (91) Rao, 1984; (92) Watson, 1891; (93) Vazuez-Bader & Gracia, 2016; (94) Wang et al., 2014; (95) Held & Wägele, 2005; (96) Kaufman, 2003; (97) Lozano-Álvarez et al., 2007; (98) Jeenkoed et al., 2016; (99) Roser et al., 2013; (100) Stamps et al., 1998; (101) Frank, 1999; (102) Tziouveli & Smith, 2009; (103) Barki et al., 1992; (104) Grittner et al., 2022; (105) Suh & Nemoto, 1988; (106) Tavares & Campinho, 1998; (107) Narendra et al., 2011; (108) Dietemann et al., 2002; (109) Clark, 1951; (110) Lindley, 1982; (111) Ogoshi et al., 2012; (112) Dheri et al., 2013; (113) Komata & Sota, 2017; (114) Kunte & Ravikanthachari, 2020; (115) Fischer et al., 1981; (116) Smith, 1858; (117) Hoddle et al., 2020; (118) Lurz et al., 2005; (119) Aydin, 2017; (120) Griffiths & Brandt, 1983; (121) Jalil et al., 2020; (122) Butterfly Conservation, 2024; (123) MNHN & OFB, 2024; (124) Australian Museum, 2024; (125) India Biodiversity, 2024; (126) RSPB, 2024; (127) Antweb, 2024; (128) Discover Life, 2024; (129) Encyclopaedia Britannica, 2024; (130) Antstore, 2024; (131) Dimensions, 2024; (132) Conti et al., 2022; (133) Headrick & Wilen, 2011; (134) InsectIdentification, 2024; (135) The Animal Facts, 2024; (136) Global Invasive Species Database, 2024; (137) BirdID Nord University, 2024; (138) George & Jones, 1982; (139) Cowles, 2005; (140) Encyclopedia of Life, 2024; (141) Zborowski, 1998; (142) Slow Food Foundation for Biodiversity, 2024; (143) antARK, 2024; (144) O'Donnell & Jeanne, 1991; (145) Kuhn-Neto et al., 2009; (146) Monterey Bay Aquarium, 2024; (147) Aquariumbreeder, 2024; (148) Naturalis Biodiversity Center, 2024a; (149) Naturalis Biodiversity Center, 2024b; (150) Holthuis, 1991

References

Abecassis, M., Dewar, H., Hawn, D., & Polovina, J. (2012). Modeling swordfish daytime vertical habitat in the North Pacific Ocean from pop-up archival tags. *Marine Ecology Progress Series*, *452*(April), 219–236. https://doi.org/10.3354/meps09583

Ali, M. A., & Kobayashi, H. (1968). Electroretinogram—flicker fusion frequency in albino trout. *Experientia*, *24*, 454–455.

antARK. (2024). Weaver ants. http://antark.net/ant-species/weaver-ant-oecophylla-smaragdina/

Antstore. (2024). Camponutus rufipes. https://www.antstore.net/shop/en/ants/Ants-from-America/Camponotus-rufipes.html

Antweb. (2024). California Academy of Science. https://www.antweb.org/description.do?genus=atta&species=sexdens&rank=species

Aquariumbreeder. (2024). Red-white cleaner shrimp – Detailed guide: care, diet and breeding. https://aquariumbreeder.com/red-white-cleaner-shrimp-detailed-guide-care-diet-and-breeding/

Australian Museum. (2024). Insects. https://australian.museum/learn/animals/insects

Aydin, M. (2017). Some biological parameters of painted comber (Serranus scriba L., 1758) in the Black Sea. *Turkish Journal of Maritime and Marine Sciences*, *3*(1), 34–41.

Barki, A., Karplus, I., & Goren, M. (1992). Effects of size and morphotype on dominance hierarchies and resource competition in the freshwater prawn Macrobrachium rosenbergii. *Animal Behaviour*, *44*, 547–555.

BirdID Nord University. (2024). Collared flycatcher (Ficedula albicollis). https://www.birdid.no/bird/eBook.php?specieID=1267

Bobkova, M. V., Tartakovskaya, O. S., Borissenko, S. L., Zhukov, V. V., & Meyer-Rochow, V. B. (2004). Restoration of morphological and functional integrity in the regenerating eye of the giant African land snail Achatina fulica. *Acta Zoologica*, *85*(1), 1–14. https://doi.org/10.1111/j.0001-7272.2004.00152.x

Bok, M. J., Nilsson, D. E., & Garm, A. (2019). Photoresponses in the radiolar eyes of the fan worm Acromegalomma vesiculosum. *Journal of Experimental Biology*, *22*(23). https://doi.org/10.1242/jeb.212779

Boström, J. E., Dimitrova, M., Canton, C., Håstad, O., Qvarnström, A., & Ödeen, A. (2016). Ultra-Rapid vision in birds. *PLoS ONE*, *11*(3), 3–9. https://doi.org/10.1371/journal.pone.0151099

Brill, R. W., Horodysky, A. Z., Place, A. R., Larkin, M. E. M., & Reimschuessel, R. (2019). Effects of dietary taurine level on visual function in European sea bass (Dicentrarchus labrax). *PLoS ONE*, *14*(6), 1–18. https://doi.org/10.1371/journal.pone.0214347

Brodrick, E. A., How, M. J., & Hemmi, J. M. (2022). Fiddler crab electroretinograms reveal vast circadian shifts in visual sensitivity and temporal summation in dim light. *Journal of Experimental Biology*, *225*(5), 1–12. https://doi.org/10.1242/jeb.243693

Bullock, T. H., Hofmann, M. H., New, J. G., & Nahm, F. K. (1990). Dynamic properties of visual evoked potentials in the tectum of cartilaginous and bony fishes, with neuroethological implications. *Journal of Experimental Zoology*, *256*(5 S), 142–155. https://doi.org/10.1002/jez.1402560519

Buschbeck, E. K., Ehmer, B., & Hoy, R. R. (2003). The unusual visual system of the Strepsiptera: External eye and neuropils. *Journal of Comparative Physiology A:*

Neuroethology, Sensory, Neural, and Behavioral Physiology, *189*(8), 617–630. https://doi.org/10.1007/s00359-003-0443-x

Butterfly Conservation. (2024). http://butterfly-conservation.org/

CABI. (2024). CABI Compendium. Wallingford, UK. CAB International. https://www.cabidigitallibrary.org/

Cagle, F. R. (1950). The Life History of the Slider Turtle , Pseudemys scripta troostii (Holbrook). *Ecological Monographs*, *20*(1), 31–54.

Camp, D. K., & Heard, R. W. (1988). Booralana tricarinata, a new species of isopod from the western Atlantic Ocean (Crustacea: Isopoda: Cirolanidae). *Proceedings of the Biological Society of Washington*, *101*(3), 603–613.

Caves, E. M., Frank, T. M., & Johnsen, S. (2016). Spectral sensitivity, spatial resolution and temporal resolution and their implications for conspecific signalling in cleaner shrimp. *Journal of Experimental Biology*, *219*(4), 597–608. https://doi.org/10.1242/jeb.122275

Chan, T., & Yu, H.-P. (1988). An uncommon deep-sea shrimp Eugonatonotus crassus (A. Milne Edwards, 1881) (Crustacea: Decapoda: Eugonatonotidae) from Taiwan. *Bulletin of Institute of Zoology, Academia Sinica*, *27*(4), 259–263.

Chatterjee, P., Mohan, U., Krishnan, A., & Sane, S. P. (2020). Evolutionary constraints on flicker fusion frequency in Lepidoptera. *Journal of Comparative Physiology A: Neuroethology, Sensory, Neural, and Behavioral Physiology*, *206*(5), 671–681. https://doi.org/10.1007/s00359-020-01429-3

Chung, W. S., Marshall, N. J., Watson, S. A., Munday, P. L., & Nilsson, G. E. (2014). Ocean acidification slows retinal function in a damselfish through interference with GABAA receptors. *Journal of Experimental Biology*, *217*(3), 323–326. https://doi.org/10.1242/jeb.092478

Clark, J. (1951). *The Formicidae of Australia*. Commonwealth Scientific and Industrial Research Organisation, Australia.

Conti, C., Desvignes, T., & Didierlaurent, S. (2022). Carassius spp. *DORIS*. https://doris.ffessm.fr/ref/specie/2552

Cowles, D. (2005). Ligia (Megaligia) occidentalis Dana, 1853. *Invertebrates of the Salish Sea. https://inverts.wallawalla.edu/Arthropoda/Crustacea/Malacostraca/Eumalacostraca/Peracarida/Isopoda/Oniscoidea/Family_Ligiidae/Ligia_occidentalis.html*

Crozier, W. J., Wolf, E., & Zerrahn-Wolf, G. (1938). Critical illumination and flicker frequency, as a function of flash duration: for the sunfish. *Journal of General Physiology*, *21*(3), 313–334. https://doi.org/10.1085/jgp.21.3.313

Crozier, W. J., & Wolf, E. (1939) -a. The flicker response contour for the isopod Asellus. *The Journal of General Physiology*, *22*(4), 451–462.

Crozier, W. J., Wolf, E., & Zerrahn-wolf, G. (1939) -b. The flicker response function for the turtle Pseudemys. *The Journal of General Physiology*, *22*(3), 311–340.

Crozier, W. J., & Wolf, E. (1939) -c. The flicker response contour for the gecko (rod retina). *The Journal of General Physiology*, *22*(5), 555–566.

Crozier, W. J., & Wolf, E. (1940). The flicker response curve for Fundulus. *The Journal of General Physiology*, *34*(6), 677–694.

Crozier, W. J., & Wolf, E. (1941) -a. The flicker response contour for phrynosoma (horned lizard; cone retina). *The Journal of General Physiology*, *24*(3), 317–324.

Crozier, W. J., & Wolf, E. (1941) -b. The simplex flicker threshold contour for the zebra finch. *The Journal of General Physiology*, *24*(5), 625–633. https://doi.org/https://doi.org/10.1085/jgp.24.5.625

Crozier, W. J., & Wolf, E. (1944). Flicker response contours for the sparrow, and the theory of the avian pecten. *The Journal of General Physiology*, *27*(4), 315–324. https://doi.org/10.1126/science.65.1678.208-a

Décima, M., Ohman, M. D., & De Robertis, A. (2010). Body size dependence of euphausiid spatial patchiness. *Limnology and Oceanography*, *55*(2), 777–788. https://doi.org/10.4319/lo.2009.55.2.0777

Dheri, B., Mehmood, S. A., & Ahmad, T. (2013). Diversity of butterfly fauna of Union Council Koaz. *Journal of Entomology and Zoology Studies*, *1*(6), 113–117.

Dietemann, V., Hölldobler, B., & Peeters, C. (2002). Caste specialization and differentiation in reproductive potential in the phylogenetically primitive ant Myrmecia gulosa. *Insectes Sociaux*, *49*(3), 289–298. https://doi.org/10.1007/s00040-002-8316-9

Dimensions. (2024). Beagle. https://www.dimensions.com/element/dogs-beagle

Discover Life. 2024. Bombus morio (Swederus, 1787). https://www.discoverlife.org/mp/20q?search=Bombus+morio

Dreyfert, T., Holmberg, K. A. J., & Struwe, G. (1979). Critical flicker fusion frequency of the river lamprey (Lampetra fluviatilis). *Vision Research*, *19*(5), 551–553. https://doi.org/https://doi.org/10.1016/0042-6989(79)90140-8

Encyclopaedia Britannica. (2024). Blow fly. https://www.britannica.com/animal/blow-fly-insect

Encyclopedia of Life. (2024). https://eol.org

Fenk, L. M., & Schmid, A. (2011). Flicker-induced eye movements and the behavioural temporal cut-off frequency in a nocturnal spider. *Journal of Experimental Biology*, *214*(21), 3658–3663. https://doi.org/10.1242/jeb.060855

Fischer, W., Bianchi, G., & Scott, W. B. (1981). FAO Species Identification Sheets for Fishery Purposes, Eastern Central Atlantic. *Department of Fisheries and Oceans, Canada*, *6*, 1–304. https://www.ptonline.com/articles/how-to-get-better-mfi-results

Fleishman, L. (1988). The Social Behavior of Anolis auratus, a Grass Anole from Panama. *Journal of Herpetology*, *22*(1), 13–23.

Florida Museum of Natural History. (2024). Discover – Species profiles. https://floridamuseum.ufl.edu

Frank, T. M. (1999). Comparative study of temporal resolution in the visual systems of mesopelagic crustaceans. *Biological Bulletin*, *196*(2), 137–144. https://doi.org/10.2307/1542559

Fritsches, K. A., Brill, R. W., & Warrant, E. J. (2005). Warm Eyes Provide Superior Vision in Swordfishes. *Current Biology*, *15*, 55–58. https://doi.org/10.1016/j

Froese, R., & Pauly, D. (2024). FishBase. World Wide Web electronic publication. https://www.fishbase.org

Garm, A., Simonsen, S. H., Mendoza-González, P., & Worsaae, K. (2021). Have the eyes of bioluminescent scale worms adapted to see their own light? A comparative study of eyes and vision in Harmothoe imbricata and Lepidonotus squamatus. *Journal of Experimental Biology*, *224*(14). https://doi.org/10.1242/jeb.242501

George, R.W., & Jones, D. S. (1982). A revision of the fiddler crabs of Australia (Ocypodinae: Uca). *Record of the Western Australian Museum – Supplement*, 14:1–99.

Global Invasive Species Database. (2024). Columba livia. https://www.iucngisd.org/gisd/species.php?sc=1052

Goller, B., Fellows, T. K., Dakin, R., Tyrrell, L., Fernández-Juricic, E., & Altshuler, D. L. (2019). Spatial and Temporal Resolution of the Visual System of the Anna's Hummingbird (Calypte anna) Relative to Other Birds. *Physiological and Biochemical Zoology : PBZ*, *92*(5), 481–495. https://doi.org/10.1086/705124

Graf, V. A. (1972). Behavioral visual functions for Chrysemys picta picta. *Brain, Behavior and Evolution*, *5*, 155–175. https://www.inaturalist.org/observations/152396164

Graham, J. H. (1989). Foraging by sunfishes in a bog lake. In *Freshwater Wetlands and Wildlife. U.S. Department of Energy Symposium Series No. 61. Office of Scientific and Technical Information. Oak Ridge, Tennesse*.

Gramoni, R., Ali, M.A. (1970). L'électroretinogramme et sa fréquence de fusion chez Amia Calva (Linné). *Revue de Canadienne De Biologie, 29,* 353-363.

Green, D. G., & Siegel, I. M. (1975). Double branched flicker fusion curves from the all-rod skate retina. *Science*, *188*(4193), 1120–1122. https://doi.org/10.1126/science.1215989

Griffiths, F., & Brandt, S. (1983). Distribution of mesopelagic decapod Crustacea in and around a warm-core eddy in the Tasman Sea. *Marine Ecology Progress Series*, *12*(January 1983), 175–184. https://doi.org/10.3354/meps012175

Grittner, R., Baird, E., & Stöckl, A. (2022). Spatial tuning of translational optic flow responses in hawkmoths of varying body size. *Journal of Comparative Physiology A: Neuroethology,*

Sensory, Neural, and Behavioral Physiology, *208*(2), 279–296. https://doi.org/10.1007/s00359-021-01530-1

Haarlem, C. S., O'Connell, R. G., Mitchell, K. J., & Jackson, A. L. (2024). The speed of sight: Individual variation in critical flicker fusion thresholds. *PLoS ONE*, *19*(4 April), 1–13. https://doi.org/10.1371/journal.pone.0298007

Haigh, A. J. (2011). *The Ecology of the European hedgehog (Erinaceus europaeus) in rural Ireland.* [Doctoral dissertation, University College Cork].

Hargeby, A., Stoltz, J., & Johansson, J. (2005). Locally differentiated cryptic pigmentation in the freshwater isopod Asellus aquaticus. *Journal of Evolutionary Biology*, *18*(3), 713–721. https://doi.org/10.1111/j.1420-9101.2004.00837.x

Hasenei, A., Kerstetter, D. W., Horodysky, A. Z., & Brill, R. W. (2020). Physiological limits to inshore invasion of Indo-Pacific lionfish (Pterois spp.): insights from the functional characteristics of their visual system and hypoxia tolerance. *Biological Invasions*, *22*(6), 2079–2097. https://doi.org/10.1007/s10530-020-02241-5

Headrick, D. H., & Wilen, C. A. (2011). Indian walking stick. *Pest Notes, 74157, 1-3. https://ipm.ucanr.edu/PMG/PESTNOTES/pn74157.html*

Healy, K., McNally, L., Ruxton, G. D., Cooper, N., & Jackson, A. L. (2013). Metabolic rate and body size are linked with perception of temporal information. *Animal Behaviour*, *86*(4), 685–696. https://doi.org/10.1016/j.anbehav.2013.06.018

Held, C., & Wägele, J. W. (2005). Cryptic speciation in the giant Antarctic isopod Glyptonotus antarcticus (Isopoda: Valvifera: Chaetiliidae). *Scientia Marina*, *69*(SUPPL. 2), 175–181. https://doi.org/10.3989/scimar.2005.69s2175

Hill, M., & Matyot, P. (2001). *The dot underwing Eudocima materna (Linnaeus , 1767) (Lepidoptera , Noctuidae) in Seychelles*. 1908–1909. https://islandbiodiversity.com/Phelsuma%2011-18.pdf

Hoddle, M. S., Hoddle, C. D., & Milosavljević, I. (2020). How Far Can Rhynchophorus palmarum (Coleoptera: Curculionidae) Fly? *Journal of Economic Entomology*, *113*(4), 1786–1795. https://doi.org/10.1093/jee/toaa115

Holthuis, L.B. (1991). FAO Species Catalogue. Vol. 13. Marine lobsters of the world. An annotated and illustrated catalogue of species of interest to fisheries known to date. *crustacean; decapod FAO Fish. Synop. 125(13):292p.* Rome: FAO.

Holdich, David M. (2002). Biology of Freshwater Crayfish. London: Blackwell Science. pp. 609–613. ISBN 978-0-632-05431-2.

Horodysky, A. Z., Brill, R. W., Warrant, E. J., Musick, J. A., & Latour, R. J. (2010). Comparative visual function in four piscivorous fishes inhabiting Chesapeake Bay. *Journal of Experimental Biology*, *213*(10), 1751–1761. https://doi.org/10.1242/jeb.038117

Horodysky, A. Z., Brill, R. W., Crawford, K. C., Seagroves, E. S., & Johnson, A. K. (2013). Comparative visual ecophysiology of mid-Atlantic temperate reef fishes. *Biology Open*, *2*(12), 1371–1381. https://doi.org/10.1242/bio.20136825

Horsten, G. P. M., & Winkelman, J. E. (1962). Comparison of critical fusion frequency in diurnal and nocturnal retina of vertebrates. *Archives Internationales de Physiologie El de Biochimie*, *70*(5), 660–670.

Horváth, G., Kerekes, K., Nyitrai, V., Balázs, G., Berisha, H., & Herczeg, G. (2023). Exploratory behaviour divergence between surface populations, cave colonists and a cave population in the water louse, Asellus aquaticus. *Behavioral Ecology and Sociobiology*, *77*(1). https://doi.org/10.1007/s00265-022-03288-1

Ilić, M., Pirih, P., & Belušič, G. (2016). Four photoreceptor classes in the open rhabdom eye of the red palm weevil, Rynchophorus ferrugineus Olivier. *Journal of Comparative Physiology A: Neuroethology, Sensory, Neural, and Behavioral Physiology*, *202*(3), 203–213. https://doi.org/10.1007/s00359-015-1065-9

India Biodiversity. (2024). Species. https://indiabiodiversity.org/species/list

InsectIdentification. (2024). https://www.insectidentification.org

Jalil, Mallawa, A., Amir, F., & Safruddin. (2020). Size composition and length-weight relationships of the Yellowfin Tuna (Thunnus albacares) in Bone Bay. *E3S Web of Conferences*, *153*. https://doi.org/10.1051/e3sconf/202015301006

James, M., Nandamuri, S. P., Stahl, A., & Buschbeck, E. K. (2016). The unusual eyes of Xenos peckii (Strepsiptera: Xenidae) have green- and UV-sensitive photoreceptors. *Journal of Experimental Biology*, *219*(24), 3866–3874. https://doi.org/10.1242/jeb.148361

Jeenkoed, R., Bumroongsook, S., & Tigvattananont, S. (2016). Biology and host plants of Hippotion celerio (L.)(Lepidoptera: Sphingidae). *International Journal of Agricultural Technology*, *12*(7.2), 2089–2094.

Jenssen, T. A., & Swenson, B. (1974). An ecological correlate of critical flicker-fusion frequencies for some Anolis lizards. *Vision Research*, *14*(10), 965–970. https://doi.org/10.1016/0042-6989(74)90164-3

Johnson, M. A., & Wade, J. (2010). Behavioural display systems across nine Anolis lizard species: Sexual dimorphisms in structure and function. *Proceedings of the Royal Society B: Biological Sciences*, *277*(1688), 1711–1719. https://doi.org/10.1098/rspb.2009.2323

Kalinoski, M., Hirons, A., Horodysky, A., & Brill, R. (2014). Spectral sensitivity, luminous sensitivity, and temporal resolution of the visual systems in three sympatric temperate coastal shark species. *Journal of Comparative Physiology A: Neuroethology, Sensory, Neural, and Behavioral Physiology*, *200*(12), 997–1013. https://doi.org/10.1007/s00359-014-0950-y

Kaufman, J. (2003). On the Expensive-Tissue Hypothesis: Independent Support from Highly Encephalized Fish. *Current Anthropology*, *44*(5), 705–707.

Kingston, A. C. N., Chappell, D. R., & Speiser, D. I. (2020). A snapping shrimp has the fastest vision of any aquatic animal: Fast vision in snapping shrimp. *Biology Letters*, *16*(6). https://doi.org/10.1098/rsbl.2020.0298rsbl20200298

Komata, S., & Sota, T. (2017). Seasonal polyphenism in body size and juvenile development of the swallowtail butterfly Papilio xuthus (Lepidoptera: Papilionidae). *European Journal of Entomology*, *114*, 365–371. https://doi.org/10.14411/eje.2017.046

Kuhn-Neto, B., Contrera, F. A. L., Castro, M. S., & Nieh, J. C. (2009). Long distance foraging and recruitment by a stingless bee, Melipona mandacaia . Apidologie, 40(4), 472–480. https://doi.org/10.1051/apido/2009007

Kunte, K., & Ravikanthachari, N. (2020). Butterflies of Bengaluru. *Karnataka Forest Department (Research Wing), National Centre for Biological Sciences, and Indian Foundation for Butterflies, Bengaluru, India.*, 196.

Lafitte, A., Sordello, R., Legrand, M., Nicolas, V., Obein, G., & Reyjol, Y. (2022). A flashing light may not be that flashy: A systematic review on critical fusion frequencies. *PloS One*, *17*(12), e0279718. https://doi.org/10.1371/journal.pone.0279718

Landgren, E., Fritsches, K., Brill, R., & Warrant, E. (2014). The visual ecology of a deep-sea fish, the escolar Lepidocybium flavobrunneum (Smith, 1843). *Philosophical Transactions of the Royal Society B: Biological Sciences*, *369*(1636). https://doi.org/10.1098/rstb.2013.0039

Li, W., Zhang, Z., Lin, L., & Terenius, O. (2017). Antheraea pernyi (Lepidoptera: Saturniidae) and Its Importance in Sericulture, Food Consumption, and Traditional Chinese Medicine. *Journal of Economic Entomology*, *110*(4), 1404–1411. https://doi.org/10.1093/jee/tox140

Lindley, J. A. (1982). Population dynamics and production of euphausiids. *Marine Biology*, *66*(1), 37–46. https://doi.org/10.1007/bf00397252

Loew, E. R., Fleishman, L. J., Foster, R. G., & Provencio, I. (2002). Visual pigments and oil droplets in diurnal lizards: A comparative study of Caribbean anoles. *Journal of Experimental Biology*, *205*(7), 927–938.

Lozano-Álvarez, E., Briones-Fourzán, P., Gracia, A., & Vázquez-Bader, A. R. (2007). Relative Growth and Size at First Maturity of the Deep Water Shrimp , Heterocarpus ensifer (Decapoda, Pandalidae) from the Southern Gulf of Mexico. *Crustaceana*, *80*(5), 555–568.

Lurz, P. W. W., Gurnell, J., & Magris, L. (2005). Sciurus vulgaris. *Mammalian Species*, *769*, 1–10.

Mascaró, M., Rodríguez-Pestaña, L., Chiappa-Carrara, X., & Simoes, N. (2012). Host selection by the cleaner shrimp Ancylomenes pedersoni: Do anemone host species, prior

experience or the presence of conspecific shrimp matter? *Journal of Experimental Marine Biology and Ecology*, *413*, 87–93. https://doi.org/10.1016/j.jembe.2011.11.026

McComb, D. M., Kajiura, S. M., Horodysky, A. Z., & Frank, T. M. (2013). Comparative visual function in predatory fishes from the Indian River Lagoon. *Physiological and Biochemical Zoology*, *86*(3), 285–297. https://doi.org/10.1086/670260

Meijer, J. H., Overkamp, G. J. F., & Hermann, P. M. (1990). The Two-Oscillator Circadian System of Tree Shrews (Tupaia belangeri) and Its Response to Light and Dark Pulses. *Journal of Biological Rhythms*, *5*(1), 1–16. https://doi.org/10.1177/074873049000500101

Milosevic, M., Visnjic, Z., & Damjanović, I. (2009). Temporal analysis of electroretinographic responses in fishes with rod-dominated and mixed rod-cone retina. *General Physiology and Biophysics*, *28*, 276–282. https://doi.org/10.4149/gpb_2009_03_276

Mizutani, A., & Toh, Y. (1995). Optical and physiological properties of the larval visual system of the tiger beetle, Cicindela chinensis. *Journal of Comparative Physiology A*, *177*(5), 591–599. https://doi.org/10.1007/BF00207188

MNHN, & OFB. (2024). Sheet of Bathynectes longipes (Risso, 1816). *Inventaire national du patrimoine naturel (INPN).* https://inpn.mnhn.fr/espece/cd_nom/350546

Monterey Bay Aquarium. (2024). Mangrove box jelly. https://www.montereybayaquarium.org/animals/animals-a-to-z/mangrove-box-jelly

Mršulja, B. B., & Rakić, L. M. (1974). Circadian rhythm of glycogen content in various brain structures of serranus scriba cuv. *Journal of Experimental Marine Biology and Ecology*, *15*, 43–48.

Myers, P., R. Espinosa, C. S. Parr, T. Jones, G. S. Hammond, & T. A. Dewey. (2024). The Animal Diversity Web. https://animaldiversity.org

Nakagawa, T., & Eguchi, E. (1994). Differences in Flicker Fusion Frequencies of the Five Spectral Photoreceptor Types in the Swallowtail Butterfly's Compound Eye. *Zoological Science*, *11*, 759–762.

Narendra, A., Reid, S. F., Greiner, B., Peters, R. A., Hemmi, J. M., Ribi, W. A., & Zeil, J. (2011). Caste-specific visual adaptations to distinct daily activity schedules in Australian Myrmecia ants. *Proceedings of the Royal Society B: Biological Sciences*, *278*(1709), 1141–1149. https://doi.org/10.1098/rspb.2010.1378

Naturalis Biodiversity Center. (2024a). Sergestes arcticus. *Zooplankton and micronekton of the North Sea 2.0.* https://ns-zooplankton.linnaeus.naturalis.nl/linnaeus_ng/app/views/species/nsr_taxon.php?id=132246&epi=210

Naturalis Biodiversity Center. (2024b). Macrobenthos of the North Sea. https://ns-polychaeta.linnaeus.naturalis.nl/linnaeus_ng/app/views/species/taxon.php?id=78262&epi=93

Nelson, L. (2003). *An Investigation of the Phototransduction Cascade and Temporal Characteristics of the Retina of the Cuttlefish, Sepia Officinalis* [University of Plymouth]. https://doi.org/http://dx.doi.org/10.24382/4897

Nizinski, M. S., McClain-Counts, J. P., & Ross, S. W. (2023). Habitat utilization, demography, and behavioral observations of the squat lobster, Eumunida picta (Crustacea: Anomura: Eumunididae), on western North Atlantic deep-water coral habitats. *Deep-Sea Research Part I: Oceanographic Research Papers*, *193*(September 2022), 103953. https://doi.org/10.1016/j.dsr.2022.103953

O'Connor, M., Nilsson, D. E., & Garm, A. (2010). Temporal properties of the lens eyes of the box jellyfish Tripedalia cystophora. *Journal of Comparative Physiology A: Neuroethology, Sensory, Neural, and Behavioral Physiology*, *196*(3), 213–220. https://doi.org/10.1007/s00359-010-0506-8

O'Donnell, S., & Jeanne, R. L. (1991). Interspecific occupation of a tropical social wasp colony (Hymenoptera: Vespidae:Polistes). Journal of Insect Behavior, 4(3), 397–400. https://doi.org/10.1007/BF01048286

Ogawa, Y., Narendra, A., & Hemmi, J. M. (2022). Nocturnal Myrmecia ants have faster temporal resolution at low light levels but lower adaptability compared to diurnal relatives. *IScience*, *25*(4), 104134. https://doi.org/10.1016/j.isci.2022.104134

Ogawa, Y., Jones, L., Ryan, L. A., Robson, S. K. A., Hart, N. S., & Narendra, A. (2023). Physiological properties of the visual system in the Green Weaver ant, Oecophylla smaragdina. *Journal of Comparative Physiology A: Neuroethology, Sensory, Neural, and Behavioral Physiology*, *0123456789*. https://doi.org/10.1007/s00359-023-01629-7

Ogoshi, M., Kato, K., Takahashi, H., Ikeuchi, T., Abe, T., & Sakamoto, T. (2012). Growth, energetics and the cortisol-hepatic glucocorticoid receptor axis of medaka (Oryzias latipes) in various salinities. *General and Comparative Endocrinology*, *178*(2), 175–179. https://doi.org/10.1016/j.ygcen.2012.05.001

Petie, R., Hall, M. R., Hyldahl, M., & Garm, A. (2016). Visual orientation by the crown-of-thorns starfish (Acanthaster planci). *Coral Reefs*, *35*(4), 1139–1150. https://doi.org/10.1007/s00338-016-1478-0

Pitnick, S., & Markow, T. A. (1994). Large-male advantages associated with costs of sperm production in Drosophila hydei, a species with giant sperm. Proceedings of the National Academy of Sciences of the United States of America, 91(20), 9277–9281. https://doi.org/10.1073/pnas.91.20.9277

Potier, S., Lieuvin, M., Pfaff, M., & Kelber, A. (2020). How fast can raptors see? *Journal of Experimental Biology*, *223*(1). https://doi.org/10.1242/jeb.209031

Pusch, R., Kassing, V., Riemer, U., Wagner, H. J., von der Emde, G., & Engelmann, J. (2013). A grouped retina provides high temporal resolution in the weakly electric fish

Gnathonemus petersii. *Journal of Physiology Paris*, *107*(1–2), 84–94. https://doi.org/10.1016/j.jphysparis.2012.06.002

Rao, G. S. (1984). Notes on a collection of two species of pelagic penaeids (Crustacea: Decapoda) from the oceanic waters of the southwest Arabian Sea. *Journal of the Marine Biological Association of India*, *26*(1–2), 165–166.

Roser, M., Appel, C., & Ritchie, H. (2013). *Human Height*. Our World in Data. https://ourworldindata.org/human-height

Rospars, J. P., & Meyer-Vernet, N. (2021). How fast do mobile organisms respond to stimuli? Response times from bacteria to elephants and whales. *Physical Biology*, *18*(2). https://doi.org/10.1088/1478-3975/abcd88

Rowe, J. W., & Dalgarn, S. F. (2010). Home range size and daily movements of midland painted turtles (Chrysemys Picta Marginata) in relation to body size, sex, and weather patterns. *Herpetological Conservation and Biology*, *5*(3), 461–473.

RSPB. (2024). Little Owl. https://www.rspb.org.uk/birds-and-wildlife/little-owl

Ryan, L. A., Hemmi, J. M., Collin, S. P., & Hart, N. S. (2017). Electrophysiological measures of temporal resolution, contrast sensitivity and spatial resolving power in sharks. *Journal of Comparative Physiology A: Neuroethology, Sensory, Neural, and Behavioral Physiology*, *203*(3), 197–210. https://doi.org/10.1007/s00359-017-1154-z

Signal, T. D., Temple, W., & Foster, T. M. (2001). Visual Discrimination in the Brushtail Possum (Trichosurus vulpecula). *Australian Journal of Psychology*, *53*(3), 152–154.

Sivertsen, E., & Holthuis, L. B. (1956). Report on the scientific results of the "Michael Sars" North Atlant. Deep-Sea Exped. 1910. Crustacea Decapoda. University of Bergen, 5(12), 1–36. https://doi.org/10.31857/s0044513420100049

Slow Food Foundation for Biodiversity. (2024). Mandaçaia Bee Honey (Melipona quadrifasciata anthidiodes). https://www.fondazioneslowfood.com/en/ark-of-taste-slow-food/mandac%CC%A7aia-bee-melipona-quadrifasciata-anthidiodes-honey/

Smith, F. (1858). *Catalogue of hymenopterous insects in the collection of the british museum*. Taylor & Francis.

Snyder, D. J., & Peterson, M. S. (1999). Foraging and prey selection by bluespotted sunfish enneacanthus gloriosus (holbrook) in backwater, vegetated ponds in coastal Mississippi. *Journal of Freshwater Ecology*, *14*(2), 187–196. https://doi.org/10.1080/02705060.1999.9663670

Stamps, J. A., Mangel, M., & Phillips, J. A. (1998). A new look at relationships between size at maturity and asymptotic size. *American Naturalist*, *152*(3), 470–479. https://doi.org/10.1086/286183

Stavros, K. A., & Kiorpes, L. (2008). Behavioral measurement of temporal contrast sensitivity development in macaque monkeys (Macaca nemestrina). *Vision Research*, *48*(11), 1335–1344. https://doi.org/10.1016/j.visres.2008.01.031

Stowasser, A., Mohr, S., Buschbeck, E., & Vilinsky, I. (2015). Electrophysiology meets ecology: Investigating how vision is tuned to the life style of an animal using electroretinography. *Journal of Undergraduate Neuroscience Education*, *13*(3), A234–A243.

Suh, H. L., & Nemoto, T. (1988). Morphology of the gastric mill in ten species of euphausiids. *Marine Biology*, *97*, 79–85.

Tavares, M., & Campinho, P. (1998). Three new records of deep-sea squat lobsters of the genus Munidopsis Whiteaves from the southwestern Atlantic Ocean (Decapoda: Galatheidae). *Crustacean Research*, *27*(0), 88–100. https://doi.org/10.18353/crustacea.27.0_88

The Animal Facts. (2024). East Asian tiger beetle fact file – Cicindela chinensis. https://www.theanimalfacts.com/insects-spiders/east-asian-tiger-beetle/

Tziouveli, V., & Smith, G. (2009). Sexual maturity and environmental sex determination in the white-striped cleaner shrimp Lysmata amboinensis. *Invertebrate Reproduction and Development*, *53*(3), 155–163.

Ubels, J. L., DeJong, R. J., Hoolsema, B., Wurzberger, A., Nguyen, T. T., Blankespoor, H. D., & Blankespoor, C. L. (2018). Impairment of retinal function in yellow perch (Perca flavescens) by Diplostomum baeri metacercariae. *International Journal for Parasitology: Parasites and Wildlife*, *7*(2), 171–179. https://doi.org/10.1016/j.ijppaw.2018.05.001

Uetz, P., Freed, P., Aguilar, R., Reyes, F., Kudera, J., & Hošek, J. (2024). The Reptile Database, http://www.reptile-database.org

VanDyk, J. (2023). BugGuide.Net: Identification, Images, & Information For Insects, Spiders & Their Kin For the United States & Canada. Iowa State University. http://bugguide.net

Vázquez-Bader, A. R., & Gracia, A. (2016). Diversity and distribution of Chirostyloidea and Galatheoidea (Decapoda, Anomura) in the Southern Gulf of Mexico. *ZooKeys*, *2016*(612), 1–30. https://doi.org/10.3897/zookeys.612.9492

Wang, Z. Y., Ji, A. H., Endlein, T., Li, W., Samuel, D., & Dai, Z. D. (2014). Locomotor kinematics of the gecko (Tokay gecko) upon challenge with various inclines. *Chinese Science Bulletin*, *59*(33), 4568–4577. https://doi.org/10.1007/s11434-014-0557-2

Warrington, R. E., Hart, N. S., Potter, I. C., Collin, S. P., & Hemmi, J. M. (2017). Retinal temporal resolution and contrast sensitivity in the parasitic lamprey Mordacia mordax and its non-parasitic derivative Mordacia praecox. *Journal of Experimental Biology*, *220*(7), 1245–1255. https://doi.org/10.1242/jeb.150383

Watson, E. Y. (1891). *Hesperiidae Indicae, being a reprint of descriptions of the Hesperiidae, of India, Burma and Ceylon*. Madras, Vest.

Weihmann, T. (2013). Crawling at High Speeds: Steady Level Locomotion in the Spider Cupiennius salei-Global Kinematics and Implications for Centre of Mass Dynamics. *PLoS ONE*, *8*(6). https://doi.org/10.1371/journal.pone.0065788

Weisberg, S. B., Whalen, R., & Lotrich, V. A. (1981). Tidal and diurnal influence on food consumption of a salt marsh killifish Fundulus heteroclitus. *Marine Biology*, *61*(2–3), 243–246. https://doi.org/10.1007/BF00386666

WoRMS Editorial Board. (2024). World Register of Marine Species. https://www.marinespecies.org

Zborowski, R. (1998). Locust and grasshopper identification guide. *Australian Government, Department of Agriculture, Fisheries and Forestry.* https://www.agriculture.gov.au/biosecurity-trade/pests-diseases-weeds/locusts/about/id-guide/description_of_adults/3_migratory_locust_locusta_migratoria